FACILITY FORM 602

N66-13351 N66-13362

(ACCESSION NUMBER) (THRU)

151

(PAGES)

(CODE)

CR 68663

(NASA CR OR TMX OR AD NUMBER) (CATEGORY)

COSMIC RAY GROUP

School of Physics and Astronomy

GPO PRICE $ ____________

CFSTI PRICE(S) $ ____________

Hard copy (HC) 5.00

Microfiche (MF) 1.00

ff 653 July 65

UNIVERSITY OF MINNESOTA

CONTRIBUTIONS OF THE UNIVERSITY OF MINNESOTA

TO THE

NINTH INTERNATIONAL CONFERENCE ON COSMIC RAYS

LONDON, SEPTEMBER 1965

Technical Report
CR-82

October 1965

School of Physics and Astronomy
University of Minnesota
Minneapolis, Minnesota

TABLE OF CONTENTS

BLANK PAGE

N66-13352

Modulation of Cosmic Rays by an Electric Field*

P. S. Freier and C. J. Waddington

ABSTRACT

13352

A modulation model is discussed which assumes that the decreased intensity of the cosmic radiation is due to the energy loss experienced by particles passing through electric fields in the solar system. The model is mathematically equivalent to a heliocentric electric field. By assuming that the particle source spectra are power laws in total energy per nucleon, the modulation of the differential and integral intensities of protons and helium nuclei are calculated. The predicted modulation observed by sea level neutron monitors and meson detectors is also calculated and is given as a function of cutoff rigidity. These calculations are compared to the measurements made during the last solar cycle.

author

*Supported by the Office of Naval Research Contract No. Nonr 710(60).

It is generally agreed that the observed solar modulation of the cosmic ray intensity arises from particle interactions with interplanetary electromagnetic fields associated with the outward moving plasma of the solar wind. A major problem which is encountered in understanding this modulation is to separate the effects of energy interchanges between particles and fields from the effects of scattering without energy changes. Some models, such as that originally proposed by Parker (1963), attribute the reduced intensity entirely to such scattering processes, although in a later model Parker (1965) does take other processes into account but in a manner which does not lead to precise analytical solutions except in the limit. This paper presents an interpretation of the experimental data based on a concept of energy interchange between particles and the fields. It is shown that the observed effects can be generally interpreted in terms of a modulation produced by an equivalent electric field, and that this modulation can be simply expressed in a purely analytical form.

The equation for the instantaneous rate of energy change of a particle moving in a field is given by: $dT/dt = \bar{F} \cdot \bar{v}$, where T is the kinetic energy, $\bar{F}$ is the force on the particle and $\bar{v}$ the particle velocity. It can be seen that in order to calculate the change of kinetic energy of the particle in coming from infinity to the earth it is necessary to use the time average of $\bar{F} \cdot \bar{v}$, and to distinguish this from the dot product of the time averages of $\bar{F}$ and $\bar{v}$, which may well vanish. Such a model, in which it is assumed that the energy loss suffered by a particle in coming from outside the solar system to the earth is the main cause of the modulation at the earth, is mathematically equivalent to the electric field model of modulation originally proposed by Nagashima (1951) and Ehmert (1960), and recently re-emphasized by Freier and Waddington (1965). This model has the attractive feature that it has only one adjustable parameter apart, of course, from the question of the input parameters specifying the source spectrum which presents a problem common to all models. As a consequence, by making assumptions on these input parameters, it is possible to calculate the expected modulation effects in detail and compare them with the experimental data.

Aside from the fact that the data can be reasonably well fitted by an electric field model of the modulation (as shown by Freier and Waddington, 1965), it is necessary to ascertain whether the solar system contains fields of such a magnitude that it could be possible for particles on the average to lose as much as 600 Mev per unit charge in coming through the solar system to the earth. Such an energy loss (corresponding to a heliocentric potential of 600×10^6 volts) would be necessary to explain the modulation observed during the last period of maximum solar activity. In the model proposed by Freier and Waddington (1965), the earth is assumed to be at some positive potential V, which is heliocentric and relatively constant out to some distance from the sun which is determined by past and present solar activity. The electric field $E = \frac{\partial V}{r}$ is thus usually only present in some region outside the earth's orbit which may possibly be identified with the shock front that must occur in the region somewhere between 10 and 100 AU where the solar wind becomes subsonic.

From measurements in space it is now well established that there is a continuous flow of plasma from the sun. The radial ejection of this plasma combined with the solar rotation results in the sweeping out of magnetic lines of force whose magnitude and direction have been measured near the earth. Especially important to our knowledge of these magnetic fields is the work of Ness and Wilcox (1965) who have shown that there is a regular longitudinal sector structure in the field which co-rotates with the sun. They found in December 1963, for example, that 4/7 of the sectors had fields whose direction was away from the sun, while only 3/7 of the sectors had directions towards the sun. Thus, it seems plausible that particles arriving from outside the solar system and traversing these fields could show an average change in energy which was not zero.

When a particle of charge Ze and of high energy passes through a plasma stream carrying a frozen-in magnetic field $\overline{H}$, its energy increases or decreases by an amount $W = ZeV_o$ corresponding to the potential difference, V_o, between the boundaries of the plasma stream, Falthammar (1962). The electric field, E, inside the stream is given by $\overline{E} = \frac{\overline{W} \times \overline{H}}{c}$ where $\overline{w}$ is the velocity of the solar wind. Thus, streams travelling on the order of 500 km/sec carrying fields of 5γ have associated electric fields of the order of 2.5×10^{-3} volts/meter. It is possible that such plasma streams of the dimensions of 10^{10}m have potential differences of 25×10^6 volts between their boundaries. Such a modulating potential experienced by all cosmic ray particles would, for example, change the counting rate of a sea level high latitude neutron monitor by about 0.8%. Larger or more extensive fields are necessary to explain Forbush decreases and the 11 year cycle modulation, but the quiet time solar wind velocities and magnetic fields can account for the magnitude of the daily variations in neutron monitors.

In order to calculate the expected particle spectra after modulation, it is necessary to assume some form for the spectra outside the solar system. In order to obtain the best possible fit to the existing data at high energies, it has been assumed that the source spectrum of helium nuclei has the form:

$$J_{He} (\geq E) = 380\ E^{-1.45} \text{ particles/m}^2 \text{ ster.sec}$$

where E is the total energy per nucleon in GeV. The same spectral form is used for the protons with a constant 15 times as large as for helium.

$$J_p (\geq E) = 15\ J_{He} (\geq E) = 5700\ E^{-1.45} \text{ particles/m}^2 \text{ ster.sec}$$

The modulated forms of the differential and integral intensities have been calculated from these spectra on the basis of the electric field model and passage through 3 g/cm^2 of interstellar matter, Freier and Waddington (1965) and show reasonable agreement with those spectra observed during the last solar cycle. Figure 1 shows the differential intensities as a function of kinetic energy for the power law in total energy, after passage through 3 g/cm^2 of interstellar neutral hydrogen, and after modulation by various potentials. Figure 2 shows the integral intensities as a function of magnetic rigidity.

The latitude effect that should be observed by sea level neutron monitors has also been calculated and is compared in Figure 3 to latitude surveys made during solar maximum and solar minimum. This figure shows the predicted latitude curves and the experimental observations made in 1954 and 1955 by Rose et al (1956), and during 1957 and 1958 by Fukushima et al (1964) which were recently summarized by Mathews and Kodama (1964).

A similar calculation of the 11-year variation in the counting rates of meson counters at sea level as a function of cutoff rigidity predicts a form for the modulation which agrees well with that observed. In Figure 4 are shown the predicted curves for sunspot minimum (V=100 Mv) and sunspot maximum (V=600 Mv) along with the intensities measured by sea level meson counters, Quenby (1964).

Predicted Forbush decrease changes do not agree quite as well with measured intensity changes as do the changes characteristic of the solar cycle. High energy detectors tend to show <u>more</u> change than is predicted by the model. For example, during the solar cycle the maximum change predicted for an underground (60 m.w.e.) meson detector is 1.5% and only one-half that much for the November 1960 Forbush decreases. However, underground meson detectors showed as much as a 1.5% decrease during the November event, Mathews (1963). This large decrease lasted for only a brief time, and recovery from this abnormally high modulation occurred definitely sooner than recovery for sea level detectors.

Figure 5 shows the variation in the modulating potential during the last solar cycle. The continuous line is the potential corresponding to the average monthly counting rate of the Ottawa neutron monitor. Individual determinations of V from various intensity measurements of protons and helium nuclei made during balloon flights are also shown. Measurements made during Forbush decreases are identified by arrows.

With this model for the input spectra and the form of modulation, detailed calculation of abundance ratios of protons and helium nuclei can be made. Figure 6 shows the predicted ratio of the differential intensities of protons and helium nuclei as a function of magnetic rigidity. The experimental ratios are those measured in emulsions and reported at this conference, Waddington and Freier (1965). With the assumed form of input spectra, the ratio of protons to helium nuclei is not constant with rigidity; modulation changes the ratio somewhat at low rigidities.

The presence of a positive potential at the earth should result in the acceleration of negative electrons. A large flux of electrons of a few hundred MeV would be expected at least during solar maximum. Instead, observations show that the electron flux >100 MeV is only 4% or less of the primary proton flux above the same energy. Thus, it becomes necessary to postulate some loss mechanism for electrons which removes them as they are being accelerated and before they reach earth. Electrons being of lower rigidity than protons of the same energy will be much more affected by any rigidity dependent sweeping in the solar wind.

FIGURE CAPTIONS

Figure 1 The differential energy spectra of protons and helium nuclei as a function of kinetic energy per nucleon. S indicates the spectrum at the source which has been assumed to be a power law in total energy per nucleon. The effect of passage through 3 gm/cm^2 of interstellar hydrogen is shown. This is the unmodulated (V = 0) spectrum outside the solar system. The differential spectra arriving at the earth for various potentials are shown.

Figure 2 The integral rigidity spectra of protons and helium nuclei for modulating potentials from 0 - 1000 Mv.

Figure 3 Predicted counting rates for sea level neutron monitors as a function of threshold rigidity. The predicted curves are for spectra modulated by potentials of 100 Mv in 1954 and 1955, and 600 Mv for 1958-1959. The experimental points are from latitude surveys made during those years.

Figure 4 Predicted counting rates for sea level mesons at sunspot minimum (V = 100 Mv) and sunspot maximum (V = 600 Mv). The circles are experimental results quoted by Quenby (1964).

Figure 5 The time variations of the modulating potential, V, over the last solar cycle. The continuous line is the potential corresponding to the average monthly counting rate of the Ottawa neutron monitor. Individual determinations of V from various intensity measurements made during balloon flights are also shown.

During four Forbush decreases there have been several determinations of the spectra. The corresponding values of V (measured before, during and after the Forbush decrease) are shown connected by dotted lines.

Figure 6 Predicted ratio of differential intensities of protons and helium nuclei as a function of rigidity. Experimental points are from emulsion experiments in 1963 and 1964, Freier and Waddington (this conference).

REFERENCES

Ehmert, A., 1960, Proc. of Moscow International Conference on Cosmic Rays IV, 142.

Falthammar, C. G., 1962, Journal of Geophysical Research 67, 1791.

Freier, P. S. and C. J. Waddington, 1965, Space Science Reviews 4, 313-372.

Fukushima, S. M., M. Kodama, T. Makino and Y. Miyazaki, 1964, Antarctic Record (Japan) 20, 27-52.

Mathews, T., 1963, Phil. Mag. 8, 387.

Mathews, T. and M. Kodama, 1964, Journal of Geophysical Research 69, 4429.

Nagashima, K., 1951, J. Geomag. and Geoelect. 3, 100.

Ness, N. F. and J. M. Wilcox, 1965, Science 148, 1592.

Parker, E. N., 1963, Interplanetary Dynamical Processes, (Interscience, New York).

Parker, E. N., 1965, Planetary Space Science 13, 9.

Quenby, J. J., 1964, Handbuch der Physik preprint.

Rose, D. C., K. B. Fenton, I. Katzman and J. A. Simpson, 1956, Canadian Journal of Physics 34, 968.

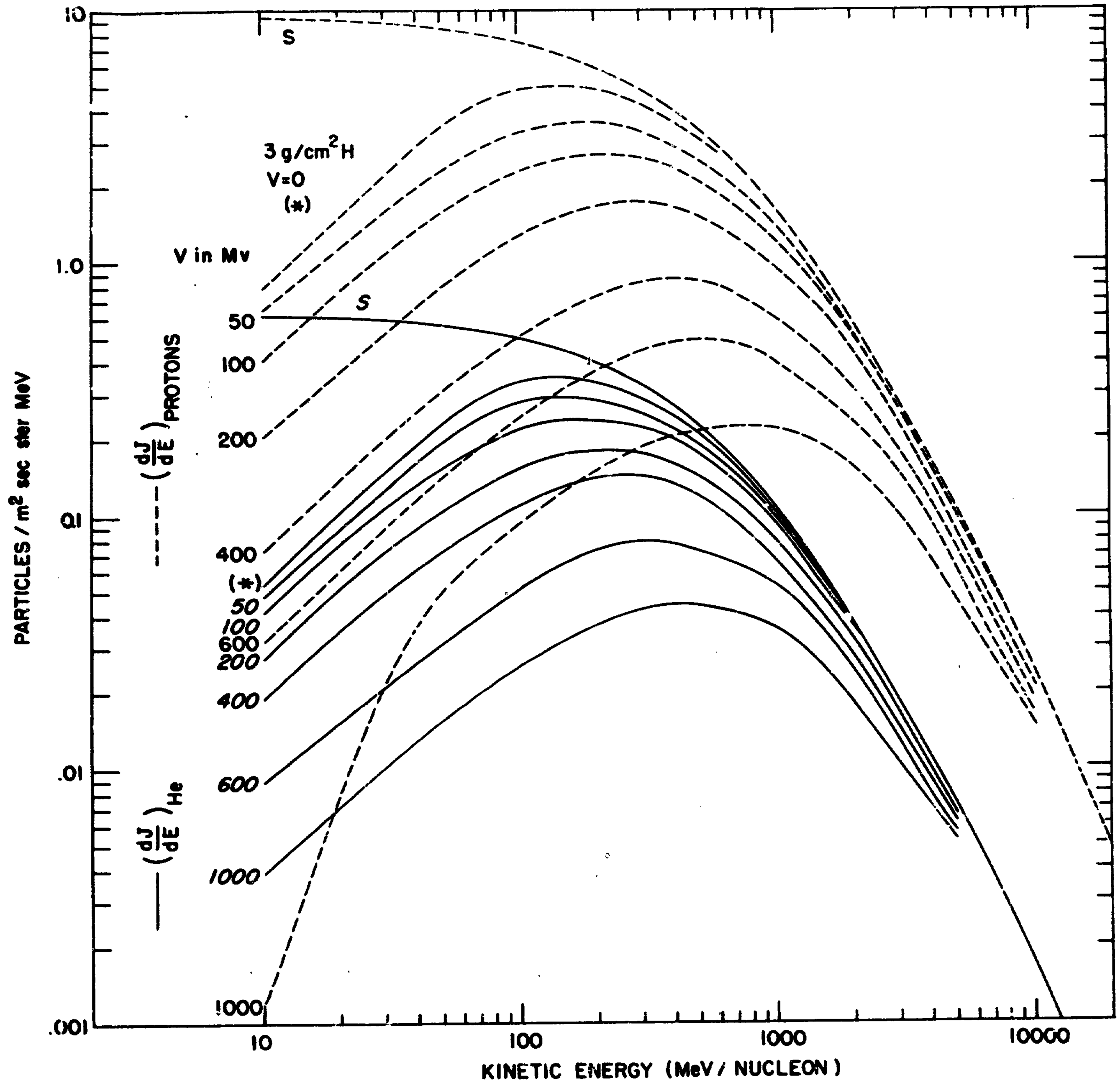

PARTICLES / m² sec ster MeV
KINETIC ENERGY (MeV / NUCLEON)
10
1.0
0.1
.01
.001
10
100
1000
10000
S
S
3 g/cm²H
V=0
(*)
V in Mv
(dJ/dE) PROTONS
(dJ/dE) He
50
100
200
400
(*)
50
100
600
200
400
600
1000
1000

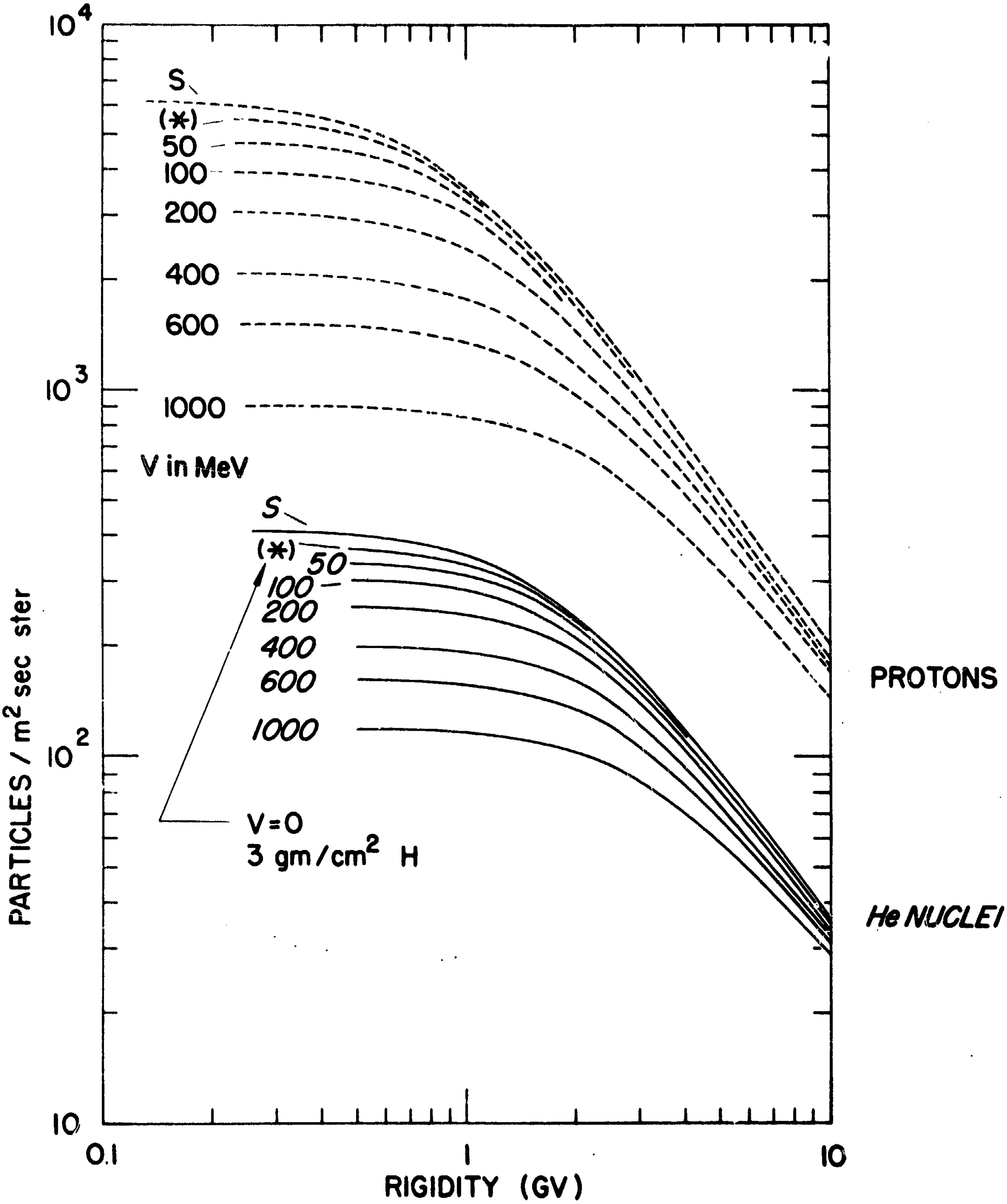

10^4
10^3
10^2
10
0.1
1
10
RIGIDITY (GV)
PARTICLES / m^2 sec ster
S
(*)
50
100
200
400
600
1000
V in MeV
S
(*)
50
100
200
400
600
1000
V=0
3 gm/cm^2 H
PROTONS
He NUCLEI

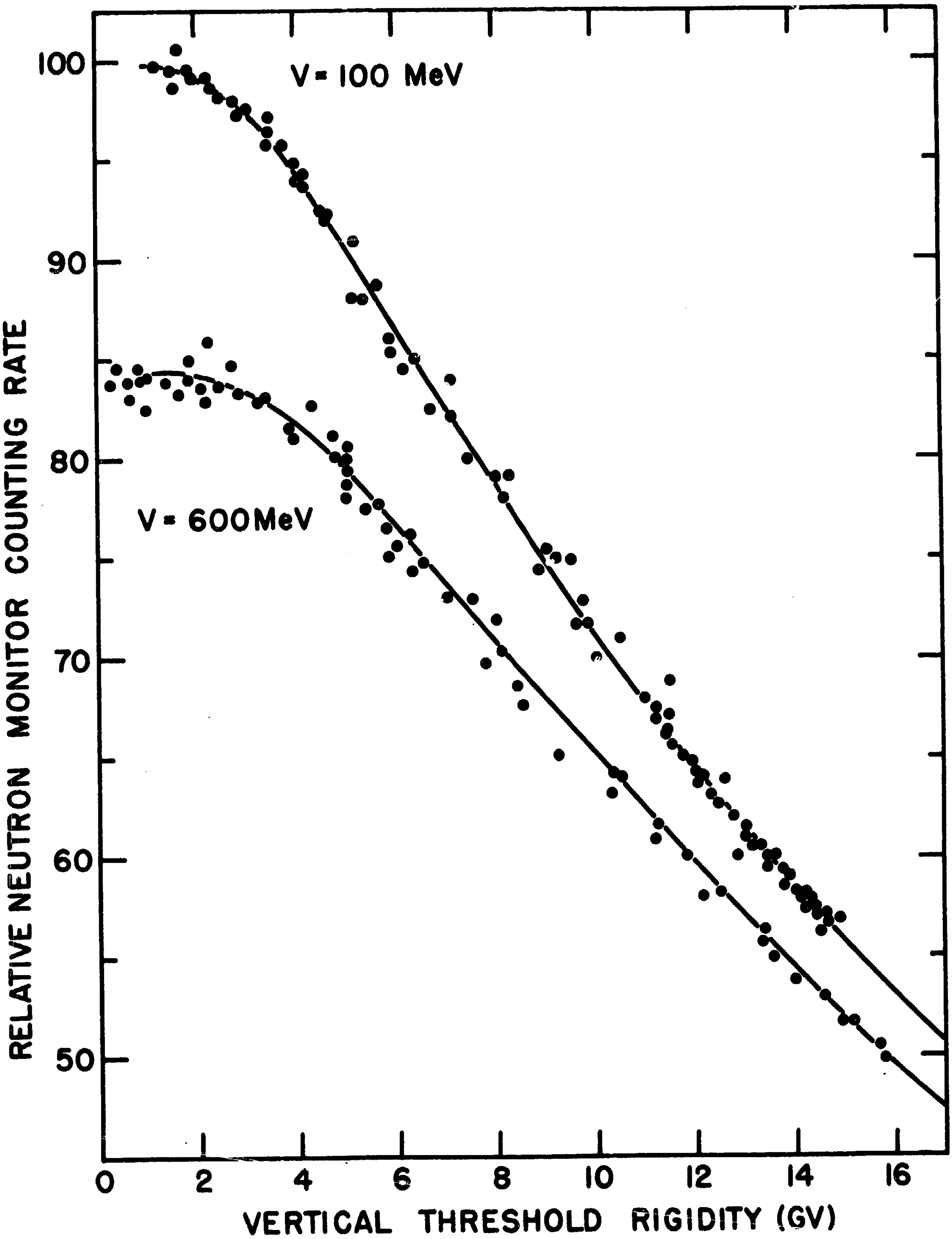

V= 100 MeV
V= 600MeV
RELATIVE NEUTRON MONITOR COUNTING RATE
VERTICAL THRESHOLD RIGIDITY (GV)
100
90
80
70
60
50
0
2
4
6
8
10
12
14
16

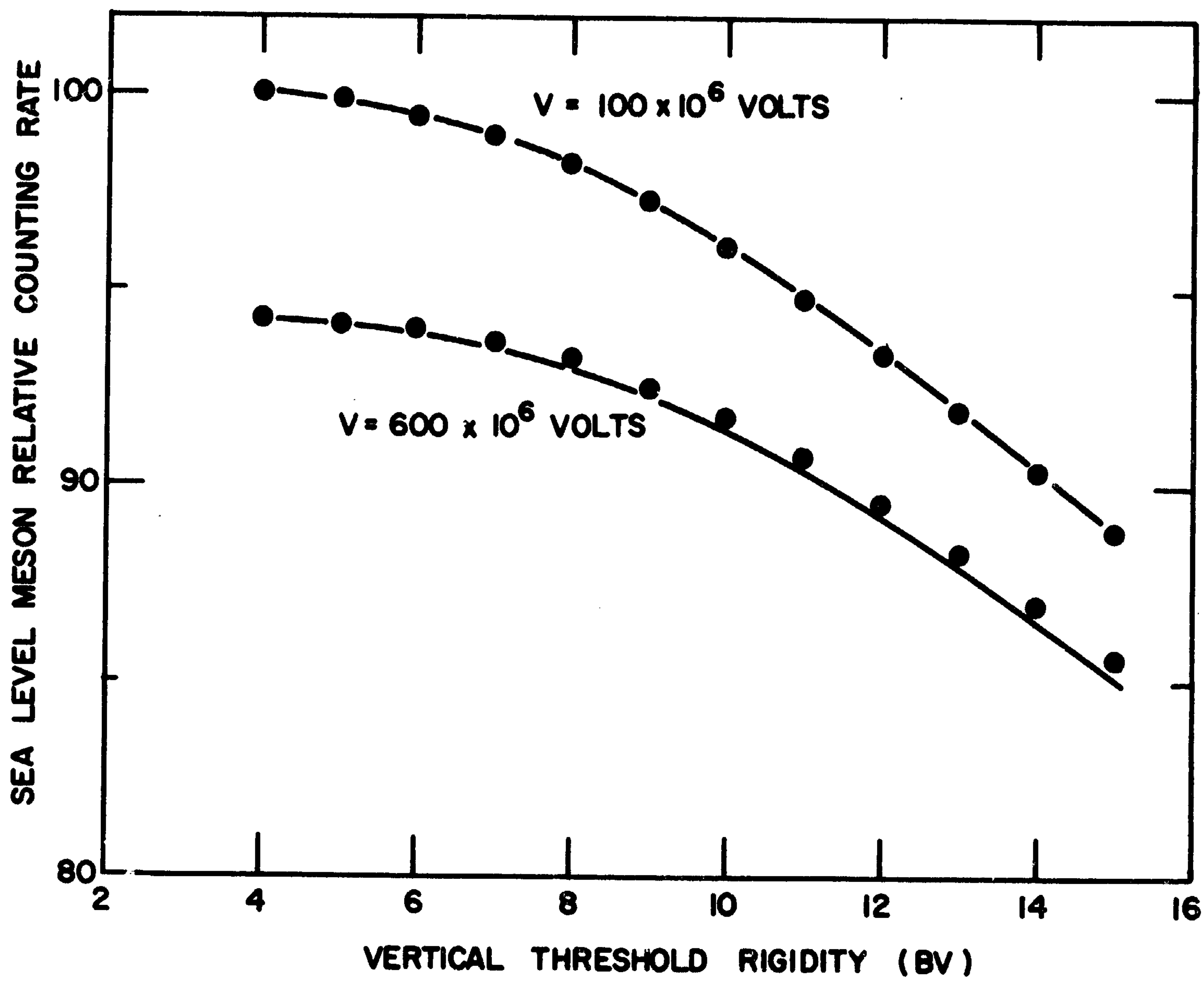

V = 100 x 10^6 VOLTS
V = 600 x 10^6 VOLTS
SEA LEVEL MESON RELATIVE COUNTING RATE
100
90
80
2
4
6
8
10
12
14
16
VERTICAL THRESHOLD RIGIDITY (BV)

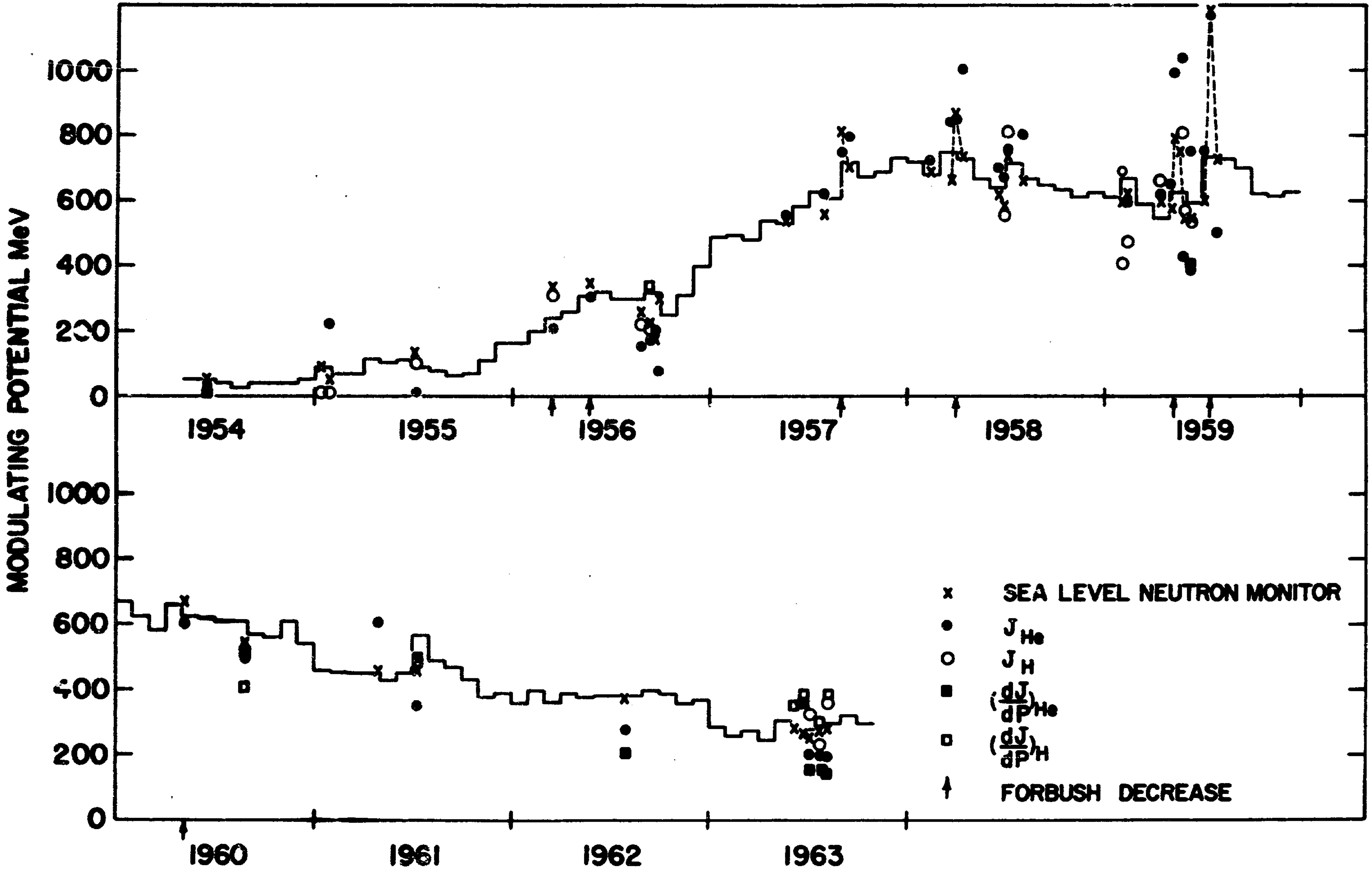

MODULATING POTENTIAL MeV
0
200
400
600
800
1000
1954
1955
1956
1957
1958
1959
1960
1961
1962
1963
SEA LEVEL NEUTRON MONITOR
J_{He}
J_H
$(\frac{dJ}{dP})_{He}$
$(\frac{dJ}{dP})_H$
FORBUSH DECREASE

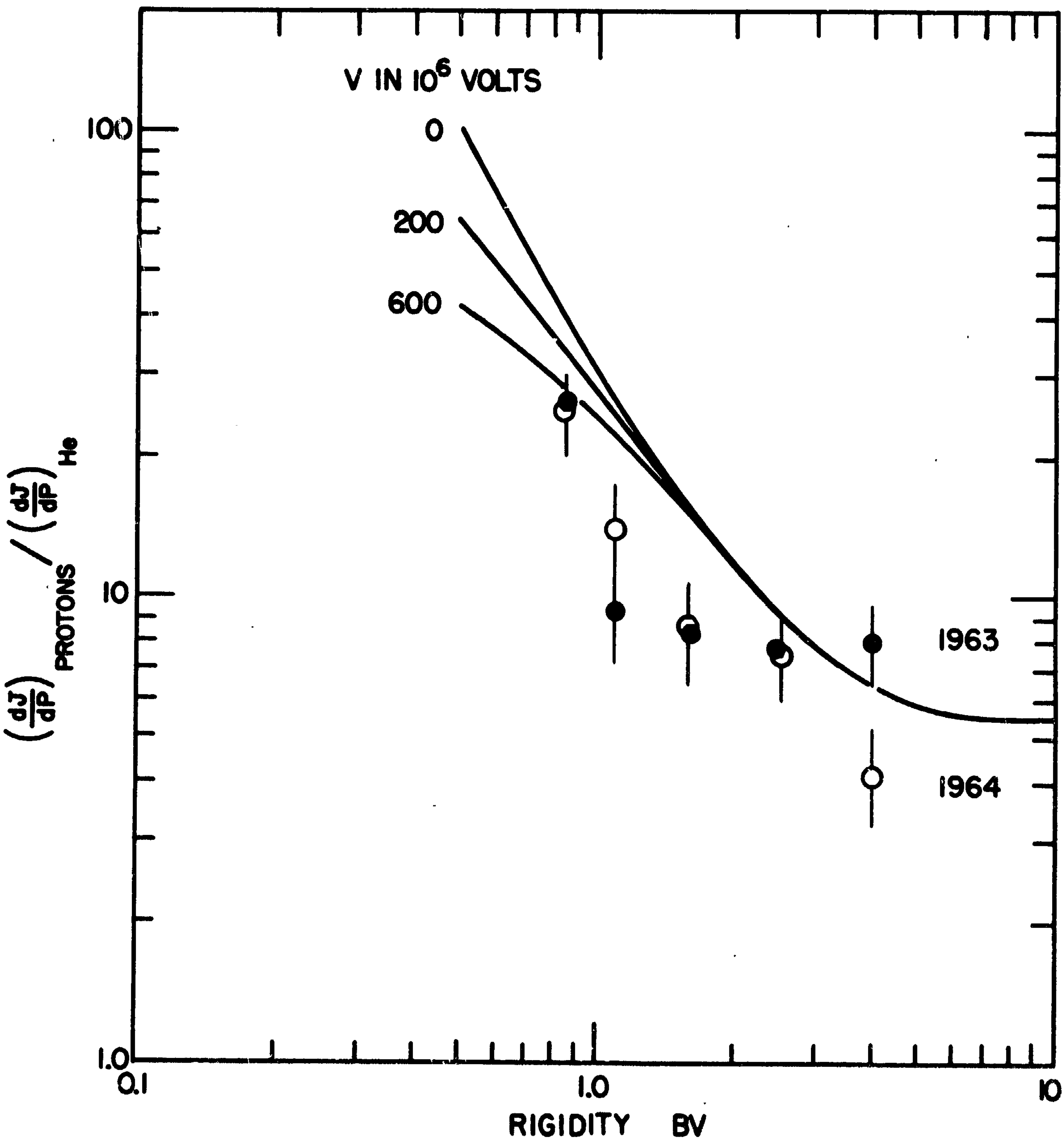

V IN 10^6 VOLTS
0
200
600
100
10
1.0
0.1
1.0
10
1963
1964
RIGIDITY BV
$\left(\frac{dJ}{dP}\right)_{PROTONS} \Big/ \left(\frac{dJ}{dP}\right)_{He}$

BLANK PAGE

N66-13353

Low Energy Multiply Charged Nuclei in the Cosmic Radiation

P. S. Freier, J. S. Eno and C. J. Waddington*

ABSTRACT

13353

Nuclear emulsions mounted in plate "shufflers" were exposed at some 2.5 g/cm^2 over Fort Churchill in 1963 and 1964. These emulsions have been examined for the tracks of multiply charged, $Z \geq 3$, nuclei, with particular emphasis being paid to those particles brought to rest in the emulsions. From these ending particles it appears that during this period near solar minimum the ratio of L to M-nuclei with $170 \leq E \leq 360$ MeV per nucleon, corrected to the top of the atmosphere, is 0.55 ± 0.18, which is appreciably greater than the value observed at higher energies. Also given are values for the total integral intensity of all $Z \geq 3$ nuclei in each year, and the differential intensity of M-nuclei derived from the ending particles. author

*Supported by Office of Naval Research Contract No. Nonr 710(60).

I. Introduction

For many years great interest has been attached to the question of the abundance of the L-nuclei, lithium, beryllium and boron in the primary cosmic radiation. However, not until 1961 at the Kyoto Conference was it possible to conclude that there was general agreement that there existed a finite intensity of L-nuclei in the primary cosmic radiation (Waddington, 1962). Even this conclusion applied only to those nuclei with kinetic energies, E, of more than 1.5 Bev per nucleon. Since then it has been generally accepted that the ratio of L to M-nuclei having $E \geq 1.5$ Bev per nucleon is about 0.28. At higher energies, the ratio was only approximately known, while at lower energies there was some evidence that the ratio increased, e.g. Koshiba et al, 1963. This increase in the ratio has frequently been interpreted as implying that lower energy particles traverse more interstellar matter than do those of higher energy. However, it has recently been pointed out by Hildebrand and Silberberg, 1965, that due to A/Z for L-nuclei being 2.2 rather than the 2.0 characteristic of M-nuclei, much of the observed variation in this ratio could, instead, be due to solar modulation. If this is indeed the case, then it might be expected that a measurement of the L to M ratio at a time near solar minimum would give an appreciably lower value than
1 those obtained in times of solar maximum. For this reason this paper describes <u>provisional</u> results on the observation of L and M-nuclei brought to rest in two emulsion stacks flown in plate shufflers in 1963 and 1964 at a time when the counting rate of the Mount Washington neutron monitor had an average value of 2350 per hour*, i.e. approximately 4% below the rate typical of solar minimum, but some 17% above that at solar maximum.

*Due to the severely limited statistics of this experiment the results of the two flights have been combined in considering the L/M ratio. In fact, the counting rates of the Mt. Washington neutron monitor differed only by 2.8% between the two flights.

II. Experimental Details

Two shuffler stacks were exposed over Fort Churchill in 1963 and 1964. The first of these floated for 11 hours at 1.8 mbs, the second for 12 hours at 2.4 mbs. The counting rates of the Deep River super neutron monitor were 6027 and 6195, respectively. Electrons, protons and helium nuclei have also been studied in these stacks (Waddington and Freier, 1965).

A scan was made along a line 4.5 mms below the top edge of the emulsions for all tracks having more than 7 times the minimum ionization, longer than 4.5 mms per plate and zenith angles less than 45°. These tracks were followed through the emulsions until the particles came to rest, left the stack, or produced nuclear interactions. An approximate indication of the charge of those identified as multiply charged nuclei was provided by δ-ray counts, while those that came to rest were identified from cumulative and differential δ-ray counts made on the ending portions of the track.

III. Results

In order to determine the L/M ratio at low energies only those nuclei which came to rest in the emulsions were considered. From the dimensions of the stack and the amount of overlying matter, it was apparent that these nuclei were only efficiently observed in the range of kinetic energies 170 to 360 Mev per nucleon. Then, by giving each ending nucleus a weight which depended on its path length and the mean free path of that species in nuclear emulsion, it was possible to calculate the observed L/M ratio as being 0.56 ± 0.18. This, when corrected to the top of the atmosphere, became:

$$\Gamma_{LM^o} \; (170 \leq E \leq 360 \text{ MeV/n}) = 0.55 \pm 0.18$$

which, even with this poor statistical weight, is appreciably greater than the value of 0.28 observed at higher energies. However, whether this difference could still be attributed to solar modulation must await the improvement of the statistical weight of this result.

One question that always arises with emulsion experiments involving measurements of charge resolution is whether charges have been correctly identified. A rough verification of the essential validity of the result obtained here is afforded by examining the absolute intensity of ending M-nuclei and comparing it with the values obtained by other workers. Figure 1 shows the value of $(1.50 \pm 0.33)10^{-2}$ nuclei/m^2ster.sec. MeV per nucleon between 170 and 360 MeV per nucleon obtained in this experiment compared with the values obtained by Lim and Fukui, 1965 from a recoverable satellite flown at a time intermediate between these two flights. The agreement is very reasonable. Also shown in this figure is a curve representing the spectrum of helium nuclei observed in the 1964 stack (Waddington and Freier, this conference) together with the same curve after it has been reduced by a factor of $6.5.10^{-2}$, the ratio of M to He-nuclei measured at higher energies (Waddington, 1962). It can be seen that this latter curve is a good fit to the data, implying that ionization energy losses have played a rather negligible role during the interstellar propagation, as otherwise the observed data would have been depressed below the predicted curve. This point is discussed in more detail and taking account of the effects of solar modulation in a paper on very heavy nuclei presented at this conference (Waddington and Freier, this conference).

The final results obtained from this experiment are those on the total intensities of $Z \geq 3$ nuclei. In a previous experiment the results were reported on a number of such measurements made at many different levels of solar modulation (Freier and Waddington, 1964). In this work, the intensities were quoted in the form of those that would be calculated from an observation made under 10 g/cm^2 of air and 1 cm of emulsion overlying the detecting line. The variation of these intensities with the counting rate of the Ottawa neutron monitor was shown as Figure 8 in the above paper. This figure is reproduced here as Figure 2, with the two intensities observed here superimposed. There is a surprisingly large difference between these intensities which, however, partially agrees with the previous data. The reason for this discrepancy is not at all clear at this time, particularly since no such difference was observed among the ending M-nuclei, and since the apparently low intensity value is the sum of two entirely separate experiments which were in extremely good agreement.

FIGURE CAPTIONS

Figure 1 The differential energy spectra of M-nuclei as observed by Lim and Fukui, 1965, and in this experiment. Also shown are the differential energy spectra of helium nuclei as observed in 1964 and when reduced by the abundance ratio of M to He-nuclei.

Figure 2 The variation of the total intensity of $Z \geq 3$ nuclei, J_{Δ}o (corr.) with the counting rate of the Ottawa neutron monitor. Curves 1 and 2 are derived from similar curves for He-nuclei with energies greater than 200 and 500 MeV per nucleon, respectively, by multiplying by the ratio of J_{Δ}o (corr.) to J_{He}. Curve 3 is the least mean square fit to all the previous data with $N > 2500$. The results from this experiment are shown by +.

REFERENCES

Freier, P. S. and C. J. Waddington 1964, Phys. Rev. 135, B724.

Hildebrand, B. and R. Silberberg, 1965, NRL Washington, Preprint.

Koshiba, M., E. Lohrmann, H. Aizu and E. Tami, 1963, Phys. Rev. 131, 2692.

Waddington, C. J. 1962, J. Phys. Soc. Japan 17, Supp. A-111, 63.

Waddington, C. J. 1962, Proc. of XIX Scuola Inter. de Fisica, Academic Press, 135.

Waddington, C. J. and P. S. Freier, 1965, this conference.

Lim, Y. K. and K. Fukui (1965) Preprint Air Force Cambridge.

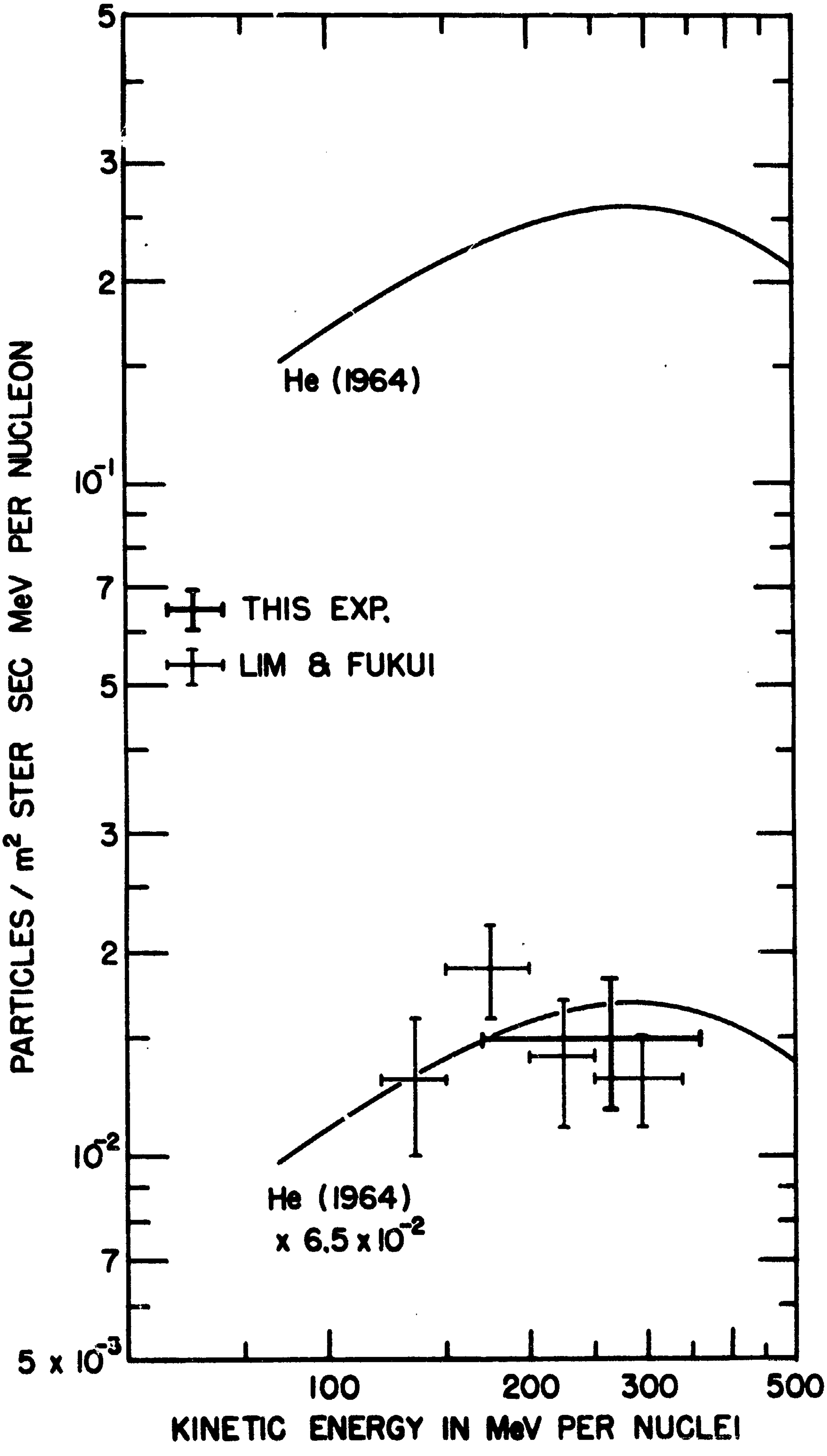

5
3
2
10^{-1}
7
5
3
2
10^{-2}
7
5×10^{-3}
PARTICLES / m^2 STER SEC MeV PER NUCLEON
He (1964)
THIS EXP.
LIM & FUKUI
He (1964)
$\times 6.5 \times 10^{-2}$
100
200
300
500
KINETIC ENERGY IN MeV PER NUCLEI

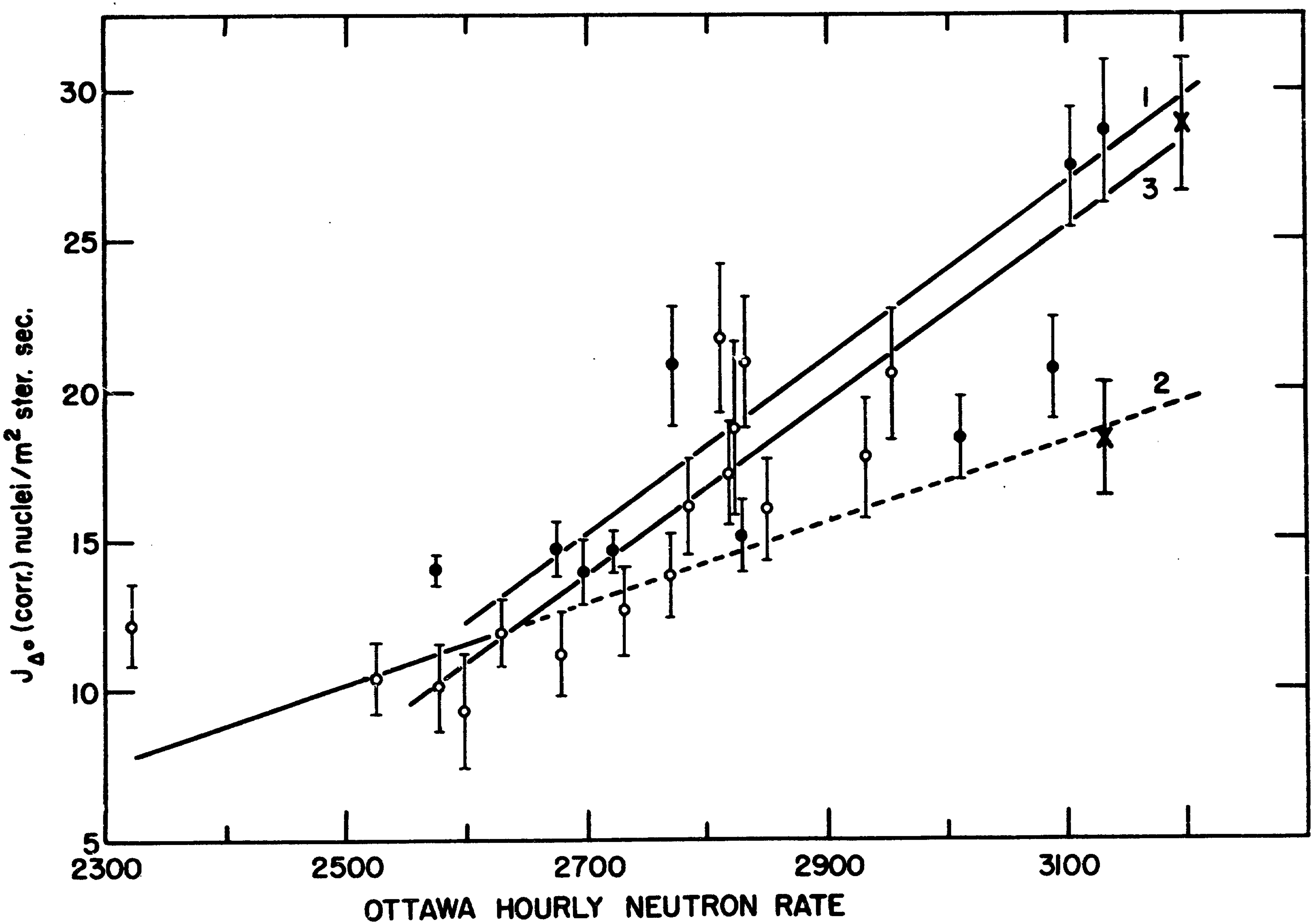

30
25
20
15
10
5
2300
2500
2700
2900
3100
1
2
3
OTTAWA HOURLY NEUTRON RATE
J_{Δ° (corr.) nuclei/m² ster. sec.

BLANK PAGE

N66-13354

VERY HEAVY LOW ENERGY COSMIC RAY NUCLEI*

C. J. Waddington and P. S. Freier

13354

ABSTRACT

A stack of nuclear emulsions having a surface area of 900 cm^2 and mounted in a pressure activated emulsion "camera" was exposed during 1964 at a residual pressure of 2.1 mbs over Fort Churchill. These emulsions are being used to measure the intensity of all nuclei having charges of 20 or greater and the differential energy spectrum of these $Z \geq 20$ nuclei between 240 MeV/n and 650 MeV/n. This range of energies covers the region where nuclei of different charges might be expected to show the greatest spectral changes due to propagation or other causes. Provisional results are reported on the energy spectrum and intensities of these nuclei. These results show that, if acceleration processes are neglected, the mean amount of interstellar or source material traversed by these nuclei does not exceed 2 g/cm^2.

Author

* Supported by U. S. Office of Naval Research under Contract No. Nonr 710(60).

I. Introduction

Experimental examination of cosmic ray particles with dissimilar charge to mass ratios provides a valuable means of investigating the solar modulation process, while a similar examination of those particles having low cosmic abundances gives an indication of the nuclear fragmentations produced during propagation and thus indicates the mean amount of material traversed since the initial acceleration process. In an analogous manner, an examination of those cosmic ray particles having very high charges might be expected to provide information on the ionization effects occurring while the particles are propagating. Since such effects will be proportional to the square of the nuclear charge, clearly the highest charged particles will afford the most sensitive indicators of these effects. This report describes provisional observations on the energy spectrum and absolute abundances of the cosmic ray nuclei which have nuclear charges between those of Calcium and Nickel nuclei, $20 \leq Z \leq 28$, VH-nuclei. Less than 20% of the available data has been analyzed thus far and consequently, the final results and conclusions may differ from those quoted here.

II. Experimental Procedure

Because of the extremely low absolute intensity of VH-nuclei, any experiment which hopes to detect a reasonable number of these nuclei must have a large area-solid angle exposure time factor. In this experiment, the particles were detected in a stack of Ilford G5 600μ stripped emulsions made up of 400 12" by 2" pellicles and 50 12" by 6" pellicles. These emulsions were mounted in a vertical plane with the 12" edge horizontal so that the total collecting area of the stack was about 900 cm^2. Placed over this collecting area and acting as 'shutters' were two glass backed emulsions mounted in a mechanical frame so that they could be swung out of the way. This emulsion 'camera' was mounted in a pressure tight sphere and the shutters connected to the logic circuits of an alphatron pressure measuring device so that they would open when the pressure fell to some predetermined value and then close again after the pressure increased to some other predetermined value.

This device was flown from Fort Churchill on the 22nd of July 1964 and floated for approximately 11 hours at a mean residual pressure of 2.1 mbs. Due to a malfunction, only one of the two shutters opened at the preselected pressure of 3 mb. It had originally been intended that this flight be simultaneous with a rocket shot by Fichtel of the NASA group to study still lower energy nuclei. Adverse winds delayed the rocket shot by several days, but all indications are that these two experiments can be directly compared.

The processed emulsions have been scanned along a line 2 mms below the top edge for tracks as heavy as those produced by fast nuclei having Z=18. All such tracks having a mean projected length greater than 2 mms and with zenith angles of less than 35° were recorded. Thus far, all the scanning has been done in the area covered by the shutter that did work, but as yet no attempt has been made to identify those particles which entered while the shutter was closed. Once this has been done, it will be possible to individually remove those particles whose energies have been incorrectly calculated because they entered while the stack was under appreciably more matter than at ceiling.

Every particle found in this manner was traced through the emulsions until it came to rest, made a nuclear interaction , or passed out of the bottom of the stack. With the stack thickness employed here and for this exposure VH-nuclei will end in the emulsions, and thus reveal their energies very accurately, in the approximate energy interval 240-650 MeV per nucleon. The greatest uncertainty in these energy estimates arises from the uncertainty in the charge determination. If, for example, the uncertainty in the charge of a VH-nucleus is ± 2 units of charge, then the energy estimate has an uncertainty of less than ± 7%.

Charge determinations thus far have been based on the measurement of delta rays having a lateral range greater than 4.5μ. Assignments of charge, based on a scale built up from nuclei of small charge, such as helium and carbon, using different range delta rays for $Z \leq 8$, leads to a peak of iron nuclei and a subsiduary peak at calcium. Furthermore, there is a clear absence of particles between the assigned charges of 20 and 16. These features all resemble those observed at higher energies and give confidence to the general correctness of the charge assignments. Nuclei which did not come to rest in the emulsion were examined for changes in ionization by making delta ray counts at each end of the track. These measurements allowed the velocities of VH-nuclei to be reasonably determined up to the region where the ionization becomes essentially independent of velocity and consequently, allowed charges to be assigned to these faster nuclei. In the case of nuclei making interactions, the velocity could in every case be determined either by ionization change, or from a study of the fragmentation products.

III. Results

From the measurements outlined in the previous section, it was possible to determine the differential energy spectra of VH-nuclei between 240 and 650 MeV per nucleon, the integral intensity of VH-nuclei above 240 MeV per nucleon and a differential intensity of nuclei with $16 \geq Z \geq 14$ between 210 and 350 MeV per nucleon.

The differential energy spectrum of the VH-nuclei is shown in Figure 1 and is based on the observation of 93 nuclei. These data have been corrected to the top of the atmosphere by using a simple absorption mean free path of VH-nuclei in air of 15 g/cm^2, which for an extreme altitude flight such as this, only results in an approximately 20% correction. Figure 1 shows the results of smaller statistical weight reported by Lim and Fukui (1965) for VH-nuclei observed in emulsions flown on a recoverable satellite at a time when the sea level neutron monitor counting rate was 3.4% less than that prevailing during this experiment. By analogy with observations on helium nuclei, Waddington and Freier (this conference), these satellite results would be expected to be not more than 20% lower than those of this experiment due to solar modulation. In fact, Figure 1 shows qualitative agreement.

The integral intensity of VH-nuclei having $E \geq 240$ MeV per nucleon, after correction to the top of the atmosphere, was:

$$J_{VH}\ (E \geq 240\ \text{MeV/n}) = 1.40 \pm 0.10\ \text{nuclei/m}^2\text{.ster.sec.}$$

This value, taken together with the comparable intensity of helium nuclei measured in a flight made four days earlier, when the neutron monitor counting rate was 0.7% less, of J_{He} ($E \geq 240$ MeV/n) = 266 ± 17 nuclei/m^2. ster.sec. Waddington and Freier (this conference), leads to a ratio of VH to helium nuclei of (5.27 ± 0.50) 10^{-3}. This can be compared to the value of $5.9 . 10^{-3}$ previously measured for high energy, $E \geq 1.5$ BeV per nucleon, nuclei, Waddington (1962).

Finally, it is possible to calculate a single differential intensity value for those nuclei having $16 \geq Z \geq 14$ between 210 and 350 MeV per nucleon. This value is: $(dJ/dE) = (11.5 \pm 2.4) \times 10^{-4}$ nuclei m^{2}ster.sec. MeV per nucleon.

IV. Discussion

The differential energy spectrum of the VH-nuclei can be compared directly with that observed for the helium nuclei four days earlier, Waddington and Freier (this conference). If ionization effects are unimportant, then the spectrum of the VH-nuclei should be given by that for the helium nuclei when this latter spectrum is reduced by the relative abundance of VH-nuclei to helium nuclei. Figure 2 shows the helium spectrum and the resulting predicted VH spectrum. It should be noted that very little difference would be made if instead of using the VH-nuclei to helium nuclei ratio for E $\geq$ 240 MeV per nucleon given above, the ratio for E $\geq$ 650 MeV per nucleon were used, $(5.5 \pm 0.6)\ 10^{-3}$.

Examination of Figure 2 shows that, with the possible exception of the lowest energy point, the data are in reasonable agreement with the predicted curve, which implies essentially no measurable effect due to ionization losses. An indication of the expected effect of passage through as little as 2 g/cm^2 of interstellar matter, neglecting fragmentation, which would further reduce the predicted spectra, can be obtained in the following manner. If it is assumed that the source spectrum of these nuclei is a power law in total energy per nucleon, so that $(dJ/dE) = K_i (E + m_o c^2)^{-2.5}$, then it is simple to calculate the shape of the unmodulated helium and VH-nuclei spectra resulting from the passage through 2 g/cm^2 of interstellar hydrogen. This unmodulated spectrum of helium nuclei can be normalized to the observed modulated spectrum by assuming an arbitrary value for the integral intensity at some energy. Figure 2, for example, shows the resultant spectrum when J_{He} (E > 240 MeV/n) is assumed to be 300 nuclei/m^{2}ster.sec. MeV per nucleon. The differences between this spectrum and that experimentally observed represent the modulation functions at every energy. The unmodulated spectrum of the VH-nuclei, after passage through 2 g/cm^2 can now be similarly normalized, using the VH to helium nuclei ratio. This ratio should be that of the unmodulated spectra, but since it is being implicitly assumed that both these groups of nuclei are similarly modulated, the ratio should be unaffected. The resulting unmodulated spectrum is shown in Figure 2, together with the spectrum produced when this unmodulated spectrum is operated on by the modulation functions found from the spectra of the helium nuclei. Because of this feature of operating on the theoretical spectrum with the deduced modulation function, it is apparent that the resultant predicted spectrum is largely independent of the original J($\geq$ E) intensity value chosen to normalize the theoretical spectrum. Furthermore, since the modulation is presumably a Z dependent function, while ionization loss is Z^2 dependent the predicted spectra will be still further depressed if it is assumed that the mean amount of matter traversed is greater than 2 g/cm^2.

Examination of Figure 2 shows that the observed intensities are about a factor of two higher than those predicted after traversal through 2 g/cm^2, but in reasonable agreement with those expected if ionization plays no appreciable role during propagation. In view of the provisional nature of this data, and the uncertain assumptions underlying the analysis given above, it is presumably just possible to reconcile these data with the passage of 2 g/cm^2 of interstellar matter, but this must surely be an upper limit. If this result is incompatible with path lengths derived from the composition, then it will be necessary to conclude that some acceleration processes take place during the majority of the time while the particles traverse the matter so as to overcome the influence of the de-accelerative ionization losses.

FIGURE CAPTIONS

Figure 1 The differential energy spectrum of VH-nuclei as measured in this experiment and compared with the data of Lim and Fukui (1965).

Figure 2 Differential energy spectra of helium and VH-nuclei for various assumptions and models, see text.

REFERENCES

Lim, Y. K. and K. Fukui (1965) Preprint, Air Force, Cambridge.

Waddington, C. J. (1962) E. Fermi Inter. School of Physics Course XIX.

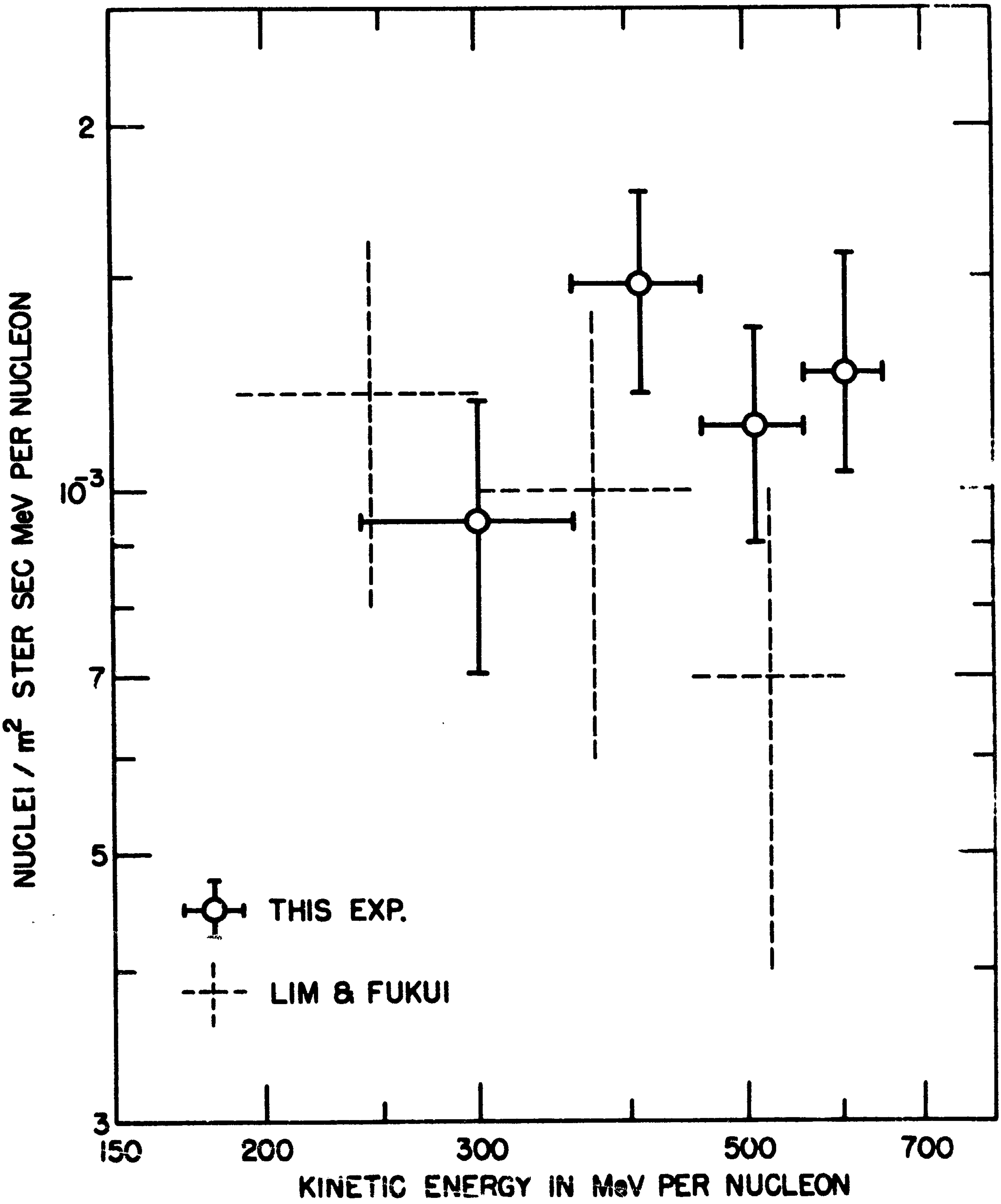

NUCLEI / m² STER SEC MeV PER NUCLEON
2
10⁻³
7
5
3
150
200
300
500
700
KINETIC ENERGY IN MeV PER NUCLEON
THIS EXP.
LIM & FUKUI

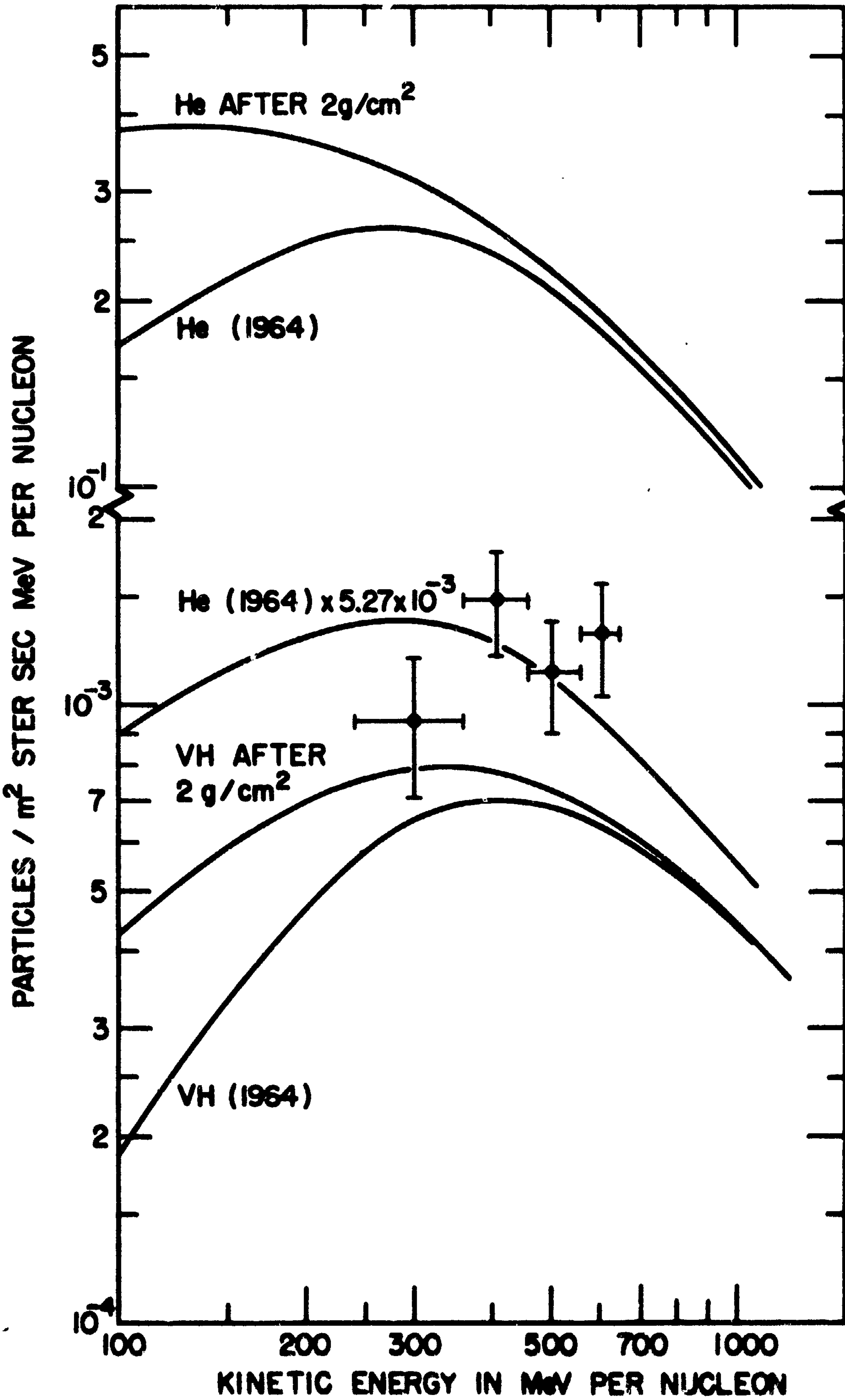
He AFTER 2g/cm²
He (1964)
He (1964) x 5.27x10⁻³
VH AFTER
2 g/cm²
VH (1964)
PARTICLES / m² STER SEC MeV PER NUCLEON
KINETIC ENERGY IN MeV PER NUCLEON
5
3
2
10⁻¹
2
10⁻³
7
5
3
2
10⁻⁴
100
200
300
500
700
1000

BLANK PAGE

N66-13355

Electrons, Hydrogen and Helium Nuclei of the Cosmic Radiation As Observed in 1963 and 1964*

C. J. Waddington and P. S. Freier

13355

ABSTRACT

Nuclear emulsions were exposed over Fort Churchill in plate "Shufflers" flown in 1963 and 1964. Preliminary data on the low energy hydrogen and helium nuclei observed in 1963 have already been reported. These observations have now been extended to cover a wider range and to include electrons. A similar analysis has been made in the shuffler stack flown in 1964 at a time when the counting rate of high latitude sea level neutron monitors had increased by 2.8%. In both stacks the energy spectrum of the hydrogen nuclei has been studied over the energy range, 80 MeV $\leq$ E $\leq$ 4 BeV, which represents a considerable extension over previously available techniques. Similarly the helium nuclei have been studied over an energy range of 70 MeV/n $\leq$ E $\leq$ 1.3 BeV/n, so that for the first time those two components have been studied over a widely overlapping range of rigidities, 0.74 $\leq$ R $\leq$ 4.0 BV. Integral and differential intensities for both years are presented, as are those on the small number of electrons observed in each stack. Analysis of these results shows that in this energy range, the modulation cannot be solely velocity dependent and that there exists a clear discrepancy between these results and some of those reported for the IMP-I satellite.

author

* Supported by U. S. Office of Naval Research under Contract No. Nonr 710(60).

I. Introduction

Electrons, hydrogen and helium nuclei present in the primary cosmic radiation were studied by the authors with a nuclear emulsion shuffler detector flown from Fort Churchill, Manitoba, in 1963, Freier and Waddington (1964, 1965a). This latter paper will henceforth be referred to as Paper I. Here the results are reported of a similar study made with a similar detector flown from the same locality a year later, in 1964, at a time when the influence of solar modulation had been appreciably relaxed and the counting rate of the Deep River neutron monitor had increased by 2.8%. The methods of analysis employed were almost exactly those described in Paper I and the reader is referred to that paper for details. The main difference between the two flights was that the second was at an average residual pressure of 2.4 mb compared with the 1.8 mb obtained in 1963.

II. Experimental Results

The observed proton intensities were corrected for the effects of the overlying atmosphere in a manner similar to that described in Paper I. Figure 1 shows the intensities of secondary protons produced in the overlying emulsion as measured in 1963 and 1964, together with the intensities predicted from interaction data. Also shown are the expected intensities of secondaries from 2.7 g/cm^2 of air, and this curve, together with the observed intensities, leads to the primary intensities shown. The use of the shuffler technique eliminates any necessity for making corrections for particles entering during the ascent phase of the flights. The remaining corrections on these nuclei, and on the helium nuclei, in particular those for absorption, follow the procedures given in Paper I.

The differential energy spectra at the top of the atmosphere of the hydrogen and helium nuclei are shown in Figure 2, together with the spectra observed in 1963, the spectra predicted from an electric field model of modulation at different modulating potentials, Freier and Waddington (1965b), and the low energy hydrogen and helium data obtained from the IMP satellite, McDonald and Ludwig(1964); Fan et al (1965); Gloeckler(1965).

The differential energy spectra of the electrons, not at the top of the atmosphere, but under 2.7 g/cm^2, are shown in Figure 3. Also shown on this figure are the values obtained in 1963 under 2.1 g/cm^2, the magnitude of the meson spectrum, as an indication of the secondary contamination, and the spectrum recently reported by L'Heureux and Meyer (1965) under 4.1 g/cm^2. These data have not been corrected to the top of the atmosphere because of the uncertain nature of this correction. However, as an indication of the possible magnitude of such a correction, Figure 3 also shows a curve for the intensities of secondaries as proposed by L'Heureux and Meyer (1965), after being suitably corrected for the lesser atmospheric depth of this experiment.

I.i. Discussion

Long term temporal variations in the relative abundances of nuclei of a particular species are a consequence of the solar modulation mechanism. Any reasonable model of this process should be able to predict particular values for the ratio of the intensity at one time to that at another time. However, the relative abundances of nuclei of different species do not necessarily vary as a consequence of solar modulations. Indeed, it is difficult to envisage a physically reasonable model which would predict temporal variations between nuclei having similar charge to mass ratios. Nuclei with dissimilar charge to mass ratios may, on the other hand, well show changes in their relative abundances as solar modulation levels change, and any specific model should be able to predict these variations. As a consequence, a study of the variations in the relative abundances of similar nuclei at two times, and of dissimilar nuclei at a particular time, provides a strong test of any model proposed to describe the phenomena of solar modulation.

Two models of particular interest are the electric field model recently reviewed by the authors, and the solar wind model proposed by Parker (1963) in which it is assumed that an equilibrium condition is established between the sweeping out of cosmic ray particles by the solar wind and their inward diffusion through scattering by irregularities in the interplanetary magnetic field. This model leads to a modulation function of the form exp $(-\omega n/v)$, where ω is the solar wind velocity, n is the number of effective mean free paths between the point of detection and infinity and v is the particle velocity. In this model, n is a constant for low rigidity particles but inversely proportional to the square of the particle's gyro-radium at higher rigidities. This model, like the electric field model, can be expressed analytically, but does have an unfortunately large number of adjustable parameters; however, by making some rather arbitrary assumptions, it is possible to obtain predictions which can be compared with experimental data.

In order to facilitate the comparison between the predictions of the theories and the experimental observations, those data obtained from the IMP-I satellite on low energy protons and helium nuclei have been included in this analysis. Briefly, these authors report that during a time period when the counting rate of the Deep River neutron monitor increased by 1.09%, the proton intensity between 25 and 80 MeV increased by less than 10%, while during a counting rate increase of 1.35%, the intensity of helium nuclei between 30 and 80 MeV per nucleon showed an appreciable and well defined increase. In order to compare, at least approximately, these data with the results of this experiment, in which the counting rate of the neutron monitor increased by 2.8%, the percentage increases of the IMP data have been doubled.

The intensity ratios obtained in this experiment, both for protons and for helium nuclei are shown in Figure 4 as a function of kinetic energy per nucleon, $\Gamma_{ii}(E)$, together with the IMP data and the predicted variations from the electric field model. In spite of the rather poor statistics, two points are apparent. Firstly, since particles of the same energy per nucleon have the same velocity, the clear divergence between the protons and the helium nuclei ratios shows that in this energy range the modulation cannot be solely velocity dependent. Secondly, the more rapid variation of the protons than of the helium nuclei observed in this experiment can hardly be consistent with the reverse behavior exhibited by the IMP results. This is in spite of the fact that in each case the overall intensities measured are in good agreement, see Figure 2. The variation in these ratios predicted by the electric field model on the basis of a change in modulating potential from 200 to 100 Mv are also shown and seem to be in reasonable agreement with this data, but not with those from IMP.

In Figure 5, the intensity ratios are plotted as a function of rigidity, $r_{ii}(R)$. It is apparent that in the region where the protons and helium nuclei have similar rigidities these data and the IMP helium data are in good agreement with the concept of a purely rigidity dependent modulation. A modulation curve of the form proportional to inverse rigidity is shown normalized to a 100% increase at 0.5 BV rigidity. The IMP proton data are in complete disagreement with these conclusions. Also shown are the predictions of the electric field model with the same assumption as before. These predictions appear to be in reasonable agreement with the results obtained here but do not fit either the proton or helium IMP data.

Finally, Figure 6a shows the abundance ratios of the protons to helium nuclei as a function of the kinetic energy per nucleon as measured in 1963 and 1964. These data can be compared with the variations predicted by the electric field model and Parker's model. For this comparison, the predictions of Parker's model have been calculated by assuming that the differential energy spectra at different levels of modulation are those given by the electric field model and that the critical rigidity at which a particle has the same gyro-radius as the scale size of the magnetic field irregularities is that of a 300 MeV proton; or a 80 MeV per nucleon helium nucleus. With these assumptions it is possible to calculate the relative ratio of proton to helium nuclei observed to that ratio prevailing in interstellar space. This variation is shown in Figure 6b, together with that predicted by the electric field model. A comparison of Figures 6a and 6b suggests that possibly Parker's model is a somewhat better representation, but the errors are sufficiently large and the behavior at high energies sufficiently divergent, that this is not a very strong confirmation. It may be noticed that if Parker's model, with the assumptions made here, is indeed a reasonable representation, then the modulation should be purely velocity dependent for protons with energies less than 300 MeV and helium nuclei less than 80 MeV per nucleon. Once again, this does not agree with the IMP data.

FIGURE CAPTIONS

Figure 1 The differential energy spectrum of the primary and secondary protons observed in these experiments. The secondaries produced in the 3 g/cm^2 of emulsion overlying the scan line are shown for 1963 and 1964 together with the predicted curve, while those predicted for the 2.7 g/cm^2 of air above the emulsion are shown as a dashed line. Those protons observed at the scan line are labeled "primary plus secondary", while the result of making the correction for secondary protons is shown by the points labeled "primary".

Figure 2 The primary differential energy spectra of the protons and helium nuclei as observed in 1963 and 1964. The curves shown are the predictions of the electric field model of solar modulation at various modulating potentials, V in Mv. The IMP results on each species of nuclei are shown by the dotted straight lines.

Figure 3 The differential energy spectrum of electrons. Also shown are the spectra of mesons observed in the two years, as an indication of the secondary contamination, and the spectrum recently published by L'Heureux and Meyer (1965).

Figure 4 The ratio of nuclei of a particular species in 1964 to those in 1963 at a specific energy per nucleon. The predictions of the electric field modulation model are shown as dashed lines, while the IMP-I data appears as solid lines.

Figure 5 The ratio of nuclei of a particular species in 1964 to those in 1963 at a specific rigidity. Similar to Figure 4 except that a curve representing a modulation inversely proportional to rigidity is also shown.

Figure 6 (a) The ratio of protons to helium nuclei as a function of kinetic energy per nucleon in 1963 and 1964.

(b) The ratio of the above ratio to that prevailing in interstellar space as predicted by the electric field and Parker's models of solar modulation at different levels of modulation measured in terms of equivalent electric potential in Mv.

REFERENCES

Fan, C. Y., G. Gloeckler and J. A. Simpson (1965) J. Geophys. Res. 70, 3515.

Freier, P. S. and C. J. Waddington (1964), Phys. Rev. Letters 13, 108 (1965a) J. Geophys. Res. to be published (1965b), Space Sci. Rev. 4, 313.

Gloecker, G. (1965) Univ. of Chicago Preprint.

L'Heureux, J. and P. Meyer (1965) Phys. Rev. Letters 15, 93.

McDonald, F. G. and G. H. Ludwig (1964) Phys. Rev. Letters 13, 783.

Parker, E. (1963) Interplanetary Dynamical Processes, Interscience Publ.

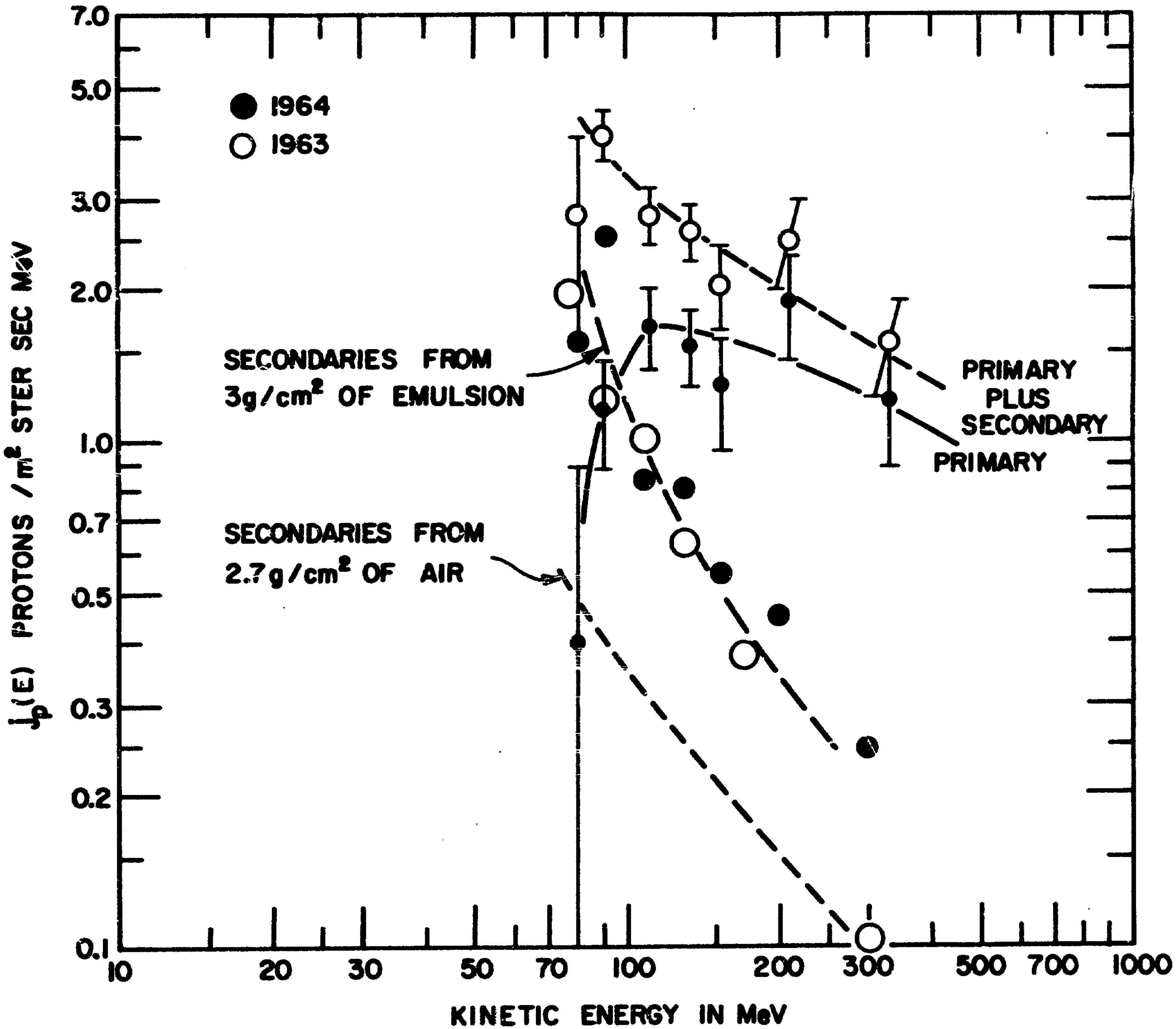

1964
1963
SECONDARIES FROM
3g/cm² OF EMULSION
SECONDARIES FROM
2.7g/cm² OF AIR
PRIMARY
PLUS
SECONDARY
PRIMARY
7.0
5.0
3.0
2.0
1.0
0.7
0.5
0.3
0.2
0.1
10
20
30
50
70
100
200
300
500
700
1000
$j_p(E)$ PROTONS / m² STER SEC MeV
KINETIC ENERGY IN MeV

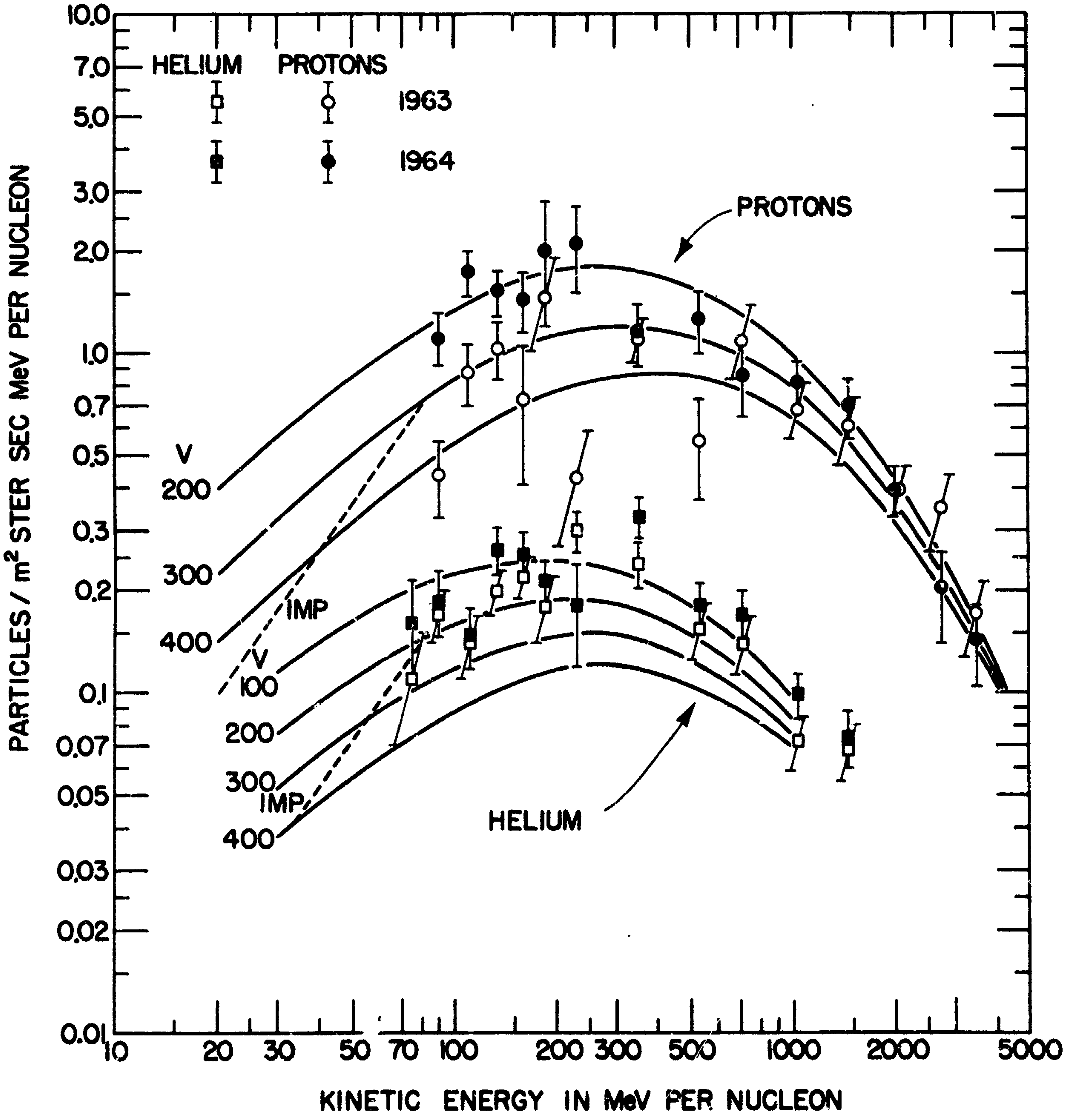

HELIUM
PROTONS
1963
1964
PROTONS
HELIUM
V
200
300
400
IMP
V
100
200
300
IMP
400
PARTICLES / m² STER SEC MeV PER NUCLEON
KINETIC ENERGY IN MeV PER NUCLEON
10.0
7.0
5.0
3.0
2.0
1.0
0.7
0.5
0.3
0.2
0.1
0.07
0.05
0.03
0.02
0.01
10
20
30
50
70
100
200
300
500
1000
2000
5000

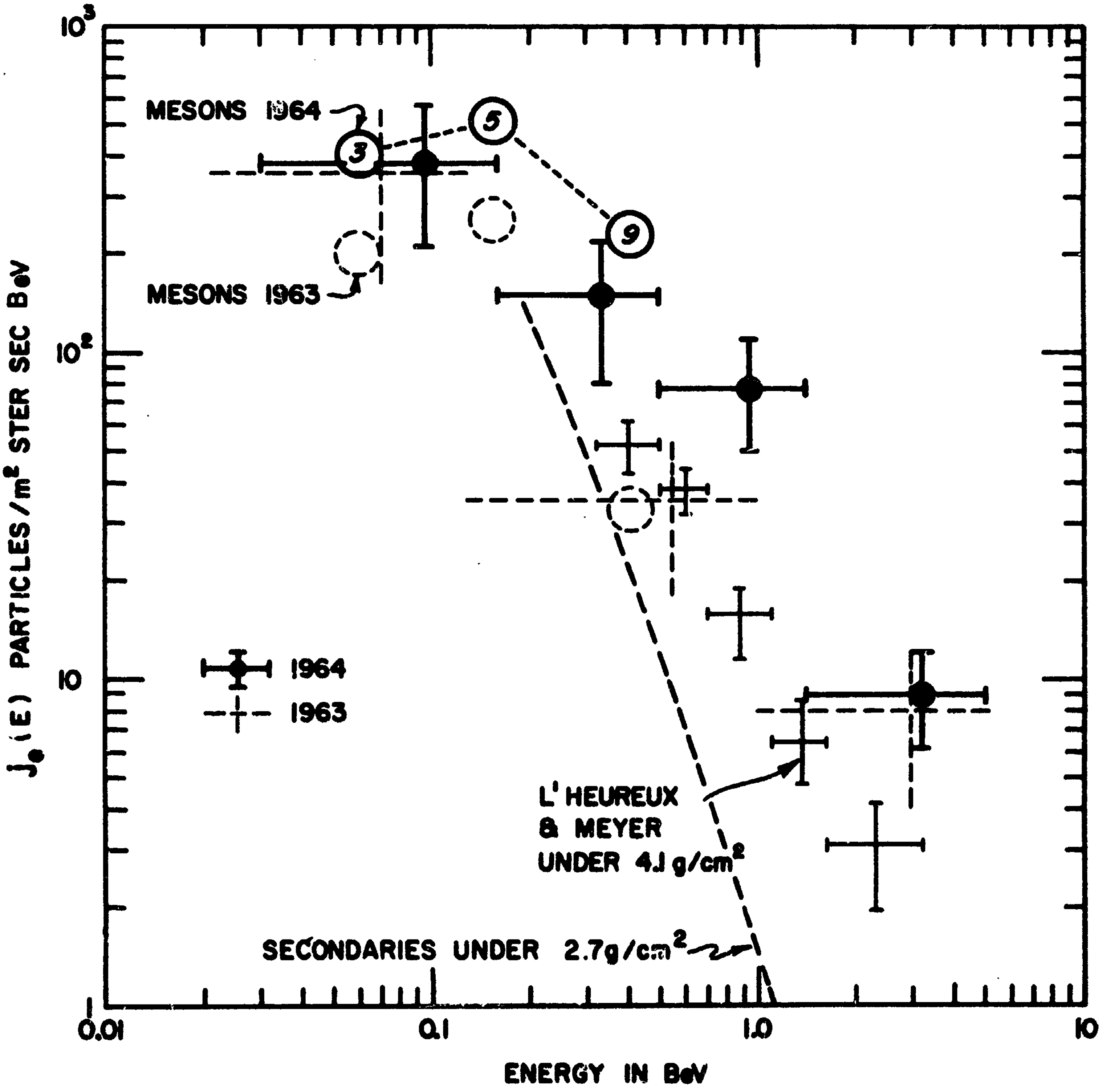

MESONS 1964
MESONS 1963
3
5
9
1964
1963
L' HEUREUX
& MEYER
UNDER 4.1 g/cm²
SECONDARIES UNDER 2.7g/cm²
$J_e(E)$ PARTICLES/m² STER SEC BeV
ENERGY IN BeV
10³
10²
10
1
0.01
0.1
1.0
10

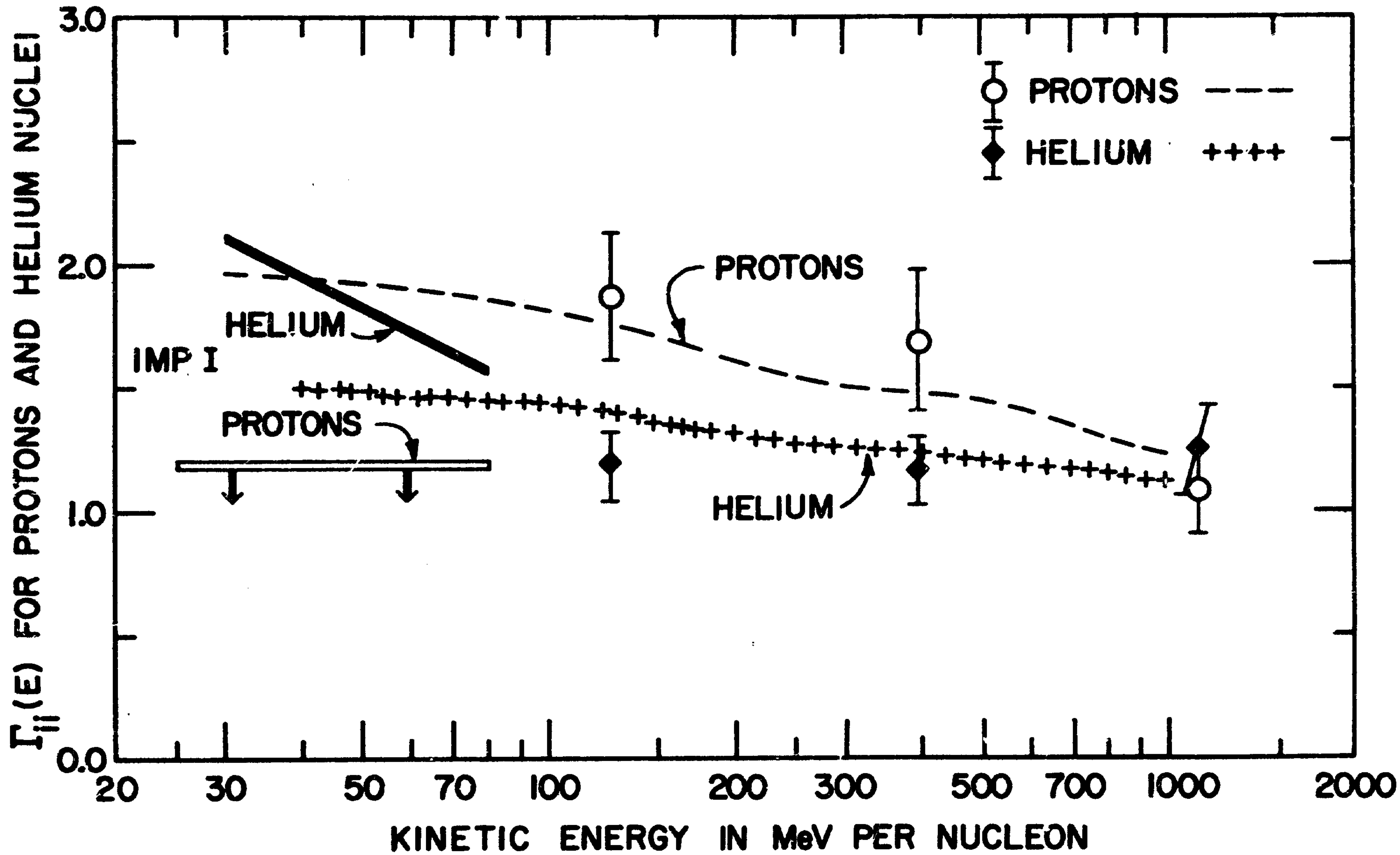

PROTONS
HELIUM
PROTONS
HELIUM
IMP I
HELIUM
PROTONS
PROTONS
HELIUM
3.0
2.0
1.0
0.0
20
30
50
70
100
200
300
500
700
1000
2000
KINETIC ENERGY IN MeV PER NUCLEON
$\Gamma_{||}(E)$ FOR PROTONS AND HELIUM NUCLEI

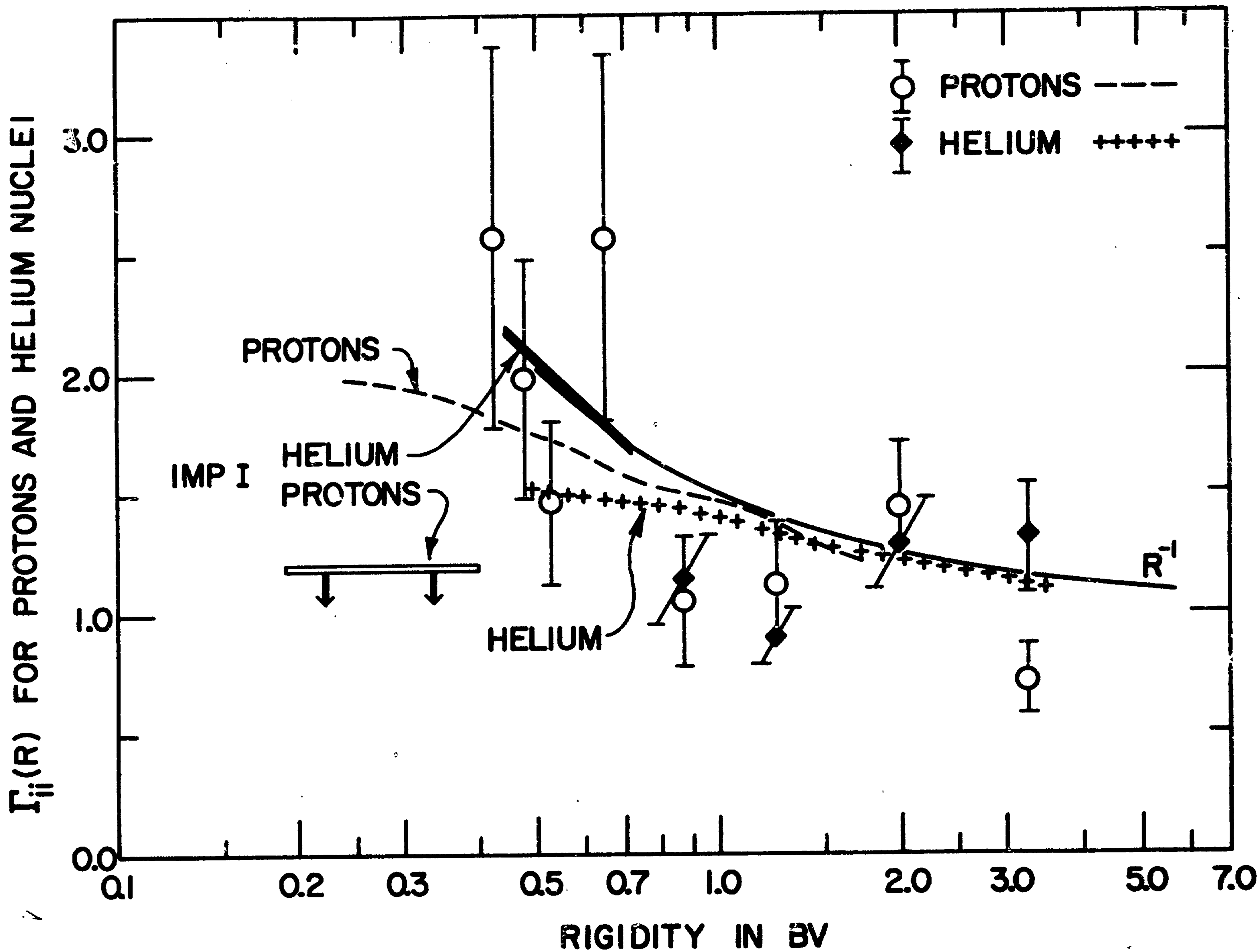

$\Gamma_{ii}(R)$ FOR PROTONS AND HELIUM NUCLEI
3.0
2.0
1.0
0.0
0.1
0.2
0.3
0.5
0.7
1.0
2.0
3.0
5.0
7.0
RIGIDITY IN BV
PROTONS
HELIUM
PROTONS
HELIUM
IMP I
PROTONS
HELIUM
R^{-1}

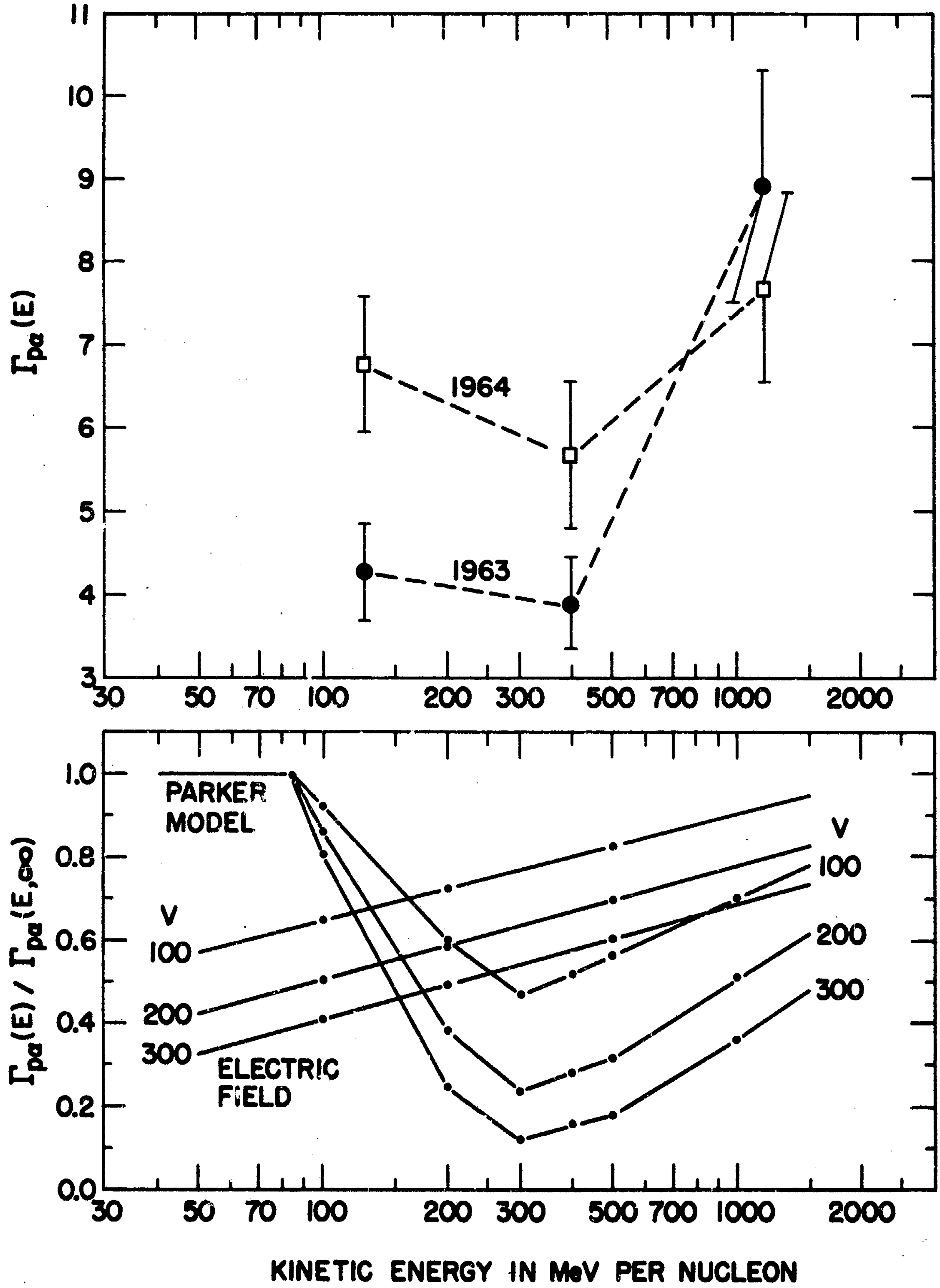

11
10
9
8
7
6
5
4
3
$\Gamma_{p\alpha}(E)$
1964
1963
30
50
70
100
200
300
500
700
1000
2000
1.0
0.8
0.6
0.4
0.2
0.0
$\Gamma_{p\alpha}(E) / \Gamma_{p\alpha}(E,\infty)$
PARKER MODEL
V
100
200
300
ELECTRIC FIELD
KINETIC ENERGY IN MeV PER NUCLEON

BLANK PAGE

N66-13356

Studies of Primary Cosmic Rays with Ionization Chambers*

S. R. Kane and J. R. Winckler
School of Physics and Astronomy

and

R. L. Arnoldy
Honeywell Research Center
Hopkins, Minnesota

13356

ABSTRACT

It is shown that the response of ion chambers in the atmosphere and in free space is peaked over narrow rigidity intervals; these are 1.5 - 2.5 bv, 2.5 - 3.5 bv and 3.0 - 4.0 bv for free space, high latitude balloon and Minneapolis balloon chambers, respectively. Using these results and measurements made with the Pioneer V, Mariner II and OGO-A ion chambers, the rigidity dependence of the long-term modulation during 1960-1965 is found to be consistent with the form $p^{-\beta}$ where $\beta \approx 0.8$. The solar cycle effect at 10 g/cm^2 as measured by balloon flights at Minneapolis and high latitudes is presented. A phase lag of about one year between the total ionization and sunspot numbers exists throughout the cycle. A correlation plot of the high latitude balloon ionization rate and the Deep River neutron monitor for 1958-1965 shows a smooth relationship between the two rigidity ranges. The rigidity dependence of the short-term modulation as measured with space ion chambers in several cases is shown to be different than the long-term. The "turn-up" in ionization in the atmosphere at high latitudes observed at solar minimum can be attributed to the presence of low energy S nuclei in the primary radiation at solar minimum. The peak ionization intensity of the present solar minimum appears to have occurred in May 1965.

author

*This work was supported by a grant from NASA under Contract NAS5-2071.

I. Mean Rigidity of Response

In this paper we shall evaluate quantitatively the rigidity response of ionization chambers flown in the high atmosphere and in deep space. The rigidity dependence of the solar cycle modulation of the primary cosmic ray spectrum will then be investigated using these results. The differential response curves for ion chambers as determined by Callender et al, 1965 and Kane et al, 1965 are summarized in Figure 1. The balloon curves are derived from latitude surveys at 10 mbs by Neher, 1965 and Neher and Anderson, 1962. The free space ion chamber repsonse curves were obtained by calculation using a known primary spectrum for the OGO-A ion chamber by Kane et al, 1965. One notes in Figure 1 that the response is peaked over a narrow rigidity range with a shift of the maximum downward at solar minimum. The mean rigidity of response is calculated by integrating the rigidity over these response curves above the appropriate cutoff as a lower limit of integration. The results obtained are: for free space, 2.9 BV decreasing to 2.1 BV at solar minimum; and for a Minneapolis 10 mb ion chamber, 4.0 BV decreasing to 3.0 BV at solar minimum. We now compare in Figure 2 the fractional increase of ion chambers during the period 1960-1964 with the fractional change in helium nuclei in various rigidity ranges. This comparison is made against the fractional increase in the Mt. Washington neutron monitor and will serve as an independent check on the correctness of the mean response rigidity evaluated above. The response rigidity inferred from the ion chamber curves in Figure 2 considered in relation to the helium nuclei curves does, indeed, agree with the calculated mean response rigidity given above.

II. Solar Cycle Variation Measured with Balloon Ion Chambers

In Figure 3 we compare the monthly average sunspot numbers with the 10 mb ionization measured at Minneapolis and at high latitude with a long series of balloon flights. The balloon data is expressed as a fractional change from the November 1958 monthly mean. Values in 1954 and 1955 are from data normalized from

H. V. Neher (see Callender et al, 1965). This figure shows the large solar cycle modulation effect in balloon ion chambers and the latitude difference between Minneapolis and Churchill which disappears at solar maximum and reappears again at solar minimum. The cosmic ray curve, like the sunspot curve, is asymmetrical, drops rapidly and recovers slowly. An apparent more or less constant phase lag of about one year exists between the cosmic ray rates and the sunspot numbers all the way through the cycle. This phase of about one year, if attributed to solar wind effects propagated from the sun with a speed of 300 km per second would imply a modulation scale size of about 100 astronomical units. In May of 1965 the high latitude ionization rates at 10 mbs have slightly exceeded their value at the previous sunspot minimum period. The smooth relationship between the long term modulation of the 3 BV range of mean rigidity and the 15 BV range is shown in Figure 4 where a correlation curve of high latitude ion chamber data and the Deep River neutron monitor is given.

III. Ionization Chambers in Free Space

In Figure 5 we have assembled on the same normalized scale, the free space ion chamber measurements made on Pioneer V, Mariner II and OGO-A. These are plotted against the Deep River neutron monitor hourly rate and cover the period 1958-1965; that is, during almost the entire upward trend in the cosmic ray rates since solar maximum. The inserts at the right of Figure 5 show expanded correlation plots during the history of each of the three satellites. The long term correlation is a linear one, but one notes that the slope may be different for the shorter term variations shown in the inserts and is markedly so for Pioneer V and also for Mariner II. Both of these spacecraft encountered large Forbush type decreases in the cosmic ray intensity. This may be taken as evidence that the rigidity dependence of the short and long term variations are not the same over the extreme range covered by the free space chambers and neutron monitors. In Figure 6 the daily average ionization rates obtained from OGO-A when the satellite was at apogee, free of the influence of the magnetosphere, are plotted through the entire history of the OGO-A and for comparison the Deep River neutron monitor. One notes the general similarity of the two curves even for short term changes. The life history of OGO-A covers what appears to be the peak cosmic ray intensity of the solar minimum period which occurred in early May 1965. The OGO-A data includes also the rather unusual sudden increase in cosmic ray intensity on approximately 1 December 1964.

IV. Low Rigidity Modulation Spectrum

Using the mean response of ion chambers and the data given in Figure 2 the rigidity dependence of the long term modulation of the primary spectrum for the time period 1960 to 1964 and in the rigidity range 1.5 - 4 BV can be determined. The fractional increase in the ion chamber rates and helium nuclei intensities are plotted versus rigidity in Figure 7. It can be seen that the observations in Figure 7 are consistent with the modulation of the form $MP^{-\beta}$. The straight line in Figure 7 corresponds to $\beta \approx 0.8$. If the total period is divided into two parts, (see Kane et al, 1965), one finds that for 1960-1962, $\beta \approx 0.8$, whereas for 1962-1964, $\beta \approx 1.4$.

V. Comments on the "Turn-up" in ionization Curves Observed at High Altitude

As a result of balloon measurements during the 1954 solar minimum, Neher, 1962, has observed a sharp increase of ionization near the top of the atmosphere at high latitudes. This observation has been frequently discussed, but the cause has not been determined. Attempts to fit the ionization depth curve with proton spectra estimated for solar minimum conditions have not been successful. Recently, on a balloon flight at Barrow, Alaska in May 1965 conducted by D. J. Hofmann of the University of Minnesota, the ionization turn-up phenomena was observed and the primary proton and helium spectrum in the low rigidity range was simultaneously measured. The ionization measurement is shown in Figure 8. A simultaneous flight made at Minneapolis shows the latitude effect of total ionization very clearly.

For comparison, an early flight made at the period of solar maximum at Minneapolis is also included in Figure 8. For a simple method of investigating this "turn-up" phenomena, we take differences between the high latitude and Minneapolis ionization curves obtained from the simultaneous flights. This difference must be due to primary particles having a rigidity equal to or less than 1.3 BV which is the Minneapolis cutoff. In Figure 9 this experimental latitude excess is shown by the dotted line. Using the known response of the ion chambers to the various charge components of the primary spectrum and the direct particle measurements by Hofmann on the Barrow flight, together with estimates in the higher rigidity range by Webber, 1965, we have also calculated the expected latitude difference. The differences for protons, helium nuclei and S-nuclei and the summation for total primaries are shown in Figure 9. The conclusion is that the proton spectrum as observed can never produce a turn-up in the ionization depth curve. This is because of the lack of low energy protons in the spectrum of the primaries observed by Hofmann at solar minimum. This confirms the earlier calculations about the turn-up phenomenon mentioned above. Figure 9 also shows a calculated contribution of helium nuclei based on the observed spectrum of Hofmann on the Barrow flight. The helium nuclei, likewise, cannot provide the excess ionization needed for the "turn-up" phenomenon. The contribution of heavies is included by assuming the ratio of heavies to helium to be the same over the complete range of rigidities. In this case, the contribution of heavies below 200 MeV per nucleon is sufficient to produce the rapid increase of ionization as shown in Figure 9. Although this calculation is rather crude, we feel that the ionization depth "turn-up" phenomena observed at solar minimum can be satisfactorily accounted for by the primary cosmic ray spectrum and that there is no need to invoke any strange or unusual type of radiation.

FIGURE CAPTIONS

Figure 1 Differential response curves for ion chambers in space and on balloons. The former are computed using the known primary spectrum and the latter are based on Neher's latitude surveys.

Figure 2 Fractional increase in the ion chamber rates and the intensity of He nuclei in various rigidity intervals as a function of the corresponding increase in the Mt. Washington neutron monitor during the period 1960-1964. Rates in September 1964 are taken as reference levels.

Figure 3 Variation of the balloon ion chamber rates and the sunspot numbers during the last solar cycle (1954-1965). Ion chamber measurements prior to 1955 are due to Neher.

Figure 4 Relationship of the high latitude ion chamber rates (10 mb altitude) and the Deep River neutron monitor during the period 1960-1965. The neutron monitor rate corresponds to the time when the balloon attains the 10 mb level.

Figure 5 Monthly mean ion chamber rates in free space from solar maximum (1958) to solar minimum (1965) plotted against the corresponding Deep River neutron monitor rates. The inserts at the right show the correlation plots of the daily mean rates during the history of each satellite.

Figure 6 Daily mean rates of the OGO-A ion chamber and the Deep River neutron monitor during the period September 1964 - June 1965. The peak in the cosmic ray intensity apparently occurred in early May 1965.

Figure 7 Rigidity dependence of the long-term modulation of the primary cosmic rays, during the period 1960-1964. The intensity in September 1964 is taken as reference level.

Figure 8 Variation of the balloon ion chamber rates with atmospheric depth. Note the "turn-up" in the high latitude ion chamber rate at solar minimum (May 1965).

Figure 9 Observed and computed difference in Minneapolis and high latitude ion chambers at various atmospheric depths. Computations are based on the known primary spectrum at the top of the atmosphere.

REFERENCES

Callender, R. H., J. R. Manzano and J. R. Winckler, 1965, J. Geophys. Res., 70, 3189-3201.

Kane, S. R., J. R. Winckler and R. L. Arnoldy 1965, J. Geophys. Res. 70,

Neher, H. V. 1956, Phys. Rev. 103, 228-236.

Neher, H. V. and H. R. Anderson, 1962, J. Geophys. Res. 67, 1309-1315.

Webber, W. R., Handbuch der Physik, Vol. 46/2, 1965.

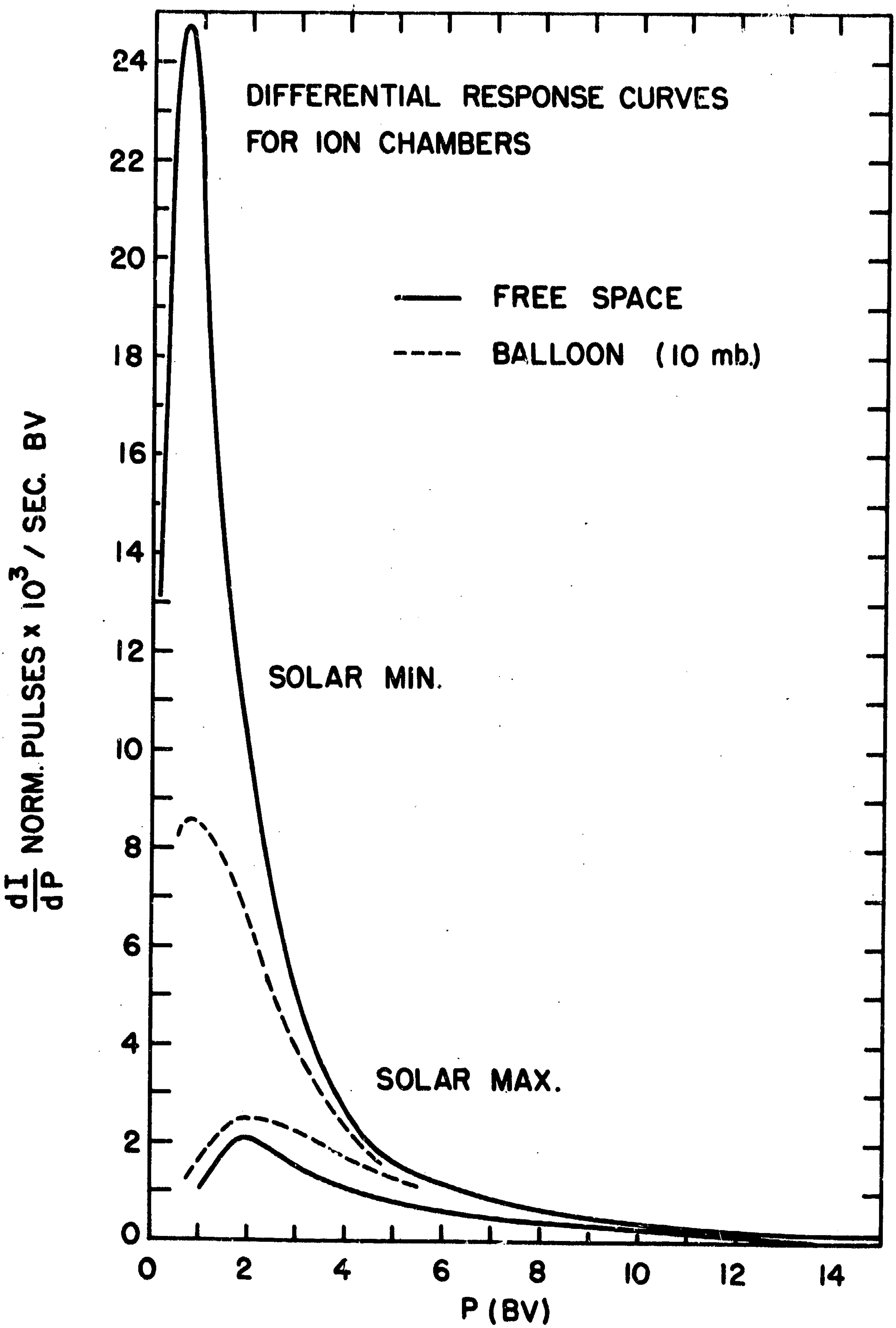
DIFFERENTIAL RESPONSE CURVES
FOR ION CHAMBERS
FREE SPACE
BALLOON (10 mb.)
SOLAR MIN.
SOLAR MAX.
$\frac{dI}{dP}$ NORM. PULSES x 10^3 / SEC. BV
P (BV)
0
2
4
6
8
10
12
14
16
18
20
22
24

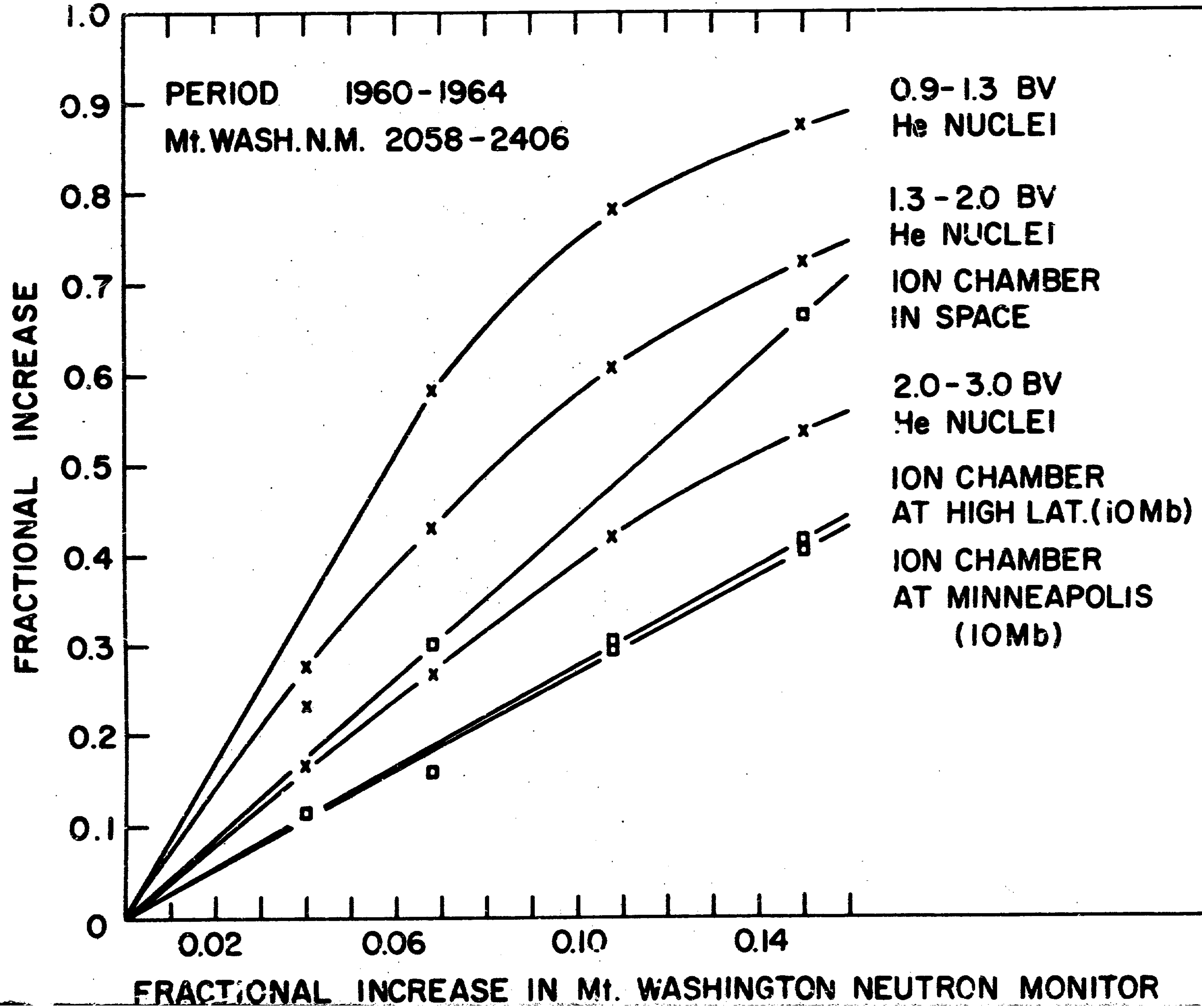

PERIOD 1960-1964
Mt. WASH. N.M. 2058-2406
0.9-1.3 BV
He NUCLEI
1.3-2.0 BV
He NUCLEI
ION CHAMBER
IN SPACE
2.0-3.0 BV
He NUCLEI
ION CHAMBER
AT HIGH LAT. (10Mb)
ION CHAMBER
AT MINNEAPOLIS
(10Mb)
FRACTIONAL INCREASE
1.0
0.9
0.8
0.7
0.6
0.5
0.4
0.3
0.2
0.1
0
0.02
0.06
0.10
0.14
FRACTIONAL INCREASE IN Mt. WASHINGTON NEUTRON MONITOR

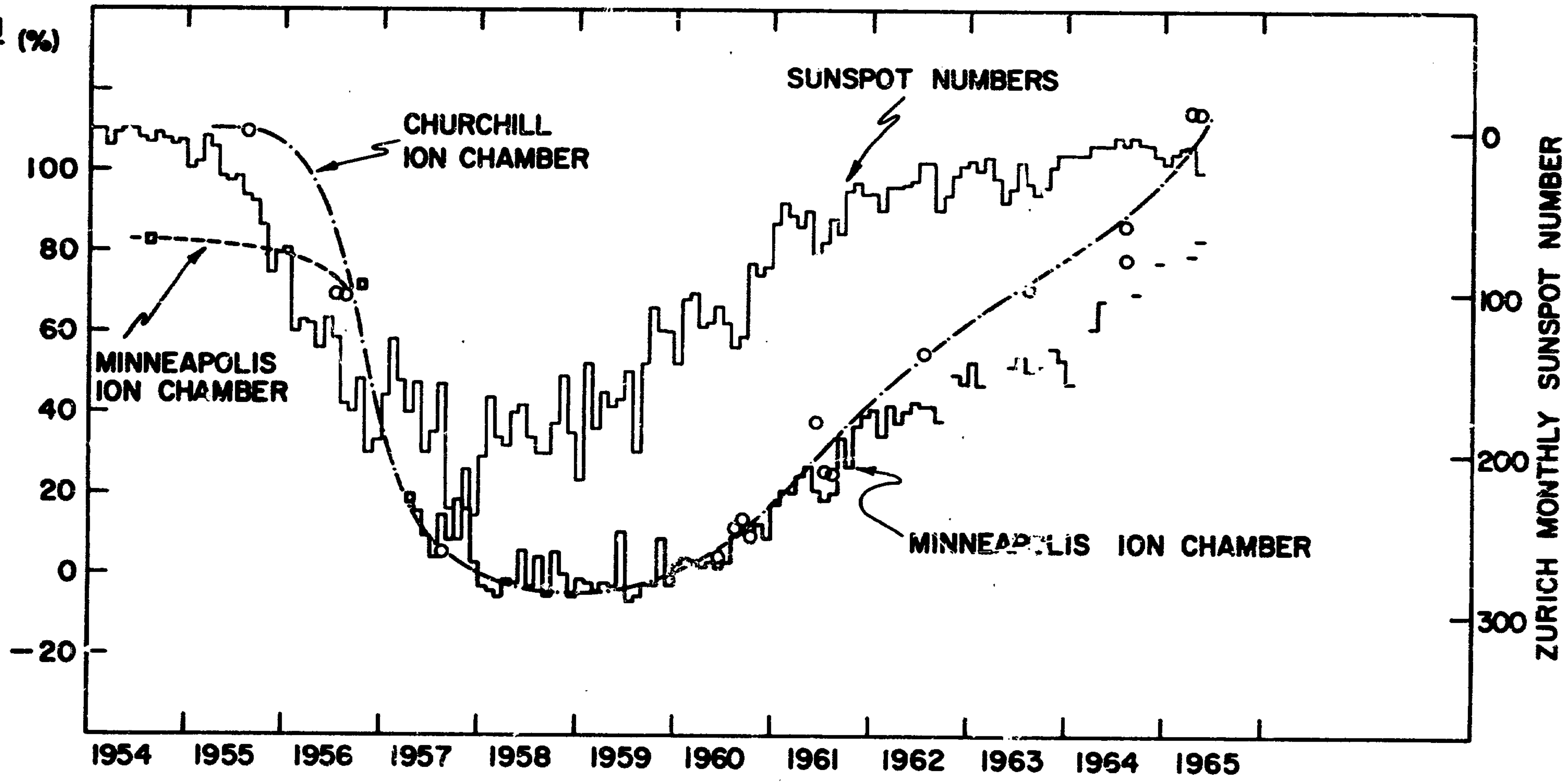

ΔN/N (%)
100
80
60
40
20
0
−20
CHURCHILL ION CHAMBER
MINNEAPOLIS ION CHAMBER
SUNSPOT NUMBERS
MINNEAPOLIS ION CHAMBER
1954
1955
1956
1957
1958
1959
1960
1961
1962
1963
1964
1965
0
100
200
300
ZURICH MONTHLY SUNSPOT NUMBER

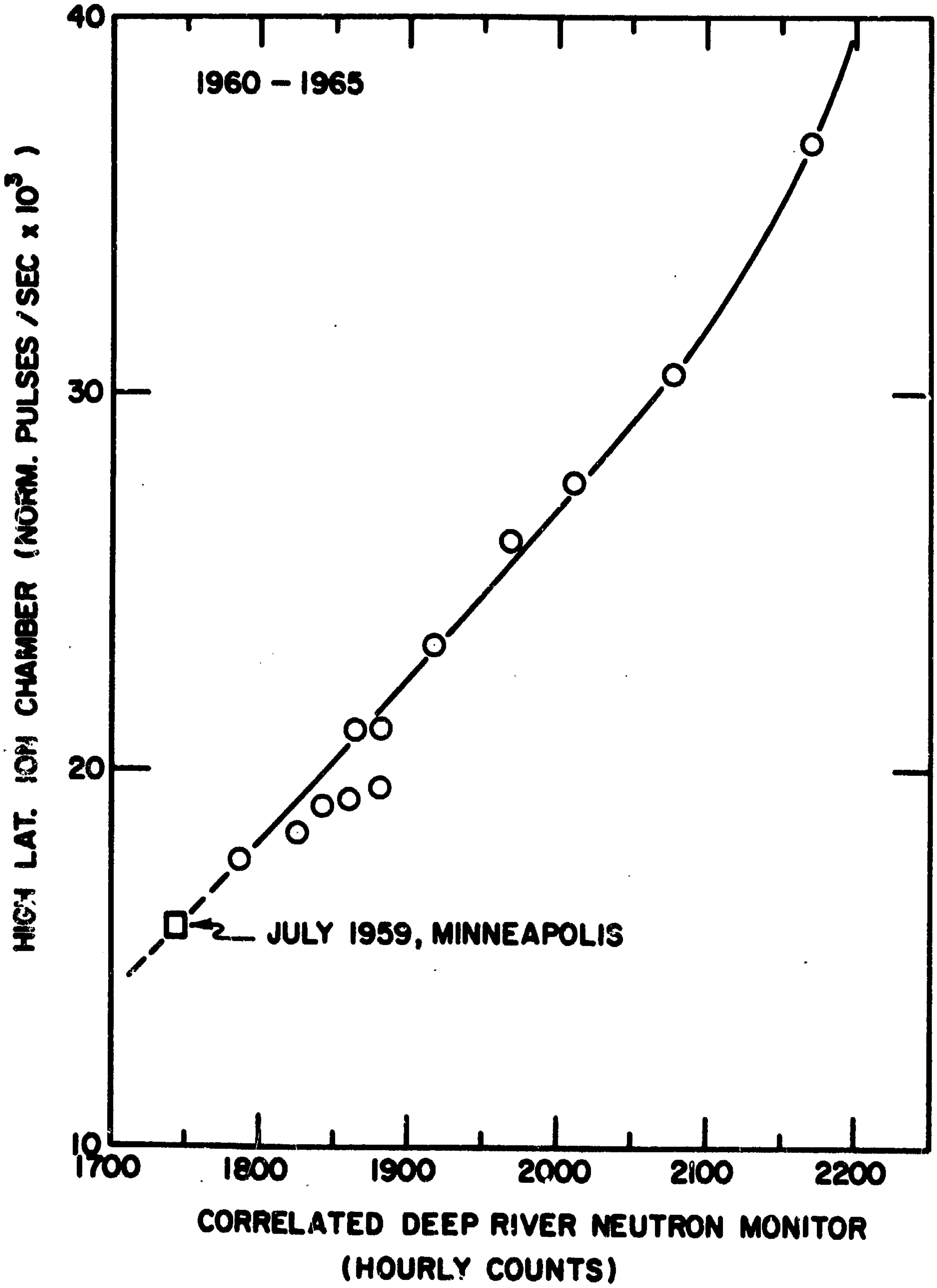
1960 - 1965
JULY 1959, MINNEAPOLIS
HIGH LAT. ION CHAMBER (NORM. PULSES / SEC x 10^3)
CORRELATED DEEP RIVER NEUTRON MONITOR
(HOURLY COUNTS)
40
30
20
10
1700
1800
1900
2000
2100
2200

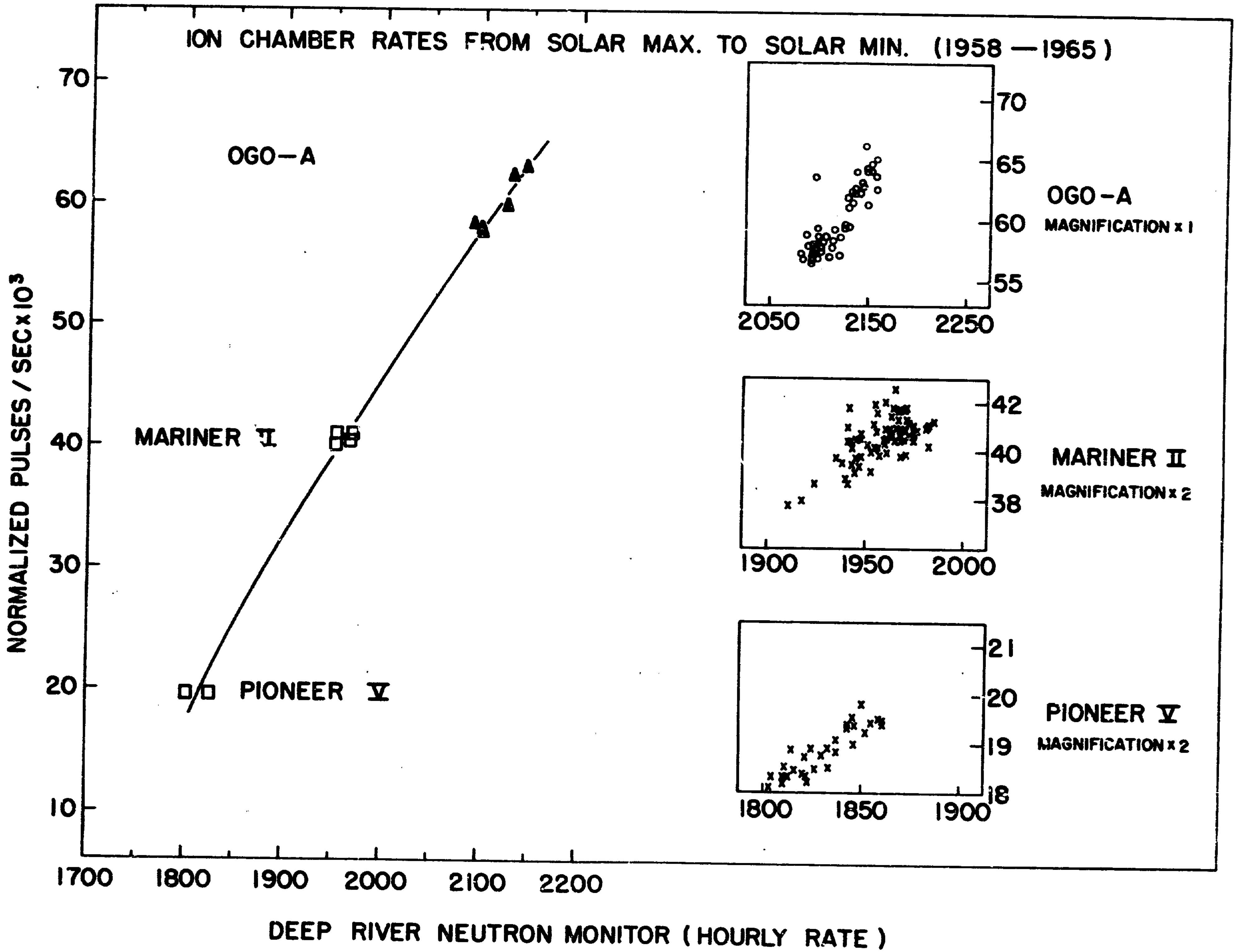
ION CHAMBER RATES FROM SOLAR MAX. TO SOLAR MIN. (1958 — 1965)
OGO-A
MARINER II
PIONEER V
NORMALIZED PULSES / SEC x 10³
DEEP RIVER NEUTRON MONITOR (HOURLY RATE)
70
60
50
40
30
20
10
1700
1800
1900
2000
2100
2200
OGO-A
MAGNIFICATION x 1
70
65
60
55
2050
2150
2250
MARINER II
MAGNIFICATION x 2
42
40
38
1900
1950
2000
PIONEER V
MAGNIFICATION x 2
21
20
19
18
1800
1850
1900

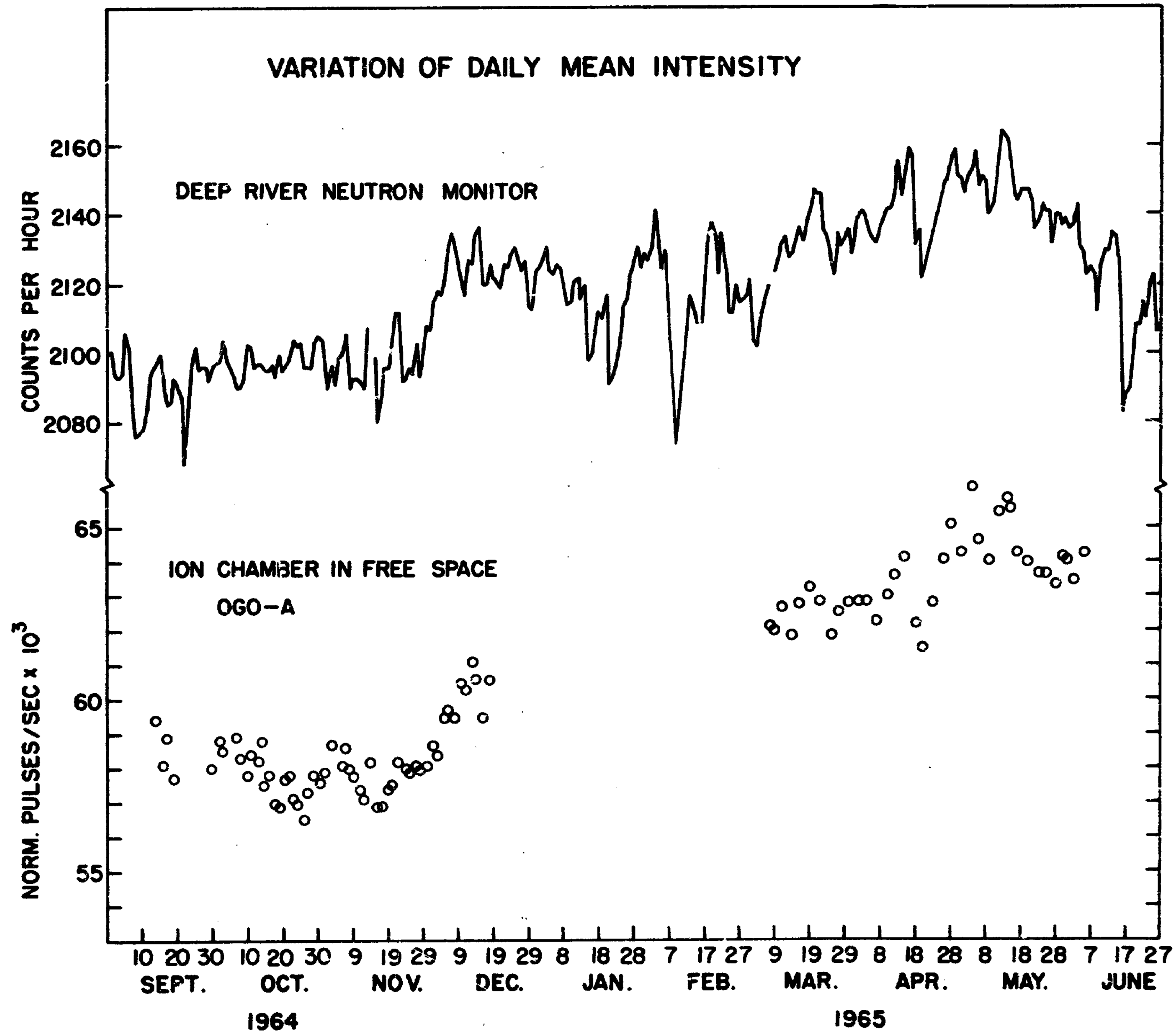

VARIATION OF DAILY MEAN INTENSITY
DEEP RIVER NEUTRON MONITOR
COUNTS PER HOUR
2160
2140
2120
2100
2080
ION CHAMBER IN FREE SPACE
OGO-A
NORM. PULSES/SEC x 10³
65
60
55
10 20 30 10 20 30 9 19 29 9 19 29 8 18 28 7 17 27 9 19 29 8 18 28 8 18 28 7 17 27
SEPT. OCT. NOV. DEC. JAN. FEB. MAR. APR. MAY. JUNE
1964
1965

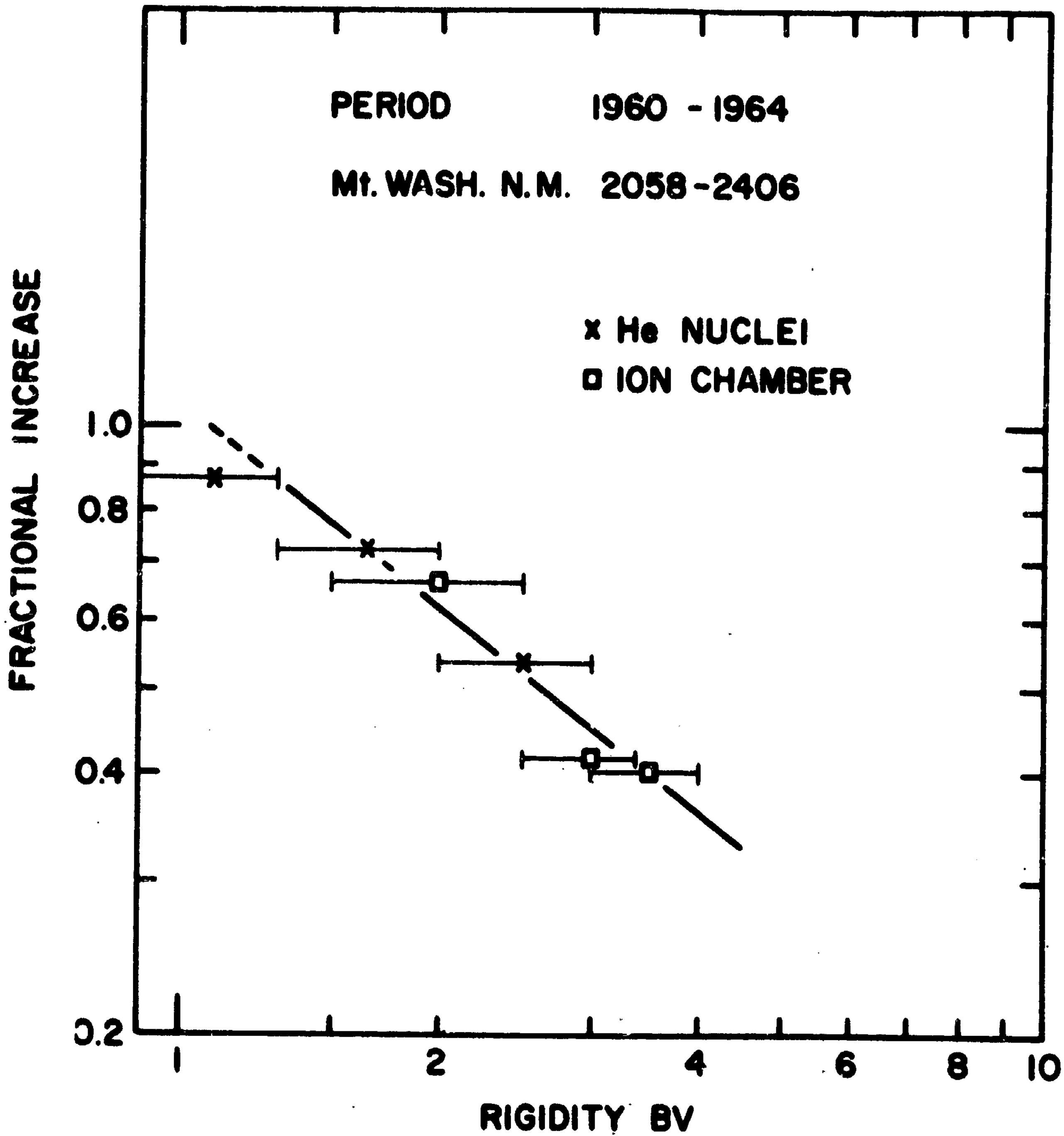

PERIOD 1960 - 1964
Mt. WASH. N.M. 2058-2406
x He NUCLEI
□ ION CHAMBER
FRACTIONAL INCREASE
1.0
0.8
0.6
0.4
0.2
1
2
4
6
8
10
RIGIDITY BV

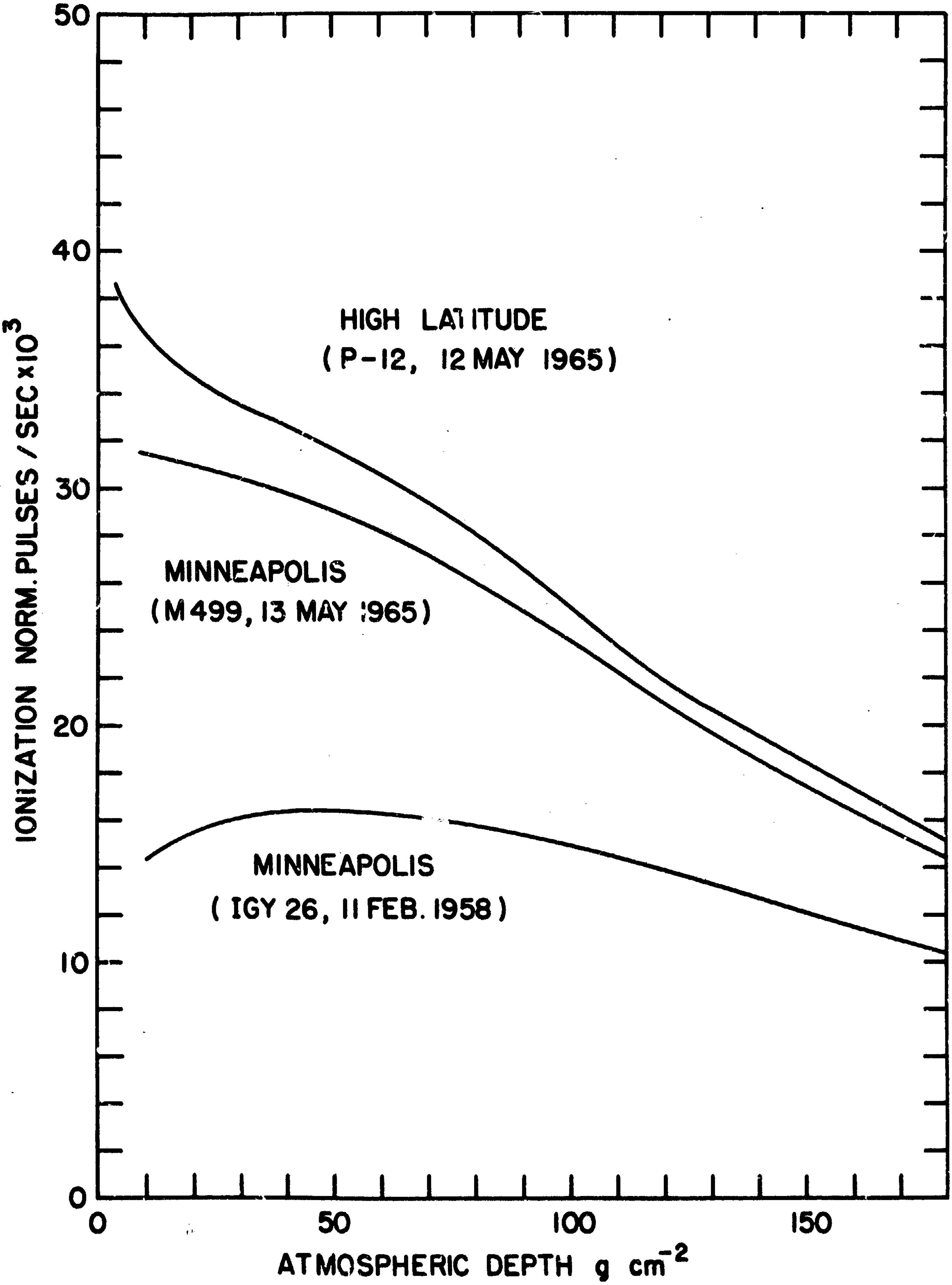

HIGH LATITUDE
(P-12, 12 MAY 1965)
MINNEAPOLIS
(M499, 13 MAY 1965)
MINNEAPOLIS
(IGY 26, 11 FEB. 1958)
IONIZATION NORM. PULSES / SEC x 10^3
ATMOSPHERIC DEPTH g cm^-2
0
10
20
30
40
50
0
50
100
150

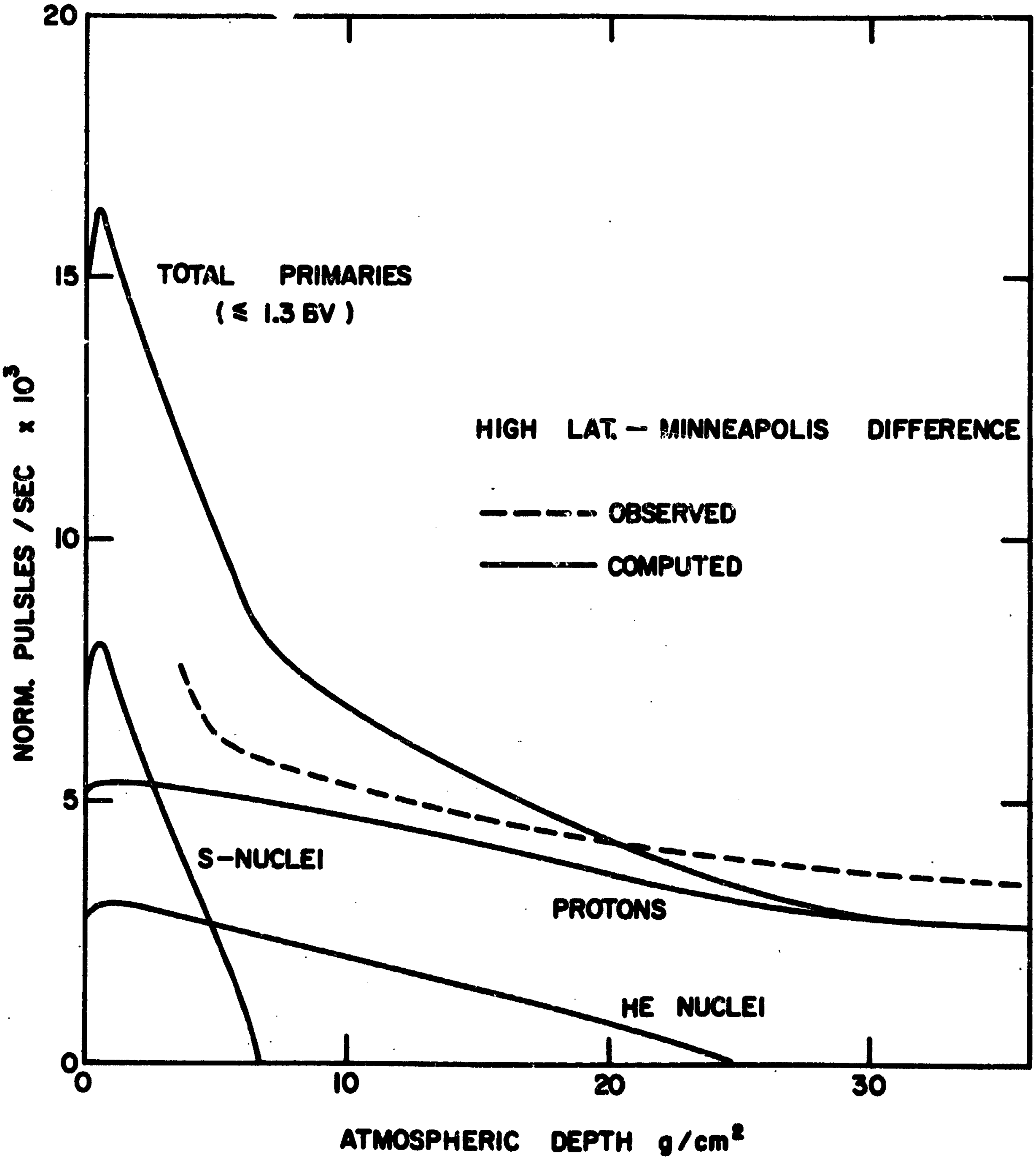

20
15
10
5
0
0
10
20
30
NORM. PULSLES / SEC x 10^3
ATMOSPHERIC DEPTH g/cm²
TOTAL PRIMARIES
(≤ 1.3 BV)
HIGH LAT. — MINNEAPOLIS DIFFERENCE
OBSERVED
COMPUTED
S-NUCLEI
PROTONS
HE NUCLEI

BLANK PAGE

N66-13357

Measurement of the Isotopic Composition of Helium Nuclei in the Primary Cosmic Radiation in the Energy Interval 80 - 150 Mev/nucleon*

D. J. Hofmann and J. R. Winckler

ABSTRACT

11357

A dE/dX - E scintillation counter device was flown at high altitude over Barrow, Alaska for a period of about 30 hours on 12 May 1965, a time of absolute solar minimum. The detector was capable of resolving protons, deuterons, He^3 and He^4 nuclei. In this paper, only the helium nuclei results will be discussed. Energy and rigidity spectra are extracted for He^3 and He^4 taken separately. The ratio He^3/He^3+He^4 is found to be constant over the energy interval 80-150 Mev/nucleon with a value of 0.19 ± 0.05 and in terms of rigidity, the ratio is found to be 0.39 ± 0.09 at .8 Bv. The relation of these ratios to the solar modulation is discussed.

author

* This work was supported by a grant from the Atmospheric Sciences Section of the National Science Foundation.

On May 12, 1965, a dE/dX - E scintillation counter device was launched on a balloon from Barrow, Alaska (69.5° N geomagnetic lat.) as a part of the IQSY polar circling balloon (POCIBO) project. Total flight time was about 31 hours with 26 hours of good data between 3.5 and 4.5 g/cm^2 atmospheric depth. On this date the Deep River neutron monitor and the OGO-A ionization chamber in free space† indicated the highest counting rate during the current solar cycle. Thus the flight was made at absolute solar minimum in terms of particle influx. During the flight, the detector measured the spectrum of protons from 10 - 128 Mev at the detector, and helium nuclei from 25 - 100 Mev/nucleon at the detector. The inherent mass resolution of the detector and the increased amount of data gathered (220 helium nuclei), compared with previous balloon measurements, permits the energy spectrums of the two resolved isotopes He^3 and He^4 to be evaluated separately and thus to examine for the first time, the dependence of the ratio He^3/He^3+He^4 on energy and rigidity.

Figure 1 is a two-dimensional pulse height distribution from the dE/dX - E scintillation counters showing all events in the low gain helium mode during 26 hours of the flight. The smooth curves are the theoretical positions of the He^3 and He^4 lines. Background due to nuclear interactions in the crystals is only a serious problem below 100 Mev total kinetic energy and this data has been excluded from the analysis. Data in the region >25 Mev/nucleon from the 26 hours is shown as a mass histogram in figure 2. Also shown are Gaussian distributions with 10% half-widths, the estimated resolution of the dE/dX scintillator for particles of this energy. Figures 3 and 4 show the differential energy/nucleon and rigidity spectrums of the He^3 and He^4 components taken separately and grouped together and treated as He^4. The data has been extrapolated to 0 gm/cm^2 using appropriate range energy data for the two species and the only flux correction amounted to an 8% increase due to atmospheric absorption and production by heavier nuclei, using the data of Freier and Waddington (1965). Thus the errors indicated in the figures are purely statistical. Also given in figures 3 and 4 are the ratios He^3/He^3+He^4 in terms of energy/nucleon. Over the interval from 80 - 150 Mev/nucleon, the ratio appears to be constant with energy/nucleon, having a value of .19 with a statistical deviation of $\pm$ .05 at any one energy/nucleon and $\pm$ .035 if all particles are grouped together. The rigidity spectrums overlap around .8 Bv giving a ratio of .39 $\pm$ .09 and the shape of the spectrums suggest that the ratio increases with decreasing rigidity and may be as high as .5 at .4 - .5 Bv.

The He^3/He^3+He^4 ratio measured at the earth is dependent on the cosmic ray source spectrum, interstellar fragmentation of He^4 and heavier nuclei, propagational effects such as energy loss by ionization in interstellar hydrogen and acceleration or deceleration in interstellar magnetic fields, and local modulation by solar influences. The scarcity of He^3 in most stellar atmospheres implies that the major source of He^3 is spallation of He^4 and heavier nuclei in passing through interstellar hydrogen. It is of interest to note that mass spectrometer measurements of helium nuclei in a dozen iron meteorities revealed a mean He^3/He^3+He^4 ratio of .20 $\pm$ .03 (Signer and Nier, 1962). Since these data were obtained from the interiors of large meteorites, they are presumably insensitive to the primary cosmic ray abundances as the outer layers where such particles stop were burned away by passage through the atmosphere. This central concentration of He^3 is thought to be due mainly to high energy cosmic ray nucleons causing evaporation of iron nuclei. It is an observational fact that the relative abundance reported in our measurement is the same as that observed in the meteorites. A high velocity iron nucleus in the primary cosmic radiation striking an interstellar hydrogen atom constitutes the same process mentioned above for meteorites but viewed from a different reference frame. This process alone would produce the observed ratio of He^3/He^3+He^4. However, one must consider in detail the diffusion through interstellar space of all the nuclear species in the primary cosmic radiation. One is led to the requirement of He^4 in the source and this He^4 becomes a major contributor to the He^3 abundance. From several such diffusion calculations of the path length in interstellar hydrogen as a function of the ratio He^3/He^3+He^4, (Appa Rao, 1961; Foster and Mulvey, 1963; Dahanayake et al, 1964) and using our measured ratio at solar minimum, we estimate the path length to be 6.5 ± 1.5 gm/cm^2 in the energy range 80 - 150 Mev/nucleon. The interpretation of this value must be qualified by the possible effects of solar modulation. The only available measurements at other times in the solar cycle are those of Dahanayake et al (1964) who, utilizing emulsions, found a ratio of $.18 \pm .05$ in the energy interval 160 - 370 Mev/nucleon at high latitude in 1962, and Hildebrand et al (1963) report a ratio of only $.06 \pm .03$ in the energy interval 255 - 360 Mev/nucleon in 1961. Since considerable discrepancies appear to exist between these measurements and because the energy range is higher, little can be said about the energy dependence or solar modulation dependence of the ratio by a comparison of these values with those reported here. One might expect the ratio at 80 - 150 Mev/nucleon in 1965 to be significantly higher than the ratio at 160 - 370 Mev/nucleon in 1962 because (1) The path length in interstellar hydrogen may be energy dependent, causing the ratio at lower energy to be higher. (2) Most theories of solar modulation predict a maximum in the ratio at solar minimum. From our data alone we note that the observed energy/nucleon spectrum of He^3 is similar to that of He^4, and that the measurement was made as close as possible to solar minimum in terms of particle influx. Neglecting spectral changes due to energy loss or gain processes in the interstellar medium, one would expect the energy/nucleon spectrum of the two species to be similar in the near interstellar space free from solar modulation. Since the spectrums also appear similar near the earth, one concludes that at solar minimum, the modulation has little effect on the observed He^3/He^3+He^4 ratio and it is thus probably close to the interstellar value in this energy interval.

ACKNOWLEDGEMENTS

The authors wish to express their gratitude to Ralph Fuchs, John Nitardy, Mike Weed, Darwin Throne, Glenn Gerdin, Roy Lahti and Jim Adelmann for their able assistance during this phase of the project. The POCIBO program owes much to Dr. Max Britton and the Geography Branch of the Office of Naval Research for arranging the very effective support provided by the Arctic Research Laboratory in Barrow, Alaska, and to Dr. Robert Fleischer, Director of IQSY programs for the National Science Foundation. Also, we are grateful to Professor George Swenson of the Department of Electrical Engineering, University of Illinois, for construction of the 70 K.C. receivers, site surveys and advice on D. F. problems.

FIGURE CAPTIONS

Figure 1 Pulse height distribution of the energy lost in the dE/dX crystal (ΔE) plotted versus the energy lost in the E crystal ($E - \Delta E$) in the low gain helium mode. Smooth curves are the theoretical He^3 and He^4 lines. Scattering of points below 100 Mev is due to nuclear interaction background.

Figure 2 Mass histogram taken perpendicular to the helium lines between 1.5 and 5.5 mass units and $E > 25$ Mev/nucleon. Gaussian distributions superimposed were calculated for 10% half-widths as estimated for the resolution of the dE/dX scintillator.

Figure 3 Differential energy/nucleon spectrums extrapolated to the top of the atmosphere for He^3, He^4 and the two taken together and treated as He^4.

Figure 4 Differential rigidity spectrums extrapolated to the top of the atmosphere for He^3, He^4, and the two taken together and treated as He^4.

REFERENCES

M. V. K. Appa Rao, Phys. Rev. 123, 295 (1961).

M. V. K. Appa Rao, J. Geophys. Res. 67,1289 (1962).

M. V. K. Appa Rao, C. Dahanayake, M. F. Kaplon and P. J. Lavakare, Proc. Int. Cosmic Ray Conf., Jaipur 3, 95 (1963).

C. Dahanayake, M. F. Kaplon and P. J. Lavakare, J. Geophys. Res. 69, 3681 (1964).

F. Foster and J. H. Mulvey, Nuovo Cimento 27, 93 (1963).

P. S. Freier and C. J. Waddington, Space Science Reviews 4, 313 (1965).

P. Signer and A. O. C. Nier, Researches on Meteorites, John Wiley and Sons, Inc. New York (1962).

B. Hildebrand, F. W. O'Dell, M. M. Shapiro, R. Silberberg, and B. Stiller, Proc. Int. Cosmic Ray Conf., Jaipur 3, 101 (1963).

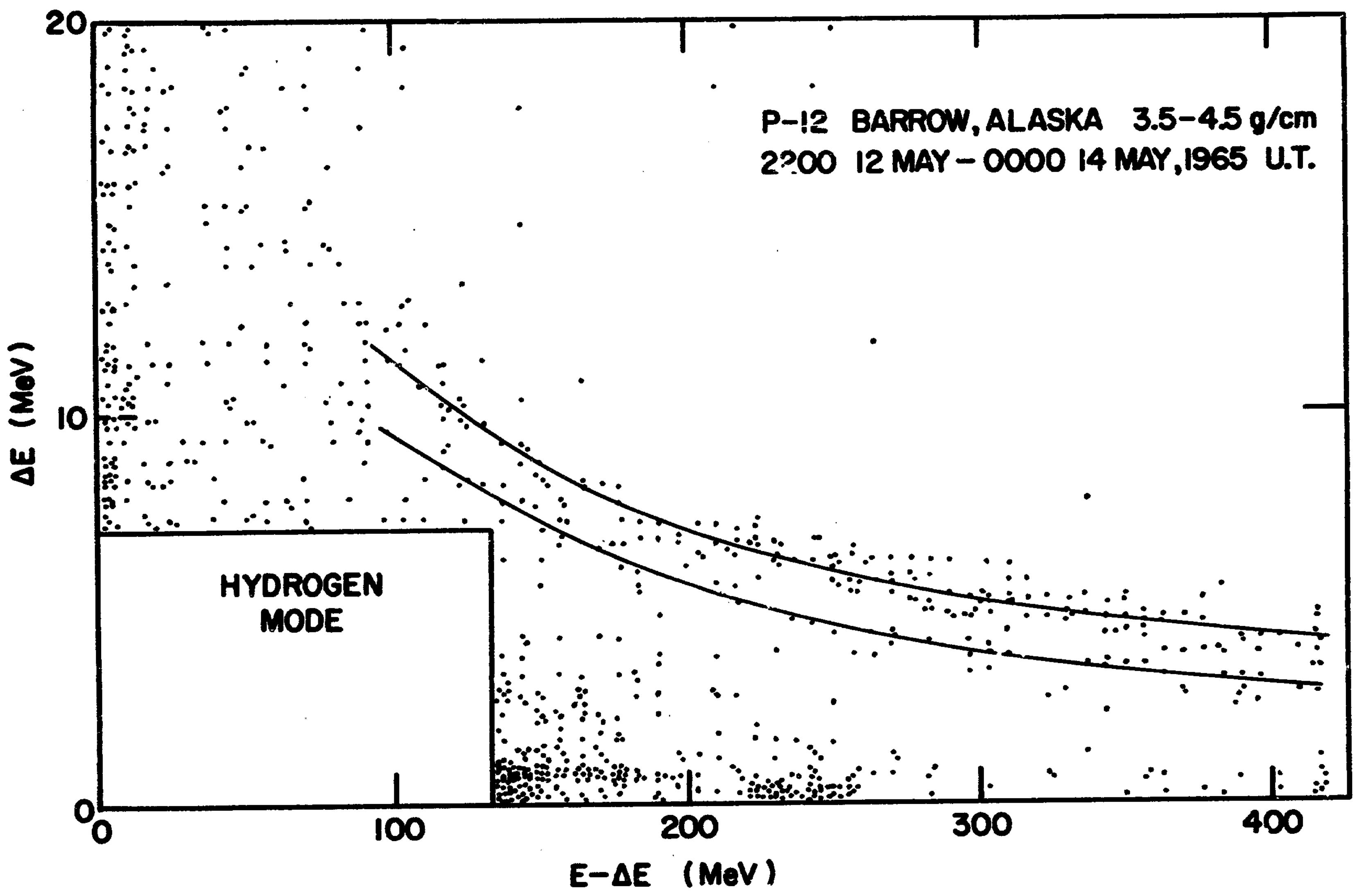
P-12 BARROW, ALASKA 3.5-4.5 g/cm
2200 12 MAY - 0000 14 MAY, 1965 U.T.
HYDROGEN
MODE
ΔE (MeV)
E-ΔE (MeV)
20
10
0
0
100
200
300
400

Fig. 1

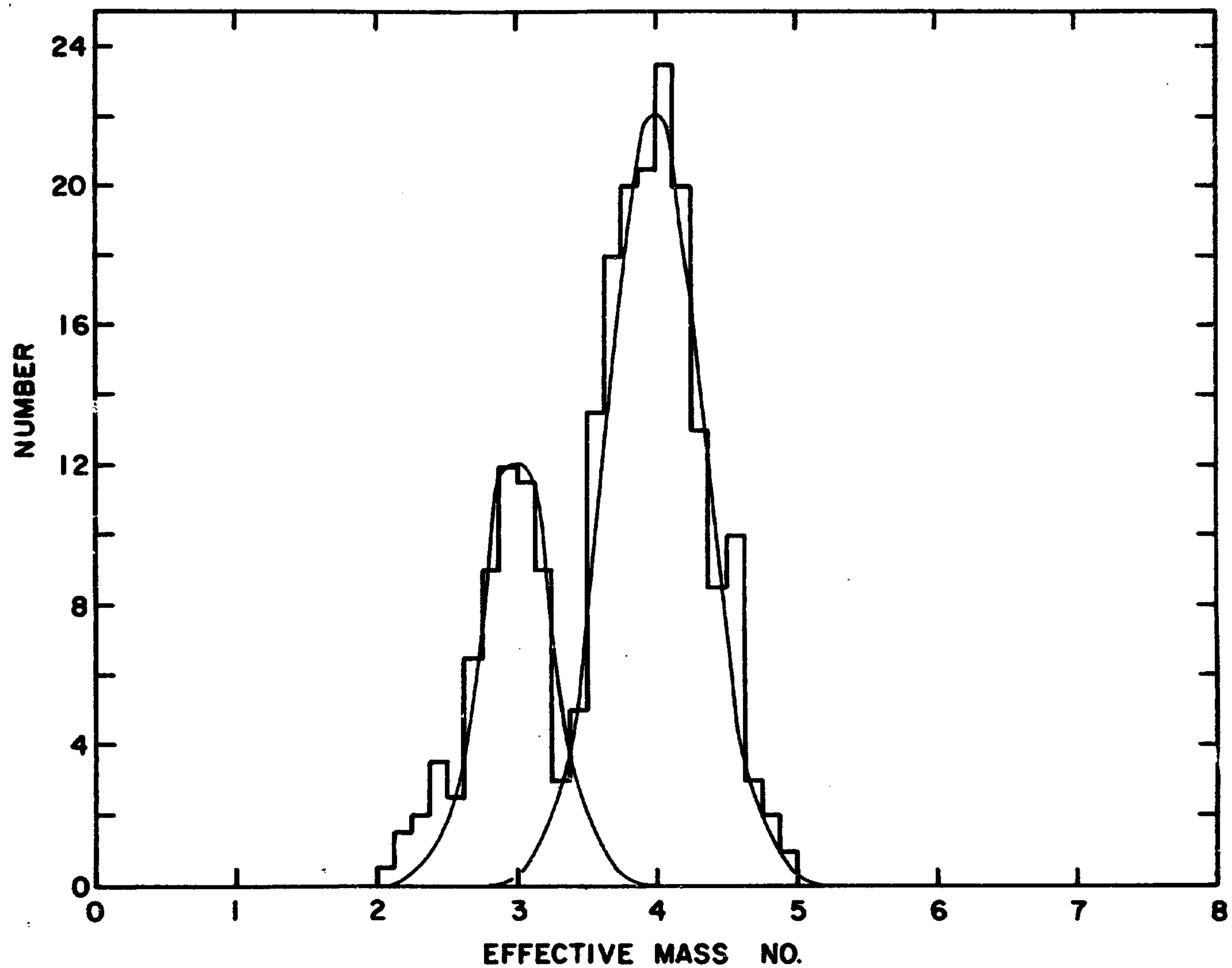

Fig. 2

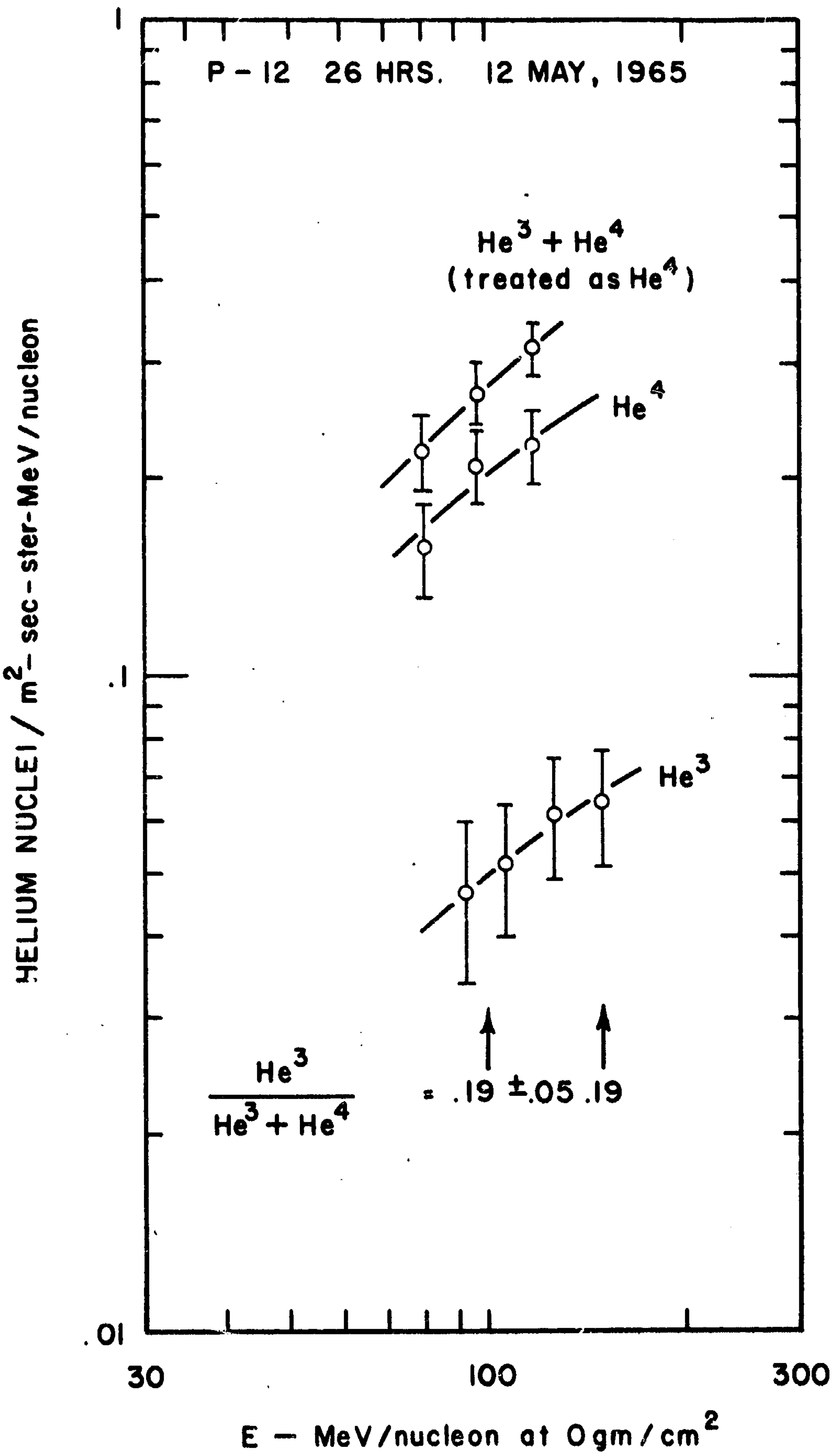

P - 12 26 HRS. 12 MAY, 1965
He3 + He4
(treated as He4)
He4
He3
He3 / He3 + He4
= .19 ±.05 .19
1
.1
.01
30
100
300
HELIUM NUCLEI / m2 - sec - ster - MeV / nucleon
E — MeV/nucleon at 0 gm/cm2

Fig. 3

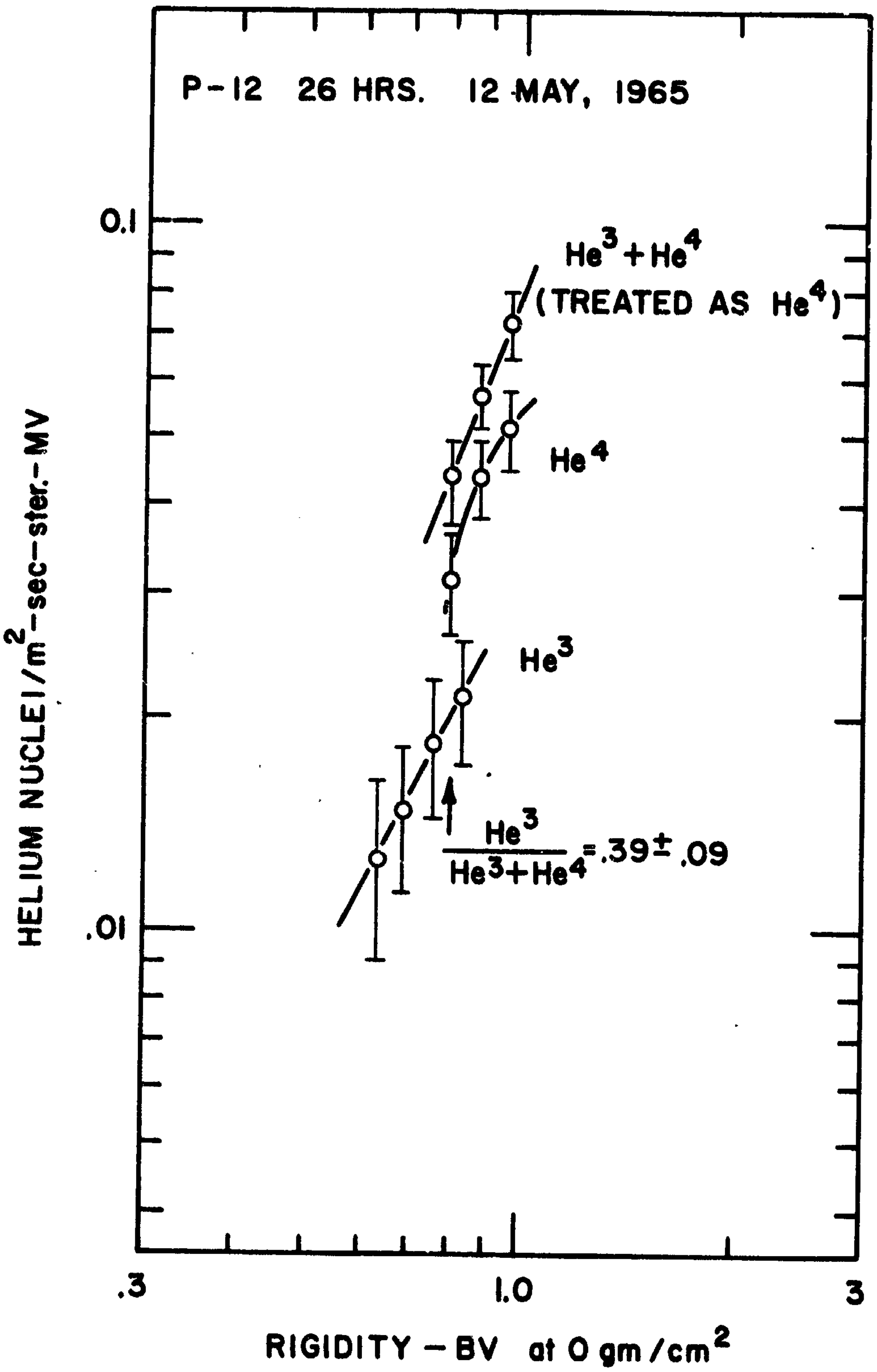

P-12 26 HRS. 12 MAY, 1965
0.1
.01
HELIUM NUCLEI/m²-sec-ster.-MV
He³+He⁴
(TREATED AS He⁴)
He⁴
He³
He³/(He³+He⁴) = .39 ± .09
.3
1.0
3
RIGIDITY – BV at 0 gm/cm²

Fig. 4

BLANK PAGE

N 66-13358

Measurements of the Primary Proton and Helium Spectra and Their Modulations Using a Balloon Borne Cerenkov-Scintillation Counter *

J. F. Ormes and W. R. Webber

13358

ABSTRACT

During the years 1963-1965, the spectra of protons and helium nuclei have been studied on eleven flights at seven geomagnetic latitudes using a modified version of the Cerenkov-scintillation counter. The flights attained depths of 2-6 g/cm^2 which coupled with the detector's large geometry factor (~50 st cm^2) enabled details of the helium intensity, and the different contributions, primary and secondary, to the singly charged distribution to be evaluated as a function of atmospheric depth. These results demonstrate that it is necessary to know in detail the contribution of all non-primary components, particularly at the lower energies, before a spectrum of primary protons can be determined. The spectra of primary protons and helium nuclei measured on these flights are presented. These spectra cover the range from ~0.6-16 Bv rigidity. Our results indicate that the lowest energy protons have increased by more than 50% between 1963 and 1965. The proton spectrum is almost flat down to 0.5 Bv in 1965, but the helium spectrum is falling sharply at the corresponding rigidities. A study of the modulation of these two components during this period reveals that (1) the modulation depends approximately on 1/β for $0.45 \leq \beta \leq 0.85$ for both components, and (2) at the same velocity, the modulation for protons is $\gtrsim 2$ x that for helium nuclei.

author

*Supported under NASA Research Grant NsG 281-62.

During the past two years eleven balloon flights have been made with a Cerenkov-scintillation telescope by the University of Minnesota group. The detector measures the energy spectrum of the individual nuclei from Z = 1-26 over an energy range from 40-1000 Mev/Nuc. Relevant data pertaining to these flights is shown in Table I.

TABLE I

Data Pertaining to Balloon Flights
of Cerenkov-Scintillation counter

Location	P_c	Date	Alt. (g/cm^2)	Mt.Wash	Inst.
Churchill	0.2	8-1-63	4.0	2297	S
Churchill	0.2	7-11-65	1.9	2425	S
Churchill	0.2	6-25-65	3.2	2445	MS
Churchill	0.2	7-2-65	4.3	2440	LAS
Ely, Minn.	0.7	6-23-64	4.1	2418	S
Devils Lake, N.D.	1.0	11-11-63	6.8	2325	S
Minneapolis, Minn.	1.2	7-4-63	6.5	2320	S
Fayetteville, Ark.	3.2	3-26-64	6.5	2378	S
Kerrville, Texas	5.6	3-29-65	5.5	2450	MS
Tucuman, Argentina	12.1	8-1- 64	5.5	2407	S
Tucuman, Argentina	12.1	8-9- 64	5.0	2410	RS

S= Standard detector
MS= Modified 3 element detector to additionally measure the low energy electron spectrum.
LAS= Large area version of standard detector with geometry factor=1000 st cm^2.
RS= Standard detector pointing at 60° to the vertical and rotating in azimuth once every 15 minutes.

The four flights at Churchill were made by outside contractors using very large plastic balloons, the remaining seven by the Minnesota group itself using 300 K or 600 K cubic ft. balloons to carry the total payload of 50 pounds to altitudes ranging from 4-6 g/cm^2. Our instrument is different than the usual Cerenkov-scintillation counter and although it has been described previously (Ormes and Webber, 1965), we would like to briefly review some of its salient features here. First, the so-called Cerenkov detector is actually a combination Lucite Cerenkov counter and plastic scintillation counter with the integrated light from both processes being viewed by a single 7" PM tube. The degree of separation of the different charge components and the ability to measure the low energy particles of different charges is determined essentially by the ratio of scintillator (S) light to Cerenkov (C) light -- the so-called S/C ratio. We have used a ratio of 0.6 in all standard flights. The response of the telescope to particles of different charge, mass and energy is shown in Figure 1. Discrimination against multiple events is carried out by studying the PHD themselves rather than with an active anti-coincidence system. We believe that this approach is superior for a telescope as large as ours where one can apply statistical methods to the analysis of the data. Furthermore, the material in and around the telescope is kept to a minimum.

Perhaps the most important feature of the detector is, however, its large geometry factor of ~50 st cm^2. This is a factor of 10-100 x that of comparable detectors flown in balloons. This large geometry factor is achieved without loss in resolution by a careful selection of components.

The flight data is d' ided into 5-10 minute intervals during the ascent and appropriate longer intervals while the balloon is at altitude. This means that the absorption of helium nuclei can be obtained as a function of altitude. The development of low energy protons can also be studied as a function of altitude -- a most important input for the separation of low energy primary and secondary protons at high latitude and high altitude. Although this data is available it will not be presented here.

During the course of a typical four hour flight at high latitude, a total of ~20,000 helium nuclei are observed. Each differential interval for helium nuclei will thus contain about 1000 counts. Unlike other detectors statistical uncertainties are not the most important source of error in the proton and helium differential spectra. For this reason, great care has been taken in the standardization of the instrumentation - both with regard to its physical properties and the analysis of the data.

The two largest sources of uncertainty in the analysis of the data are (1) the energy (or charge) calibration and (2) the identification of "true" counts as indicated by their being at the location in the PHD predicted by Figure (1) (e.g. the removal of "background" counts). (1) will be discussed in an accompanying paper on the heavier nuclei, where the energy or charge is a much more sensitive function of the known calibration of the instrument. The importance of (2) depends on the energy and charge being considered. For energies from 600-1200 Mev/Nuc for both protons and helium the pulses lie within the region of scatter of the symmetrical distributions of pulses from particles with energy > 1200 Mev/Nuc. Statistical methods are used to obtain the spectrum in this range and the accuracy varies according to how far into the symmetrical minimum ionizing distribution the pulses lie. The errors on the differential proton and helium intensities range from ~5% at the low energy end of this range to ~10% at the high energy end. The background in the proton distribution below 600 Mev runs between 20 and 40% of the true counts. Various subtraction processes and comparison with lower latitude date enable the true counts to be obtained and these counts separated into primary and secondary components. Errors on these differential points range from 3-5%. At the location where the proton and helium distributions cross, the helium nuclei dominate and the proton spectrum cannot be determined in the range 60 ± 15 Mev. The background in the helium distribution below 400 Mev runs between 10 and 25% of the true counts. Again various subtraction processes and comparison with lower latitude data enable the true counts to be obtained to an accuracy - the statistical accuracy. We estimate that the systematic errors on the integral and differential proton and helium intensities are ~ $\pm$ 3-6% for the whole series of flights; however, the relative errors when comparing individual flights are $\pm$ 2% when not limited by statistical errors. As a result the features of the modulation are defined somewhat more accurately than the spectrum itself and indeed we are able to observe statistically significant modulation effects at low energies for a 1% change in neutron monitor intensity.

The data is received in terms of a two dimensional 256 x 256 pulse height matrix with another bit signifying whether the individual pulse height should be multiplied by 8 or not. This gives a total dynamic range of 2048 in each dimension. The limits of computer storage permit the readout of only a 64 x 64 pulse height matrix, however, so it is necessary to examine the entire distribution by selecting various 64 x 64 matrices. In figure 2 we show a print-out of a matrix containing protons and relativistic helium for a typical flight.

The data we have obtained has been divided into two epochs -- one where the average Mt. Washington bihourly rate is 2320, the other where it is 2420, since a majority of flights were made at approximately these levels. Data from flights made at slightly different levels (mainly low latitude flights) have been corrected to these levels using the observed features of the modulation. The integral spectrum for protons is shown in Figure 3. The primary proton intensities at 3.2, 5.6, 10.2, 12.1 and 15.7 Bv are determined from extrapolation of the growth curve for relativistic singly charged particles (effectively protons > 1200 Mev) to the top of the atmosphere, correcting for re-entrant albedo (electrons) and using the calculated geomagnetic cut-offs appropriate to the flight locations. These absorption curves are shown in Figure 4. Determination of this part of the proton spectrum is most difficult since none of the detectors in use discriminate against either or both of the relativistic secondary mesons and protons produced in the atmosphere above the detector as well as the re-entering electrons. Our results on the intensity of primary protons and on the growth of the relativistic particles are consistent with those measured earlier at similar latitudes by McDonald (1958) and Balasubrahmanyan et al (1962). A separate study shows that the primary proton intensities at high energies previously deduced from emulsion studies are probably underestimated relative to those obtained using Cerenkov-scintillators. It should be noted that the points at 10.1 and 15.7 Bv are obtained from extrapolation of the west and east pointing portions of the rotating flight. The point at 1.9 Bv represents the extrapolation of the relativistic particle distributions in the high latitude flights. The points below 1.9 Bv are obtained directly from the differential spectrum measured by the detector and corrected for secondary protons. This differential spectrum is shown in Figure 5 along with the differential intensities obtained by comparing the 1.9, 3.2 and 5.6 Bv integral points.

The integral spectrum for helium nuclei is shown in Figure 6. The intensities at 3.2, 5.6 and 12.1 Bv are determined from the extrapolation of the exponential growth curve of these nuclei in the atmosphere (MFP ~ 55 g/cm^2). The other points are obtained directly from the differential spectra measured by the detector. These differential intensities are shown in Figure 7 along with the differential intensity obtained by comparing the 3.2 and 5.6 Bv integral points. In the case of the helium nuclei, the differential and integral spectra obtained using the detector itself and the inferred geomagnetic cut-offs overlap, and are in good agreement.

The comparative spectra and the details of the modulation of protons and helium nuclei as deduced from this study will be discussed in an accompanying paper. We summarize these results here briefly as follows:

Modulation: (1) Depends approximately on $1/\beta$ for $0.45 \leq \beta \leq 0.85$ for both components and (2) at the same velocity, the modulation for protons is ~ 2 x that for helium nuclei.

Comparative spectra: (1) Ratio of proton to helium nuclei differential intensities (P/He) remains constant at a value ~ 8 as a function of rigidity between 2 and 16 Bv. Below 2 Bv, it increases rapidly. (2) P/He as a function of energy/nucleon varies continuously from a value ~ 5 at 200 Mev/Nuc to ~ 20 above 6 Mev/Nuc. In addition, this ratio is a function of the amount of modulation.

FIGURE CAPTIONS

Figure 1 The response of the Cerenkov-scintillator telescope to particles of different charge, mass and energy.

Figure 2 64 x 64 matrix for Fayetteville flight. S output on vertical axis - S+C on horizontal. Note helium in lower right hand corner and slow proton distribution (atmospheric secondaries) running diagonally to lower center of distribution. Numbers give n where each bin has between 2^n and 2^{n+1} counts.

Figure 3 Integral spectrum of primary protons at two levels of modulation.

Figure 4 Growth curves of relativistic particles measured on 4 flights at different latitudes.

Figure 5 Differential spectrum of primary protons at two levels of modulation.

Figure 6 Integral spectrum of primary helium nuclei at two levels of modulation.

Figure 7 Differential spectrum of primary Helium nuclei at two levels of modulation.

REFERENCES

Balasubrahmanyan, V. K., S. M. Canguli, G. S. Gokhale, N. K. Ras, P. K. Kunte, M. G. K. Menon and M. S. Summi, 1962, J. Phys. Soc. Japan, Suppl. A-III, 8.

McDonald, F. B. 1958, Phys. Rev., 109, 1367.

Ormes, J. F. and W. R. Webber, 1965, Phys. Rev. 138, 416.

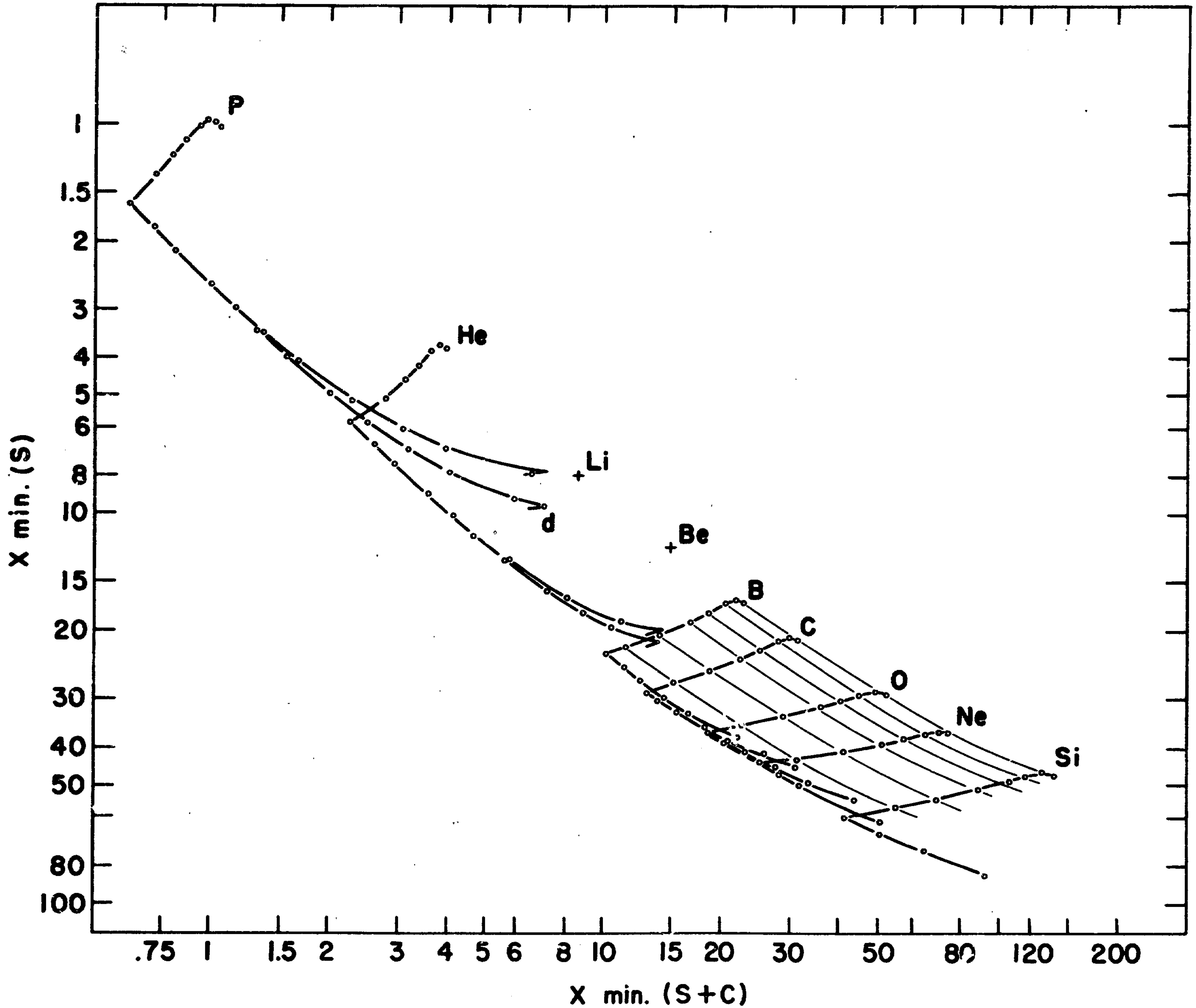
P
He
Li
d
Be
B
C
O
Ne
Si
X min. (S)
1
1.5
2
3
4
5
6
8
10
15
20
30
40
50
80
100
X min. (S+C)
.75
1
1.5
2
3
4
5
6
8
10
15
20
30
50
80
120
200

```
START TIME= 837   END TIME=1345
ALPHA  FAYETTVILLE                                                    RUN 11/6/65
 ELAPSED TIME=  17505  COUNTS LOST=   1433  NOISY  CTS =       0
  S=0  S+C=0 =       13 S=0 S+C NE 0=      33 S NE 0 S+C=0=     32
 TAPE ERRORS =       3
 160  IGNORED=      11 160   EDITED=     627 160 TIME EST=  17505
 PARITY ERRORS=       0  CHECKSUM    =-118008
   7777777777431407
              000   0000000000000000000000000000000000000000000000000000000000000000
              000   0000000011111111222222223333333344444444555555556666666677777777
              000   0123456701234567012345670123456701234567012345670123456701234567
              000
              001   0 0011 111122001001  1                            0    0 01
              002    10001112233200l    0 0      0                                  0
              003    13444445555444332331 00    10 1 011 0    101100     1  00 1    0
              004   0 5777666777766555444344433222313223122313221220012211 1000
              005     4666666676665553344333423332212221012211 00210111    1 11 211
              006   0046666666667665544434343232202222111210111011110001 02121020100
              007     46666656776655544333323332222210122112101010201O 101100021 1
              010   11567766778887665554344423322221212210011221121101211001l 110
              011   0057887789999887666554544442332212110221102120 2 1221222000121l
              012    1588888 9AAAA99877666554444433333322222332221212120122l 111110
              013   116899999AAAAA98877666555444443333332312222212210221311211101l
              014   016899899AAAAA98777666555544444333333222223333123212  211211110
              015     5899889AAAA988776665555444333322323222111211222012212201l200
              016   11588888999999877665554444443323322222221212 2222 0022111 1101 0
              017   015788888999887766554444343433221232211112210221121110011 1010
              020   0057777788888776655444334332232211220201021102111111 1    0 111
              021     5677777888776555443334332321l212 02111 1 11110021020 2110100
              022   0 467777777777655444433233211321111 121 201110010100 1 00 0011
              023   104677777777766544433333322222211212010001 11211 0 110111 0000
              024   003667777777766555343333332222112122121 001  210120 1  01001210
              025     36767676676665444333233333222000212 0100   12111 010100 00 121
              026    0356766666666554434333422332112l1 11 100    01111201001      0
              027     3566766666655533333333312122221110121001l 1 0000110 1   0 001
              030    03556666665555444333332233322120211 1101 01000010 001001 10
              031     1566666666554443322323232 22 22 00 1000012   0 11 0011 110 0
              032     356666666655543322323322112 20110 120 110001 012111 0   1 0 0
              033     14556666665554333332333222211 000001 1     20 1 1   0 1   0   01
              034     2455655555444443332322212221 010 0100 10 00011201020010101
              035     2545556565544433222212222131211l1   10 0 1   0 000   0 1
              036     14545555555443222212222 221020 0101      111   01 1 11   01002
              037      3545556554443322221121l0112000 0 00 1100 00        101000 000
              040     1444555555544332302 01 11220 1 100 1 10   00 100 0 120 0 1 000
              041     1344455555544323211222012011101 1   1 02 002 1110 2     10 0 0
              042     044444555545333221202111 01000 0 10 100001 011200111     01011
              043     2344445555344332221101112 1 0210 00022001   1110112 220200 001
              044     144433455555433322231011011010111     01 1     1010021    0   001
              045      34434445553432121110121   11 102 01 10 0111101 1 1012 00 0 1
              046     133344445444442312111101 00000   00 011100200212221222121022 2
              047     144433444554443233221200211l 12001 00111 22122232222212 0111
              050     02443444445443322231320211120l1 11   1121112223323222132222l1
              051     13334344444444333321322220201l0100 2022112222333333223232222 2
              052     123324344444443333220222 01 10101221 021232213422333334332232 2
              053     13433444443443 33232222221201111201211222334344433332332332
              054      33433444453434432322222122012211102213333233333444332233223
              055     0234444443344443342212 0121  221122212222333344444433343333222
              056     034443343444344443232223002221130022223333443445444434332323
              057     03343434333443332323223221222121221332333443444444434323232
              060     1333344444344433343333222111111 1212233233334344334443434 32233
              061     134444444444334334233213222212112212023333344343334443423222232
              062     123244444443333334333232221202211222223333334343 44332323333 2111
              063     123344333334323333333232112 02 01222323222334334332443333 3212
              064     133344333333323233333232221221212222321133333333443333 4331321223
              065     13444433442233333332323 21  012112213323333333332433223223210
              066    013343343434333222 333323122  01111223134313323344332 3323322210
              067     12333333333222222323332212221  0 2111312323222333333322l2012111
              070      23333343332233232333222111100108221333223222333332321211011
              071     0243233323232321222222112211002211111121223122122321122 01201
              072     133332232233310022322030211122022 221132221232123220 2  2 0 1
              073     033332234332331222323222211112101020113121322312121231 0 1012
              074      23333323333122212222221221310210210210210220211220200 02 010
              075     023321333222221222232222232200 1110122201222121113111120 0
              076     023312232332223130222233211220 20 111100111 211101122  100 11
              077
 START TIME= 837   END TIME=1345
```

Figure 2

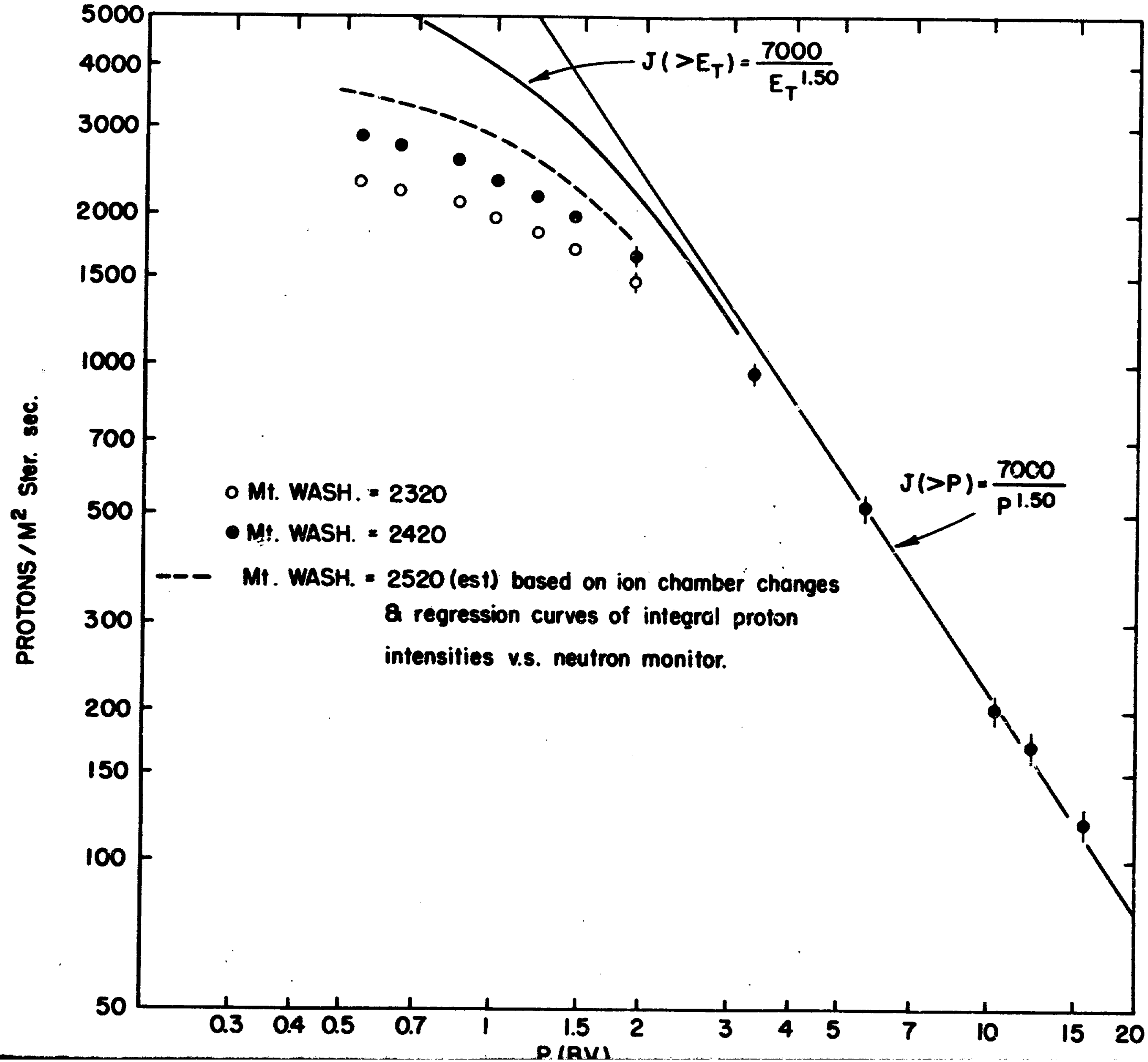

$J(>E_T) = \frac{7000}{E_T^{1.50}}$
$J(>P) = \frac{7000}{P^{1.50}}$
o Mt. WASH. = 2320
● Mt. WASH. = 2420
Mt. WASH. = 2520 (est) based on ion chamber changes & regression curves of integral proton intensities v.s. neutron monitor.
PROTONS / M² Ster. sec.
5000
4000
3000
2000
1500
1000
700
500
300
200
150
100
50
0.3
0.4
0.5
0.7
1
1.5
2
3
4
5
7
10
15
20
P (BV)

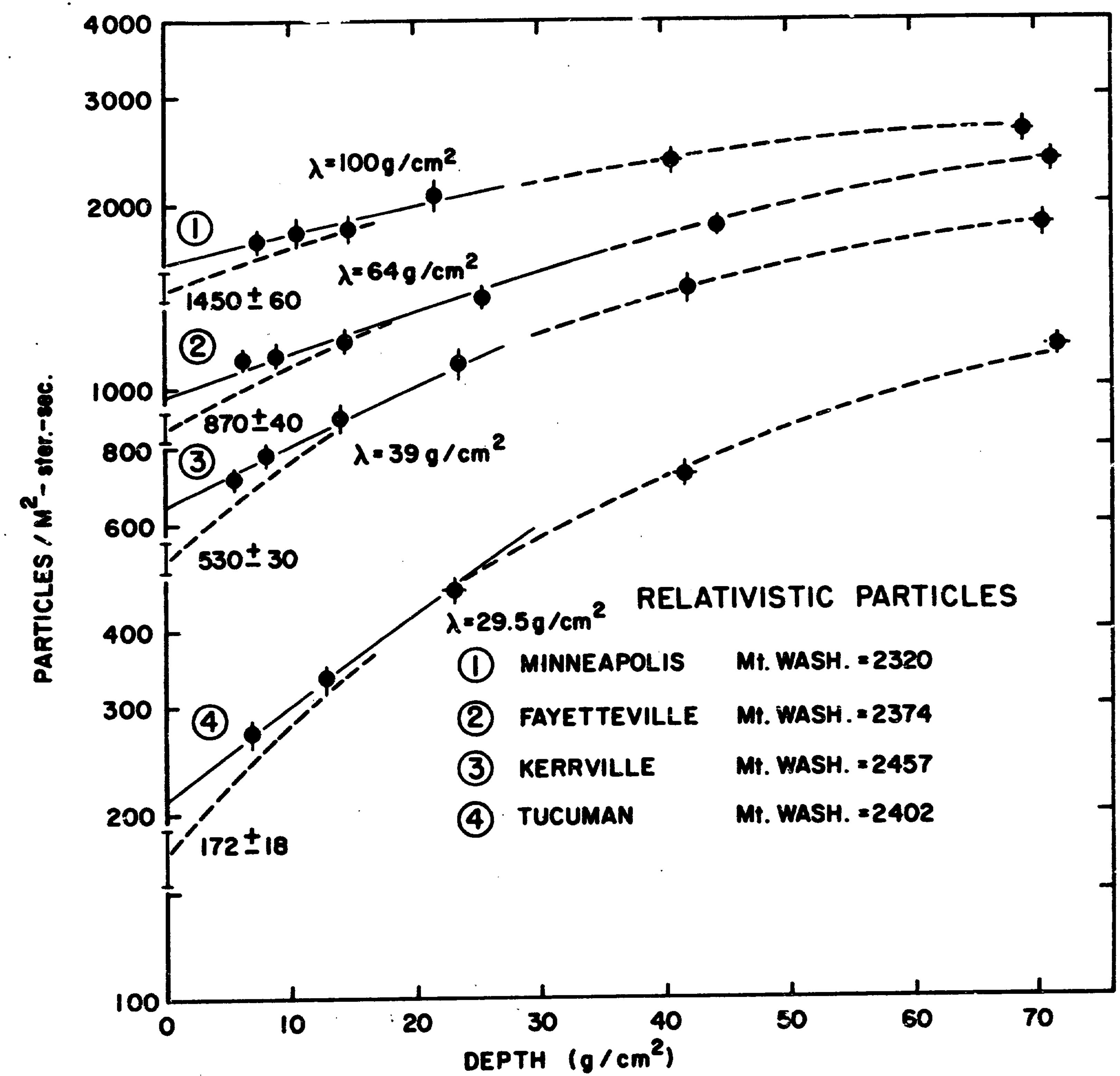

RELATIVISTIC PARTICLES
λ=100g/cm²
λ=64g/cm²
λ=39g/cm²
λ=29.5g/cm²
1450±60
870±40
530±30
172±18
① MINNEAPOLIS Mt. WASH. =2320
② FAYETTEVILLE Mt. WASH. =2374
③ KERRVILLE Mt. WASH. =2457
④ TUCUMAN Mt. WASH. =2402
PARTICLES / M² - ster.-sec.
DEPTH (g/cm²)

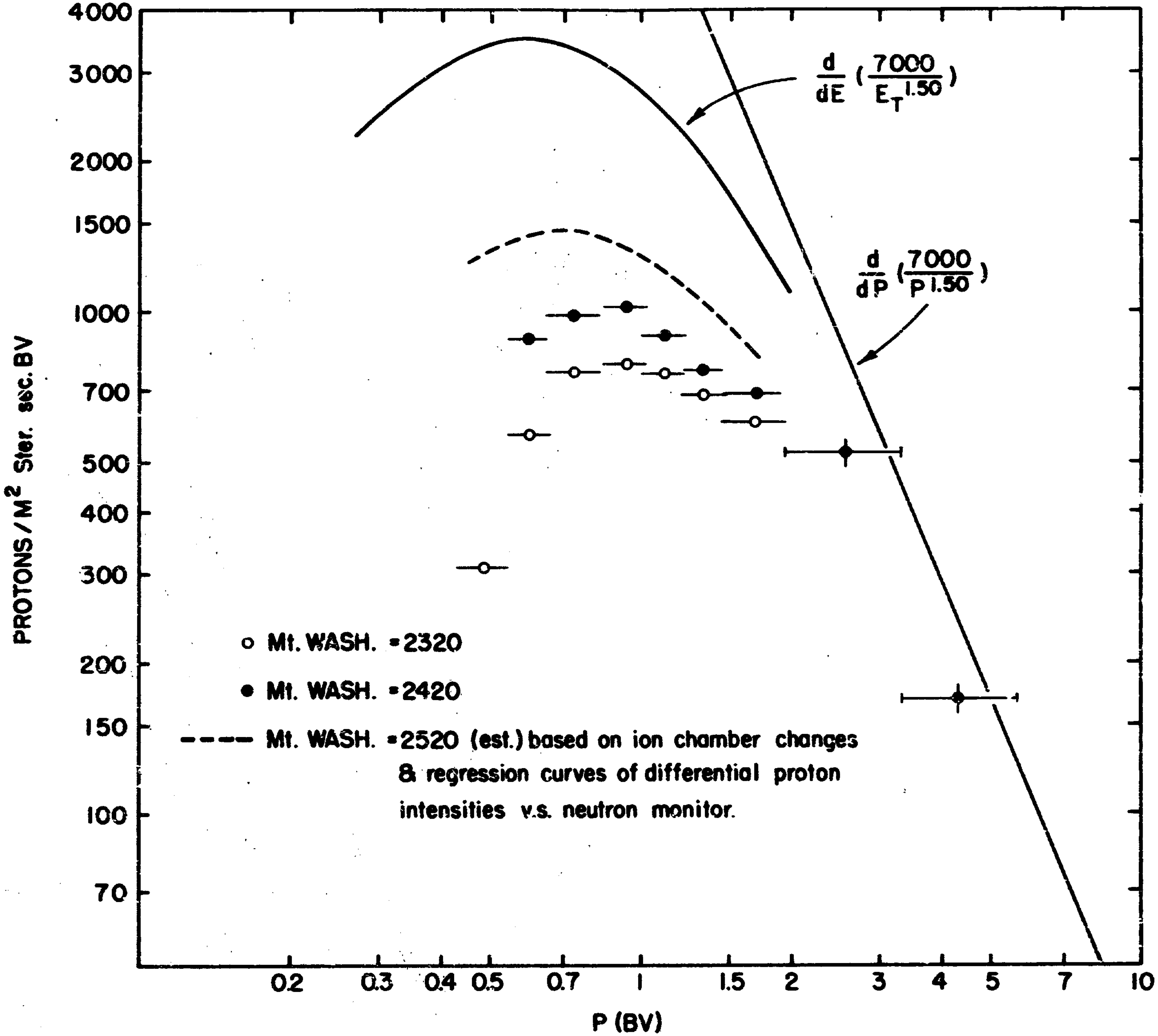

PROTONS / M² Ster. sec. BV
4000
3000
2000
1500
1000
700
500
400
300
200
150
100
70
0.2
0.3
0.4
0.5
0.7
1
1.5
2
3
4
5
7
10
P (BV)
$\frac{d}{dE}\left(\frac{7000}{E_T^{1.50}}\right)$
$\frac{d}{dP}\left(\frac{7000}{P^{1.50}}\right)$
○ Mt. WASH. =2320
● Mt. WASH. =2420
Mt. WASH. =2520 (est.) based on ion chamber changes
& regression curves of differential proton
intensities v.s. neutron monitor.

Figure 5

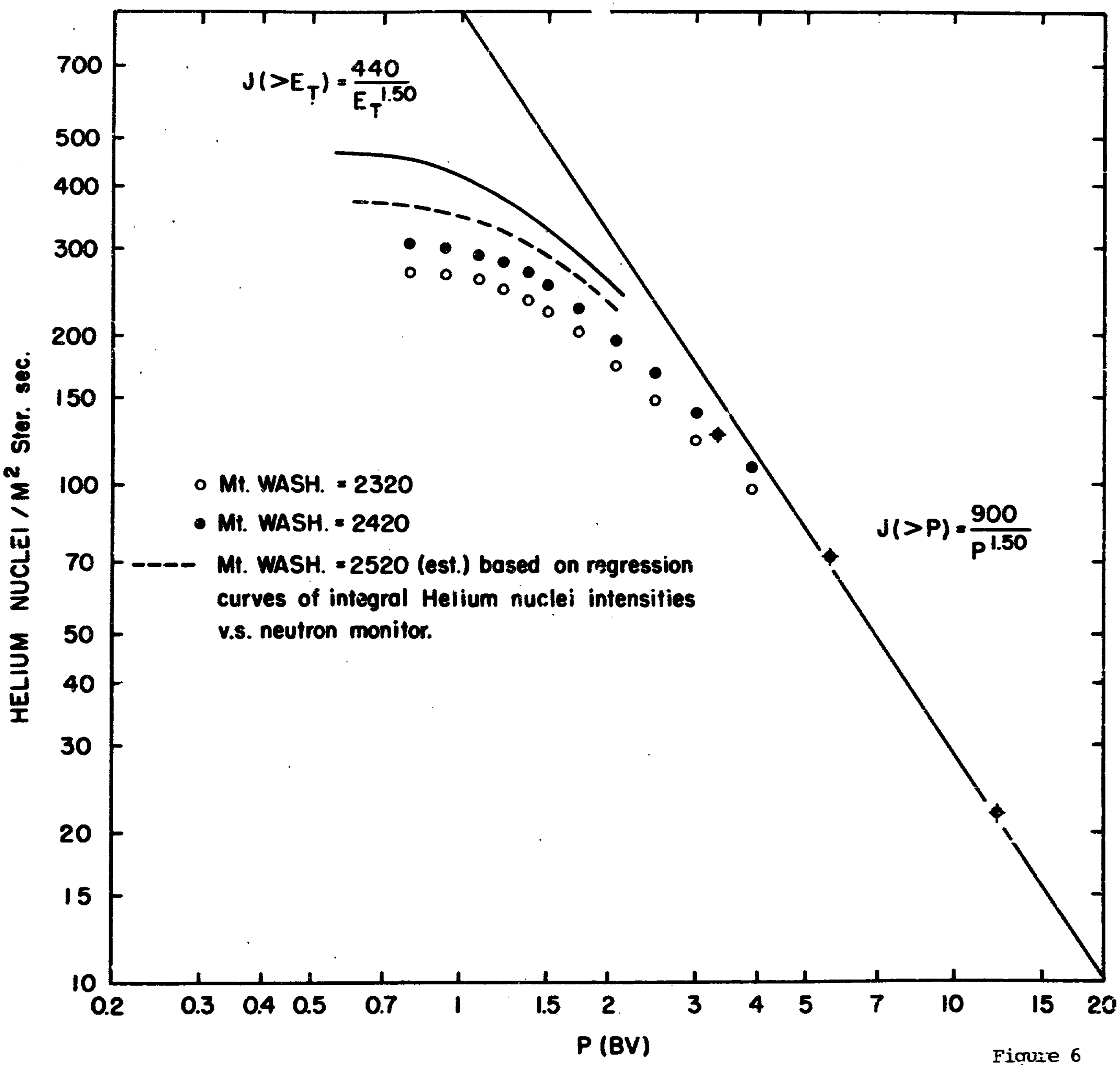

HELIUM NUCLEI / M² Ster. sec.
700
500
400
300
200
150
100
70
50
40
30
20
15
10
0.2
0.3
0.4
0.5
0.7
1
1.5
2
3
4
5
7
10
15
20
P (BV)
J(>E_T) = 440 / E_T^1.50
J(>P) = 900 / P^1.50
Mt. WASH. = 2320
Mt. WASH. = 2420
Mt. WASH. = 2520 (est.) based on regression curves of integral Helium nuclei intensities v.s. neutron monitor.

Figure 6

BLANK PAGE

N66-13359

Some Implications of the Relative Spectra of the Different Charge Components in the Primary Radiation*

W. R. Webber

13359

ABSTRACT

In accompanying papers we have presented the differential spectra of the individual charge components -- protons through heavy nuclei -- measured at different levels of solar modulation from 1963-1965. Utilizing the fact that the solar modulation affects particles of different charge to mass ratio in such a way that the ratio of intensities in differential rigidity intervals are not changed, we are able to compare the relative spectra prior to solar modulation. This comparison suggests the following: (1) The relative spectra of protons and helium nuclei are most reasonably interpreted in terms of identical rigidity spectra at the "source" rather than energy/nucleon spectra. The large increase in P/He (P) ratio at low rigidities may in large part be due to production of secondary protons as well as ionization loss in the interstellar medium. (2) The variation of the P/He, L/H and He/N ratios with energy can be interpreted in terms of ionization loss of the primary radiation moving through an amount of material which monotonically decreases with increasing energy. (3) The spectra of heavy nuclei above 3 Bv systematically become steeper with increasing charge.

Author

*Work supported under NASA Research Grant No. NsG 281-62.

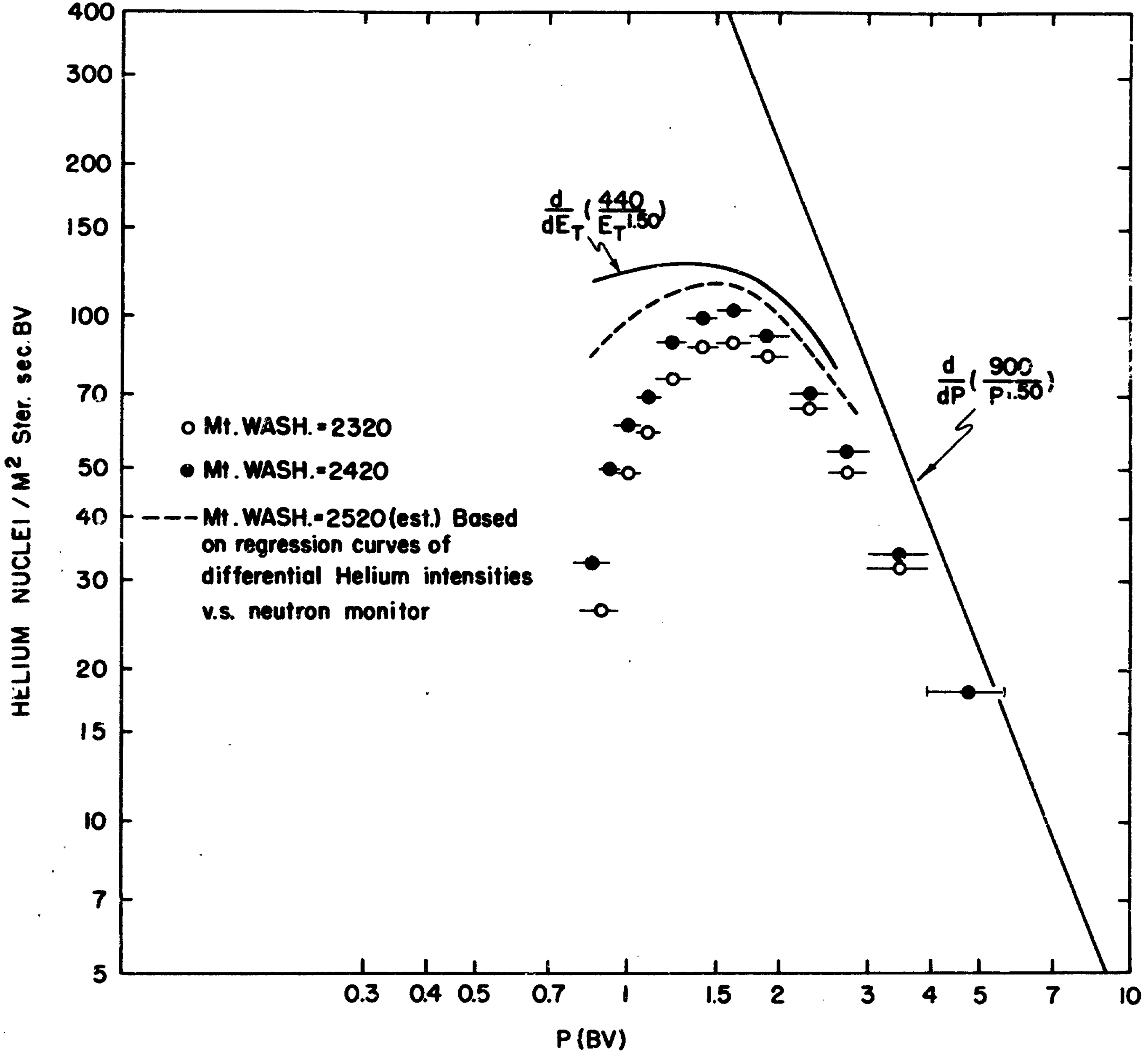

HELIUM NUCLEI / M² Ster. sec. BV
400
300
200
150
100
70
50
40
30
20
15
10
7
5
0.3
0.4
0.5
0.7
1
1.5
2
3
4
5
7
10
P (BV)
d/dE_T (440/E_T^1.50)
d/dP (900/P^1.50)
o Mt. WASH. = 2320
● Mt. WASH. = 2420
Mt. WASH. = 2520 (est.) Based on regression curves of differential Helium intensities v.s. neutron monitor

In accompanying papers, we have presented the rigidity spectra of the charge components in the primary radiation -- measured from ~ 1-16 Bv. These spectra have been measured at different levels of solar modulation. Analysis of this modulation shows that it affects particles of different charge (charge to mass ratio) in such a way that the ratios of intensities in differential rigidity intervals are not changed whereas the relative differential energy per nucleon ratios are. We shall use this fact throughout the remaining discussion whenever the effects of the solar modulation are to be considered and shall proceed to a study of the astrophysical significance of the relative unmodulated spectra of the different charge components.

Considering the protons and helium nuclei first, Figure 1 shows the ratio of the differential rigidity spectra of these two components between 0.8 and 16 Bv. Figure 2 shows the equivalent ratios for the differential energy/nucleon spectra between the corresponding limits. It is apparent that the ratio P/He (P) is sensibly constant at a value ~ 8 above about 1.5 Bv, increasing rapidly at lower rigidities to a value ~ 50 at 0.75 Bv, whereas the ratio P/He(E) seems to vary continuously over our range of measurement -- from a value ~ 5 at the lowest energies to ~ 20 at the highest energies. At even higher energies the very limited available data suggests that P/He (E) is more or less constant with a value ~ 20 (Waddington 1960).

The results on the solar modulation suggest that P/He (P) remains constant during this process so that we may regard the measurements in Figure 1 as appropriate to the unmodulated beam as well. As can be seen, however, P/He(E) changes with modulation. In order to estimate what these unmodulated ratios might be, we need to know the degree of modulation at sunspot minimum. Lacking this, we can still determine (from the known energy dependence of the modulation and the measured ratios) that the solar modulation process can never produce

P/He (E) = constant. Furthermore, unless we are seeing only a small fraction (<50% of the true galactic particles at energies ~ 1-2 Bev/Nuc, the variation of P/He (E) that is seen must be close to that present in the unmodulated beam and certainly then P/He (E) is not a constant.

There are a number of different explanations for the behavior just described. First, if the spectra of these components are viewed in terms of energy/nucleon spectra, as is the common assumption today, then it seems that the P/He (E) ratio at the "source" must be almost identical to the measured ratio above ~1 Bev/Nuc since the effects of interstellar propagation on this ratio are believed to be minor in this energy range. For example, if a Fermi type acceleration in interstellar space were dominant and invoked to produce a changing ratio with energy, the differences in spectra arising from such a process would be expected to be much less pronounced than are actually observed. As a result, we are left with the assumption that the "source" spectra are different on an energy/nucleon basis.

If the spectra are viewed in terms of rigidity, however, the following picture emerges. The observed constancy of P/He (P) above 1.5 Bv is then a reflection of identical rigidity spectra leaving the source region and subsequently relatively unaffected by interstellar propagation. The rapid increase in P/He(P) below 1.5 Bv then reflects a number of interstellar processes, the most common assumption being different rates of energy loss by ionization (at the same rigidity) in the interstellar medium. The rapidity of the increase in P/He (P) cannot be explained by ionization loss where the path length is constant with energy, however, and we must assume that the interstellar path length increases with decreasing energy (eg. Appa Rao, 1964). We illustrate this in Figure 1 with a path length varying at $E^{-0.5}$ normalized to 2.5 g/cm^2 at 3 Bv. Although this gives a reasonable fit to the data, we should point out that previous calculations have omitted the effects of secondary protons and helium nuclei arising from nuclear interactions in this same material. Calculations by Feit and Milford (1965) show that this is a large effect for protons, with secondary protons actually dominating the spectrum below 100 Mev. Although corresponding calculations have not been carried out for He nuclei, our experience in the atmosphere shows the secondary low energy He nuclei are relatively much less important. Preliminary calculations using a diffusion model and taking into account both secondary particles and ionization loss indicate that the observed increase in P/He (P) at low energies can be explained by passage through about 3 g/cm^2 of material -- constant with energy.

Before discussing this point further, let us turn to the data on heavier nuclei. We have already seen Figure 3 -- see also accompanying papers -- that the spectra of M and LH nuclei seem to be steeper than the He nuclei above 3 Bv. The differences in the spectra of L nuclei are even more pronounced and the differential L/M ratio measured at different energies and rigidities is shown in Figure 4. The decrease in this ratio is apparent both with increasing rigidity and increasing energy/nucleon.

As in Figure 3, the dotted curves show how the ratio would vary if m, the exponent on the differential spectra differs, by 0.1, 0.2, etc. (Note from Table I of the accompanying paper that no significant change in the Be/B ratio is apparent with energy. The limitations this presents on the decay of Be^{10} and the lifetime of the cosmic rays are discussed by Durgaprasad (1963).)

The L nuclei are believed to be secondary from nuclear interactions in interstellar space thus energy/nucleon seems to be the appropriate quantity to study the L/M ratio since these two groups of nuclei have slightly different charge to mass ratios. This will mean that solar modulation effects will change this ratio somewhat, but we shall neglect this effect which must certainly be small compared to the observed change. Accurate data on the L/M ratio at high energies is lacking and the previous results are conflicting. (Waddington, 1960;

Durgprasad, 1963; Mathiesen and Stenman, 1965). Our data, while based on the observation of only 36 L nuclei, is statistically the most accurate reported to date. The difference in the exponents of the L and M spectra of 0.5 ± 0.15 is certainly significant. An energy dependent L/M ratio has been speculated before and is usually interpreted in terms of passage of the M and H nuclei through an energy dependent amount of material. This might occur in the source regions or in the interstellar medium itself. If our results are interpreted in terms of such an effect, then the amount of material, $X \sim E^{-0.5}$. It is also possible that energy dependent fragmentation probabilities for the L nuclei can produce this effect. Our atmospheric attenuation results for the L and M components -- while showing some deviations from 1st order fragmentation theory -- are not sensitive enough to detect such an energy dependence.

The final aspect of the data we wish to discuss concerns the relative spectra of the M, LH and He nuclei. Referring again to Figure 3, we see that both He/M (P) and HE/LH (P) begin increasing below about 2.5 Bv rigidity. Our results are in good agreement with those found at still lower rigidities by Fichtel, et al (1964) and Lim and Fukui (1965) and interpreted again in terms of ionization loss in interstellar space by Fichtel, et al. In Fichtel's study, 3 g/cm^2 of material -- constant with energy -- was sufficient to produce the changes in He/M. The above estimate was made assuming the spectra of these nuclei were identical at higher energies. If, in fact, the M and LH spectra are steeper as our results seem to indicate, then the amount of material must increase with decreasing energy approximately at $E^{-0.5}$. This is illustrated in Figure 3. If this occurs or indeed if the particles have passed through more than 1-2 g/cm^2 of material the He/VH ratio should increase rapidly below 2-3 Bv. It is clear from Figure 3 that this does not occur. The He/VH ratio might remain essentially constant in the 1.5 - 3 Bv range only if the VH spectrum were substantially steeper than the He spectrum at high energies. Again, this does not seem to occur although our results cannot rule out a systematic increase in spectral index with increasing charge. The slightly steeper M and LH nuclei spectra suggest that this may be occurring. It is interesting to recall that such an increase (more pronounced than the ones measured here) was originally suggested by Singer (1958) on the basis of measurements up to 1956. More recent summaries, Waddington (1960) and Webber (1965), have indicated that the differences in the spectra of heavier nuclei are small if they exist at all. Our measurements at high energies are statistically as accurate as any reported to date (>200 nuclei having been observed) and have the added advantage that all components are measured simultaneously at one latitude and the same detector is used for measurements at different latitudes.

In summary, our results on the relative spectra of the different charge components suggest the following: (1) The relative spectra of protons and helium nuclei are most reasonably interpreted in terms of similar source rigidity spectra rather than energy nucleon spectra. The differences in these rigidity spectra at low energies is due to both the production of secondary protons and ionization loss in the interstellar medium. (2) The variation of the P/He, L/M and He/N ratios at low and intermediate energies can be interpreted in terms of the passage of primary radiation after acceleration through an amount of material which monotonically decreases with increasing energy. (3) A systematic steepening of the spectra of heavier multiply charged nuclei with increasing charge appears to exist.

Some of these features are less well defined than others, however, and our results show the clear need for measurements on each charge group in the rigidity range 5-50 Bv with a numerical accuracy up to 10 x that obtained in our experiments. This is not only to define the characteristics of these spectra at high energies but to enable the definitive measurements that can be obtained at very low energies to be interpreted more easily. To cite one example, the very powerful means that a measurement of the comparative spectra of the different charges at low energies gives us for determining the distribution of cosmic ray sources cannot be fully utilized without a knowledge of the comparative spectra at higher energies.

FIGURE CAPTIONS

Figure 1 Differential proton and helium nuclei intensities compared as a function of rigidity for two levels of solar modulation.

Figure 2 Differential proton and helium nuclei intensities compared as a function of energy/nucleon for two levels of solar modulation.

Figure 3 Ratios of helium to H, LH and VH nuclei respectively. Differential rigidity measurements in 1964 are shown except for the highest rigidity point which is an integral above 12.1 Bv.

Figure 4 Ratio of differential L to M intensities -- compared as a function of rigidity (A/Z of L nuclei assumed to be = 2.2) and energy/nucleon.

REFERENCES

Appa Rao, M. V. K., and S. Ramadurai, 1964, J. Geophys. Res. 69, 3729.

Durgaprasad, N. 1963, Int. Conf. on Cosmic Rays (Jaipur) 3, 17.

Feit, J., and S. N. Milford, Grumman Research Report.

Fichtel, C. E., D. E. Guss and K. A. Neelakantan, Res. Report, GSFC, Nov. 1964.

Lim, Y. K. and K. Fukui, submitted for publication 1965, J. Geophys. Res.

Mathiesen, O., and A. Stenman, 1965, Nuclear Physics Report ES 6501, University of Lund.

Singer, S. F., 1958, Prog. in Cosmic Ray Phys. 4, 205.

Waddington, C. J., 1960, Prog. Nuclear Physics 8, 1.

Webber, W. R. to be published 1965, Handbuch der Physik, 47.

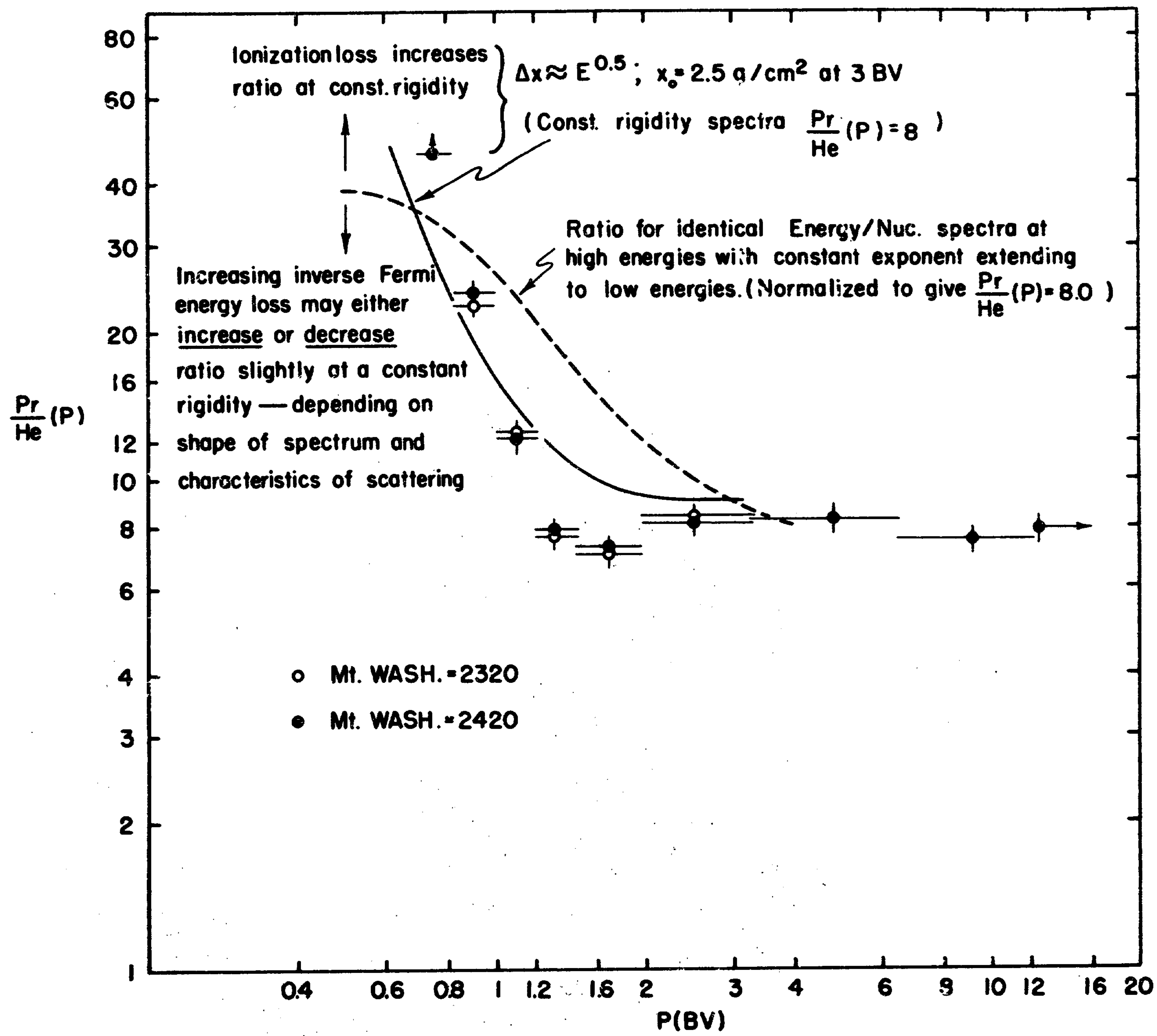

80
60
40
30
20
16
12
10
8
6
4
3
2
1
Pr/He (P)
Ionizationloss increases ratio at const. rigidity
Δx ≈ E^0.5 ; x₀ = 2.5 g/cm² at 3 BV
(Const. rigidity spectra Pr/He (P) = 8)
Ratio for identical Energy/Nuc. spectra at high energies with constant exponent extending to low energies. (Normalized to give Pr/He (P) = 8.0)
Increasing inverse Fermi energy loss may either increase or decrease ratio slightly at a constant rigidity — depending on shape of spectrum and characteristics of scattering
Mt. WASH. = 2320
Mt. WASH. = 2420
0.4
0.6
0.8
1
1.2
1.6
2
3
4
6
9
10
12
16
20
P(BV)

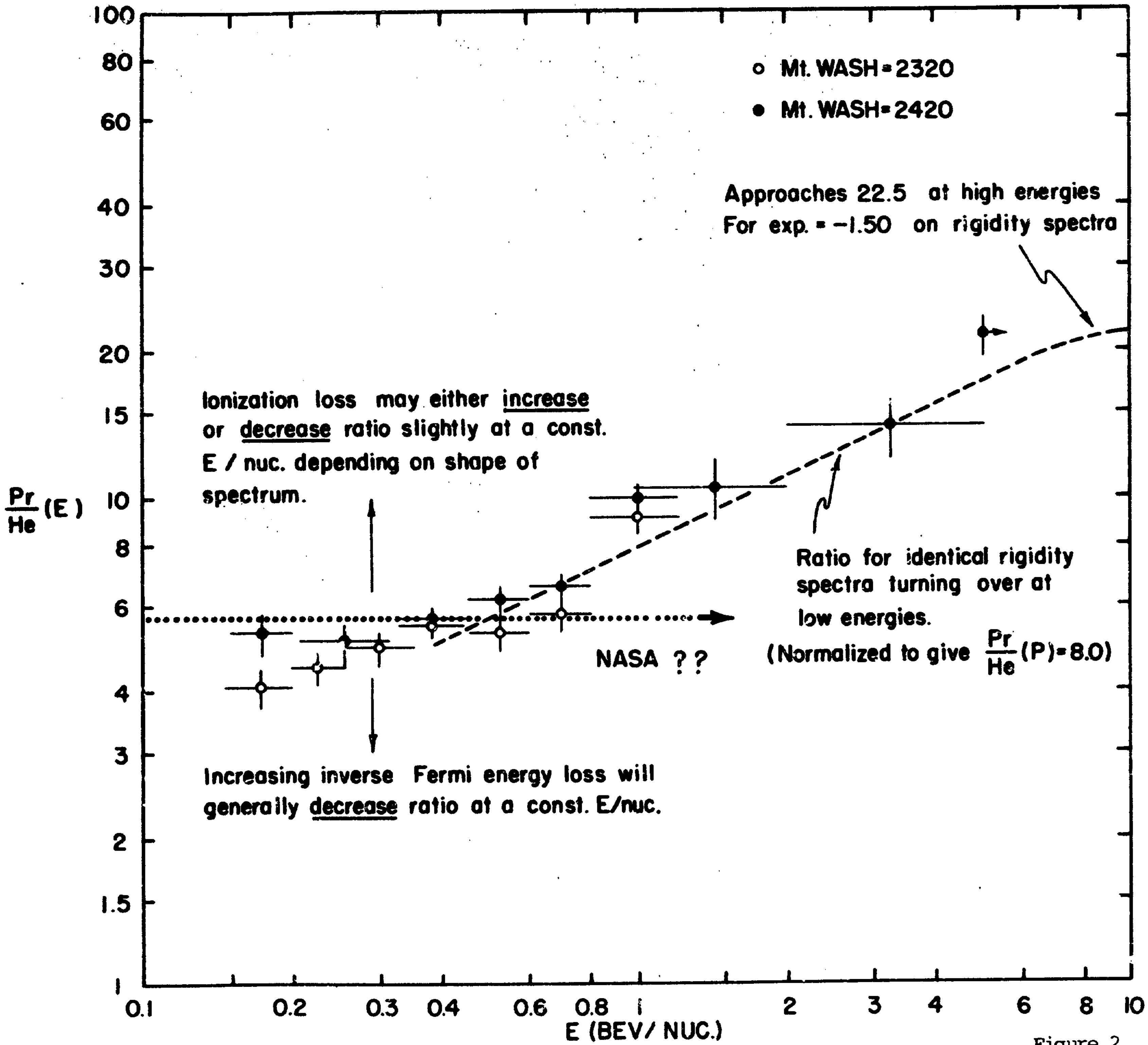

○ Mt. WASH=2320
● Mt. WASH=2420
Approaches 22.5 at high energies
For exp. = −1.50 on rigidity spectra
Ionization loss may either increase or decrease ratio slightly at a const. E / nuc. depending on shape of spectrum.
Ratio for identical rigidity spectra turning over at low energies.
(Normalized to give Pr/He (P)=8.0)
NASA ??
Increasing inverse Fermi energy loss will generally decrease ratio at a const. E/nuc.
Pr/He (E)
E (BEV/ NUC.)
100
80
60
40
30
20
15
10
8
6
4
3
2
1.5
1
0.1
0.2
0.3
0.4
0.6
0.8
1
2
3
4
6
8
10

Figure 2

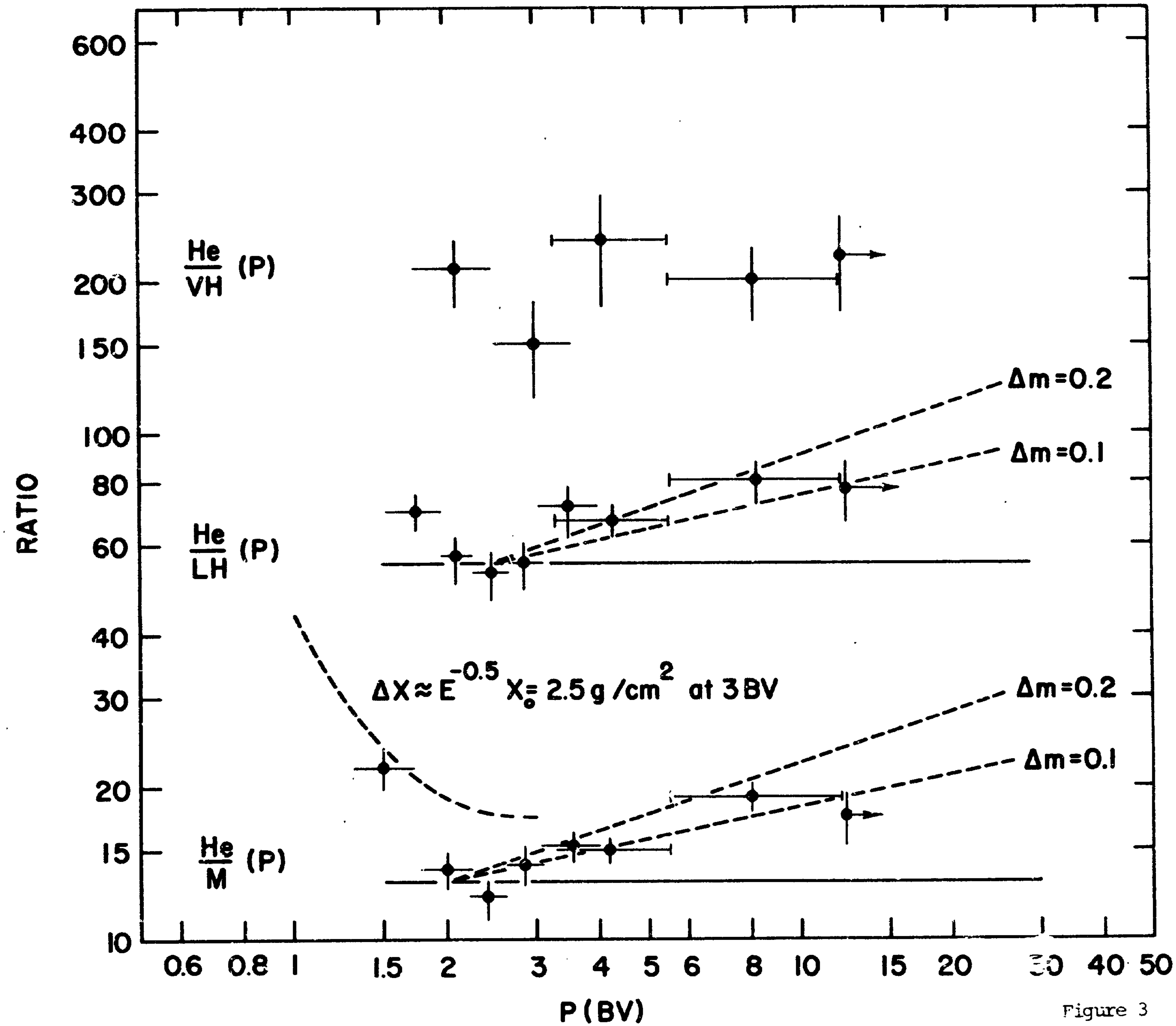

600
400
300
200
150
100
80
60
40
30
20
15
10
RATIO
He/VH (P)
He/LH (P)
He/M (P)
Δm=0.2
Δm=0.1
Δm=0.2
Δm=0.1
ΔX≈E^-0.5 X₀= 2.5 g/cm² at 3BV
0.6 0.8 1 1.5 2 3 4 5 6 8 10 15 20 30 40 50
P (BV)

Figure 3

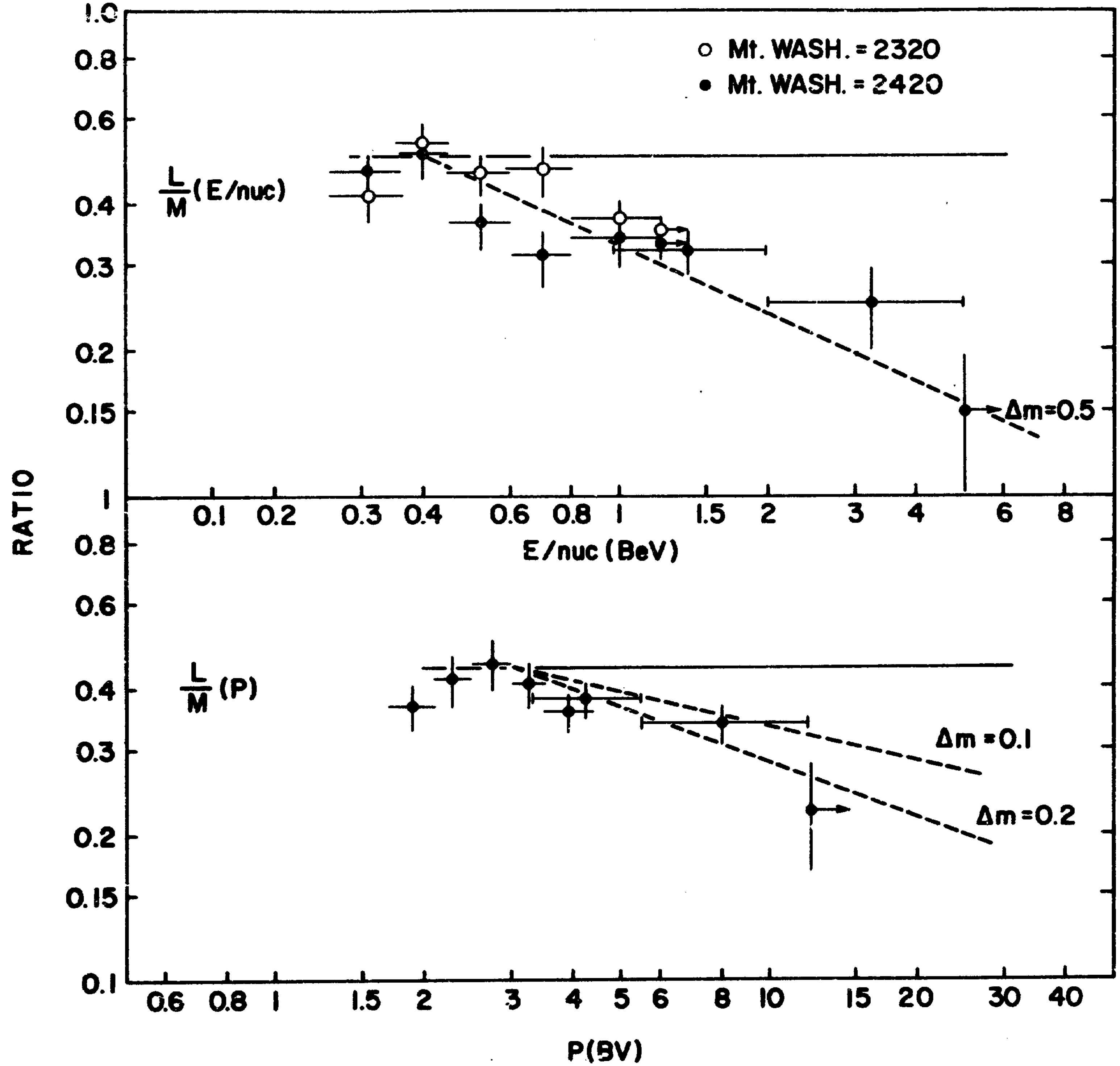

o Mt. WASH. = 2320
• Mt. WASH. = 2420
$\frac{L}{M}$(E/nuc)
Δm=0.5
E/nuc (BeV)
RATIO
$\frac{L}{M}$(P)
Δm =0.1
Δm =0.2
P(BV)

N66-13360

Measurements of the Energy Spectrum of Nuclei with Z $\geq$ 3 in the Primary Radiation Using a Balloon Borne Cerenkov-Scintillation Counter

W. R. Webber, J. F. Ormes and T. von Rosenvinge*

13360

ABSTRACT

The spectra of the so called L, M and H nuclei have been measured on eleven balloon flights at seven geomagnetic latitudes during the period 1963-1965. The instrument used is a modified version of the Cerenkov-scintillation counter. These spectra have been measured over the range 1.5 to 16 Bv. The flights attained depths of 2-6 g/cm^2 which, coupled with the detectors large geometrical factor (~50 st cm^2) has enabled details of the absorption of the L, M and H components to be studied in the upper atmosphere. The large geometrical factor has allowed identification of over 10,000 nuclei with Z $\geq$ 3, with over 2000 being observed on a single flight. A total of ~150 VH nuclei have been observed and the spectra of these nuclei has been found to be similar to that of M and LH nuclei above ~2 Bv. The spectra of the L nuclei is found to be significantly different from that of the M and H nuclei, with the exponent on a power law energy spectrum being 0.3 $\pm$ 0.1 larger. The M and LH nuclei spectra are also different than the He nuclei spectra above 3 Bv; the exponent on a power law spectrum being 0.1 $\pm$ 0.03 larger, with the integral spectrum being given by an average exponent of -1.6 $\pm$ 0.03 over the range 3-16 Bv. The solar modulation of these nuclei is found to be similar to that of the He nuclei. author

* Work supported under NASA Research Grant NsG 281-62.

In this paper we wish to discuss the energy spectra and modulation of the heavier nuclei, essentially those with $3 \leq Z \leq 26$ as measured by the Cerenkov-scintillator system discussed in a companion paper. The study of these nuclei presents a number of special problems with which we would like to concern ourselves before the actual presentation of the data.

First of all, the identification of these nuclei in the atmosphere is relatively simple and although the intensity is not great, it is possible to get meaningful absorption curves of the different components (the L, M and LH groups) as the balloon rises to altitude. These may then be used to compare with fragmentation-diffusion theory and to extrapolate the intensities of the different components to the top of the atmosphere.

During a typical four hour duration of a high latitude flight ~2000 nuclei with $Z \geq 3$ are observed. This permits breakdown into the usual L, M, LH and VH charge groups. The spectrum of the M nuclei can be determined with an accuracy formerly associated with the helium nuclei and the spectra of L and LH nuclei are each based on ~300 counts.

The identification of the different nuclei passing through the detector is controlled by two factors. First the background of unwanted counts is virtually zero for particles of all energy with $Z \geq 5$. Second, the charge resolution is good enough so that the counts due to individual charges show up as distinct groups over the range $5 \leq Z \leq 14$ in a flight at latitudes <50° and a series of successive lines (see Figure 1 of accompanying paper) at high latitudes where non-relativistic particles are entering and the energy spectrum is being measured. For values of Z >15 it is difficult to make individual charge identification, however, a grouping into "apparent" even charges is noted with a distinct grouping at a Z ~26 being the dominant feature of this part of the charge distribution. Because of the printout in 64 x 64 arrays, it is difficult to show a complete charge spectrum at the highest resolution. However, Figure 1 shows an array covering Boron, Carbon and Nitrogen for the Fayetteville flight where all of the particles are relativistic. The system linearity is calibrated by a light pulser system before each flight. In addition, the proton and helium peaks provide in-flight calibration. The ability to identify each charge peak up through Z = 14 then provides a continuous measure of the linearity of response of the system to particles of different charge and energy loss. As a result, it is possible to measure the non-linearities of energy loss in the plastic scintillator and Cerenkov-scintillator up to a charge of ~26. The results are shown in Figure 2. Our results show that the saturation effect in the scintillator becomes logarithmic at high rates of energy loss. This is in some ways an advantage since it converts a normal Z^2 charge dependence into one ~Z - giving effectively a logarithmic system and allowing us to extend our charge measurement out to Z = 26. This charge calibration has been established for several flights.

The energy spectra of the heavy nuclei are then determined in a straightforward way. An additional check is possible on the energy calibration for non-relativistic heavy nuclei by observing the location of the minimum on the S $\pm$ C output curve (as well as the slope of the S vs S [C=0] output). Detailed study of these features shows that the non-linearity is independent of charge and depends only on dE/dx in the range of energies that do not end in the scintillator.

It is to be noted that at energies somewhat below the Cerenkov threshold (<250 Mev/Nuc), it becomes impossible to resolve individual charges. In the range 100-250 Mev/Nuc, it is still possible to get the differential intensity of particles of a given charge group, however. The complete charge breakdown for all flights analyzed to date is shown in Table I.

The integral spectra of the various charge groups are shown in Figure 3. The points at 3.2, 5.6 and 12.1 Bv are evaluated in the same way as the helium nuclei, that is by extrapolating the growth curves of the individual components to the top of the atmosphere. The remaining points are obtained from the differential

TABLE I

Distribution of Particles of Different
Charge at Balloon Altitudes

Charge	Counts: Total		Counts: >12 Bv	
Li	390		14	
Be	214	1,226	5	36
B	622		17	
C	1,390		65	
N	530	3,142	15	124
O	1,132		44	
F	90		0	
Ne	301		17	
Na	110		3	
Mg	167	764	10	37
Al	65		0	
Si	121		7	
$15 \leq Z \leq 19$	103		1	
$Z \geq 20$	204		8	
$Z \sim 40$	2		0	

spectrum measured in the telescope itself. These differential spectra are shown in Figure 4 along with a point determined from the differences of the 3.2 and 5.6 Bv integral measurements. The effects of the solar modulation are clearly evident in the spectra of the M nuclei and less conspicuously so for the L and LH nuclei. As near as can be determined the solar modulation affects these nuclei (except for possibly the L nuclei) in a manner identical to the helium nuclei.

Although superficially the spectra of these heavy nuclei are similar, important differences exist, both at the low and high rigidity parts of the spectrum. These differences seem to be best illustrated by taking ratios of the differential intensities of helium nuclei to the various heavy nuclei groups. Three of these ratios are shown in Figure 5 as a function of rigidity. (Energy/nuc and rigidity are equivalent if we neglect He^3 in the helium component.) Very little can be said of the He/VH ratio - except that it shows no pronounced changes from 2-12 Bv. Even this fact has some important astrophysical implications, as will be discussed in an accompanying paper. The He/M and He/LH ratios both behave in a similar manner, however. Above about 2.5 Bv these ratios slowly increase with increasing rigidity. This increase appears to be continuous and is equivalent to the power law spectra of the M, and LH nuclei having an exponent 0.1 $\pm$ 0.03 larger than the helium nuclei. It is important to note that this result is not based on a single equatorial flight but appears in both flights -- in which over 200 of these nuclei have been recorded. This trend is also evident in the Kerrville flight at 5.6 Bv where a further 400 of these nuclei were recorded. Unless a systematic distortion exists between energies measured by the detector and those deduced from geomagnetic considerations for these charges, we must regard this effect as statistically significant.

Finally, below 2 Bv a rapid increase in these ratios occurs -- most notable for the M nuclei. The significance of these spectral differences and a discussion of the spectra of L nuclei which shows even more pronounced differences will be discussed in an accompanying paper.

FIGURE CAPTIONS

Figure 1 64 x 64 array showing a part of the pulse height distribution containing Boron, Carbon (the large group right center) and Nitrogen. S output along vertical axis, S + C output along horizontal. The geomagnetic cut-off of ~900 Mev/Nuc means that the distributions should be slightly skewed in the direction of smaller S + C outputs and this is clearly evident from the Figure.

Figure 2 Relation between energy loss (dE/dx) and light output (dL/dx) for relativistic particles of various charge in plastic scintillator (NE 102) and S + C detector.

Figure 3 Integral spectra of the L, M, LH and VH charge groups. The solid lines indicating integral rigidity spectra with exponents = -1.5 are shown for guide purposes only.

Figure 4 Differential spectra of the L, M, LH and VH charge groups. The solid lines indicating differential rigidity spectra with exponents = -2.5 are shown for guide purposes only.

Figure 5 Ratios of helium to M, LH and VH nuclei respectively. Differential rigidity measurements are shown except for the highest rigidity point which is an integral above 12.1 Bv.

```
START TIME= 837   END TIME=1345
ALPHA  FAYETTVILLE                                        RUN 11/6/65
ELAPSED TIME=  17872  COUNTS LOST=   1443  NOISY  CTS =      0
 S=0  S+C=0 =      13 S=0 S+C NE 0=     33 S NE 0 S+C=0=     32
TAPE ERRORS =      3
160  IGNORED=      11 160    EDITED=    627 160 TIME EST=  17585
PARITY ERRORS=      0  CHECKSUM   =   -384
   777777777777317
          000  4444444444444444444444444444444444444444444444444444444444444444
          000  0000000011111111222222223333333344444444555555556666666677777777
          000  0123456701234567012345670123456701234567012345670123456701234567
          400    0
          401
          402
          403
          404
          405
          406
          407             0
          410
          411
          412
          413
          414                                0
          415
          416
          417        0
          420
          421
          422                          0      1
          423           0          0  1                             0
          424                        0                              0
          425                             0      0                      0
          426                                0 0    1
          427                               0      1  0    0     0
          430                          0  0    000 1 10
          431                       0   10  101 0  00
          432                             0  00 10           0
          433                                101  0      00 0     0
          434                             0                     00 1
          435                            0   0  000   0    11 1   011 1    0
          436                             0     0      21 101121011101
          437                         0    00   0     0  011010112100011 0
          440                                6    0 10002000 0    1010000
          441                         0   0      0 0 00  10 0 1  0  000
          442                           0         0   0     0 000 000 0
          443                              00              0
          444                             0    0                  0     000 1
          445                            0              0               0  0
          446                              0 0                0 00 00   0    1
          447                                 0               0            00
          450                             0             010  00            0
          451                                                    0       0
          452                                     0        0     00     01  0
          453                                           11        0       0 0
          454                                    0       0        0      1
          455                  0                0  0             00  0    0
          456                                                       0     0
          457                                      0
          460
          461
          462
          463                                               0               0
          464
          465
          466                                    0             0        0
          467                             0
          470
          471                                          0
          472                                             0  0
          473                              0     0              0            0
          474                                                             0
          475                                     0              0
          476
          477
START TIME= 837   END TIME=1345
```

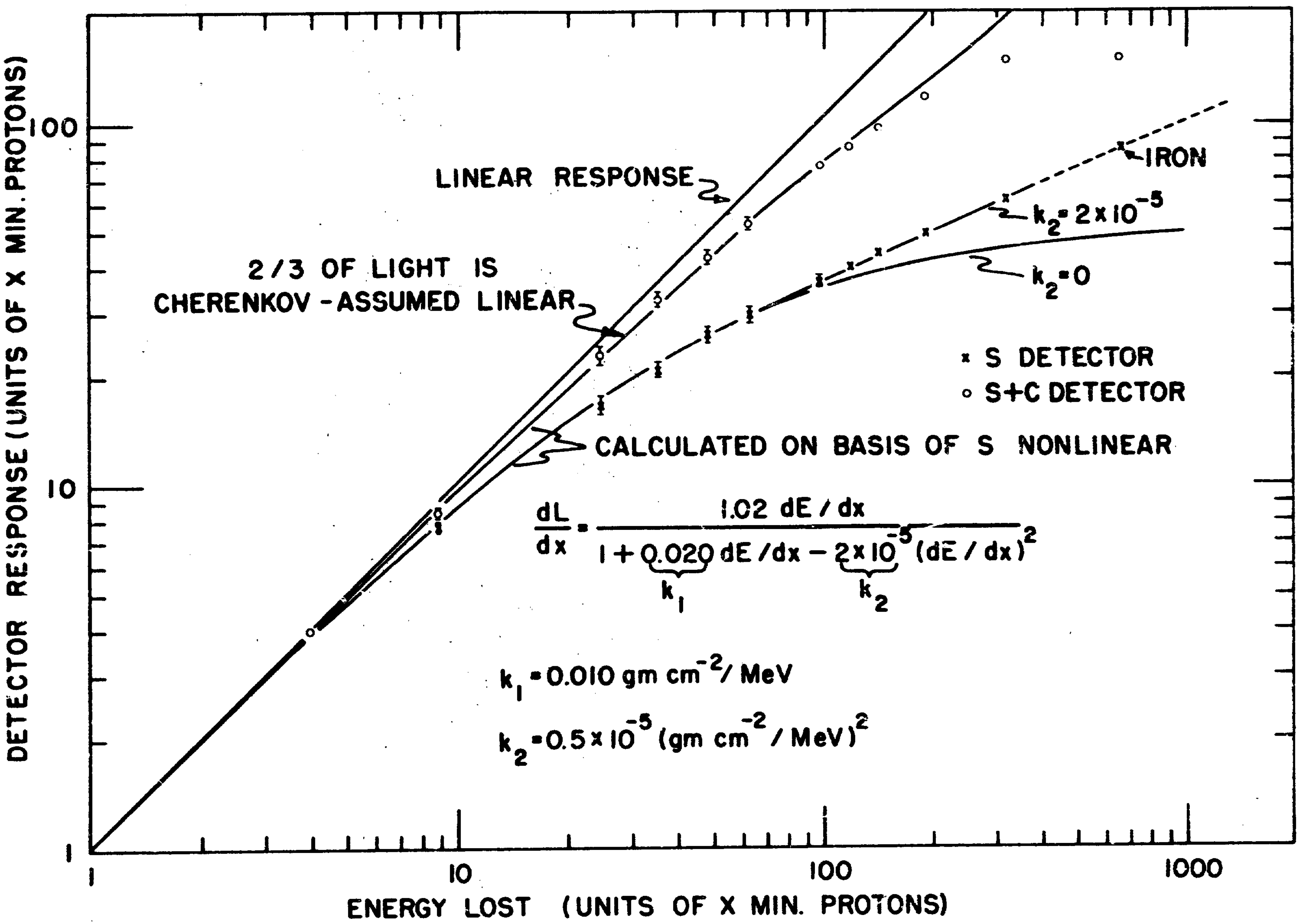
LINEAR RESPONSE
2/3 OF LIGHT IS
CHERENKOV - ASSUMED LINEAR
IRON
$k_2 = 2 \times 10^{-5}$
$k_2 = 0$
× S DETECTOR
○ S+C DETECTOR
CALCULATED ON BASIS OF S NONLINEAR
$\frac{dL}{dx} = \frac{1.02\ dE/dx}{1 + \underbrace{0.020}_{k_1} dE/dx - \underbrace{2 \times 10^{-5}}_{k_2} (dE/dx)^2}$
$k_1 = 0.010\ gm\ cm^{-2}/MeV$
$k_2 = 0.5 \times 10^{-5}\ (gm\ cm^{-2}/MeV)^2$
DETECTOR RESPONSE (UNITS OF X MIN. PROTONS)
ENERGY LOST (UNITS OF X MIN. PROTONS)
1
10
100
1000

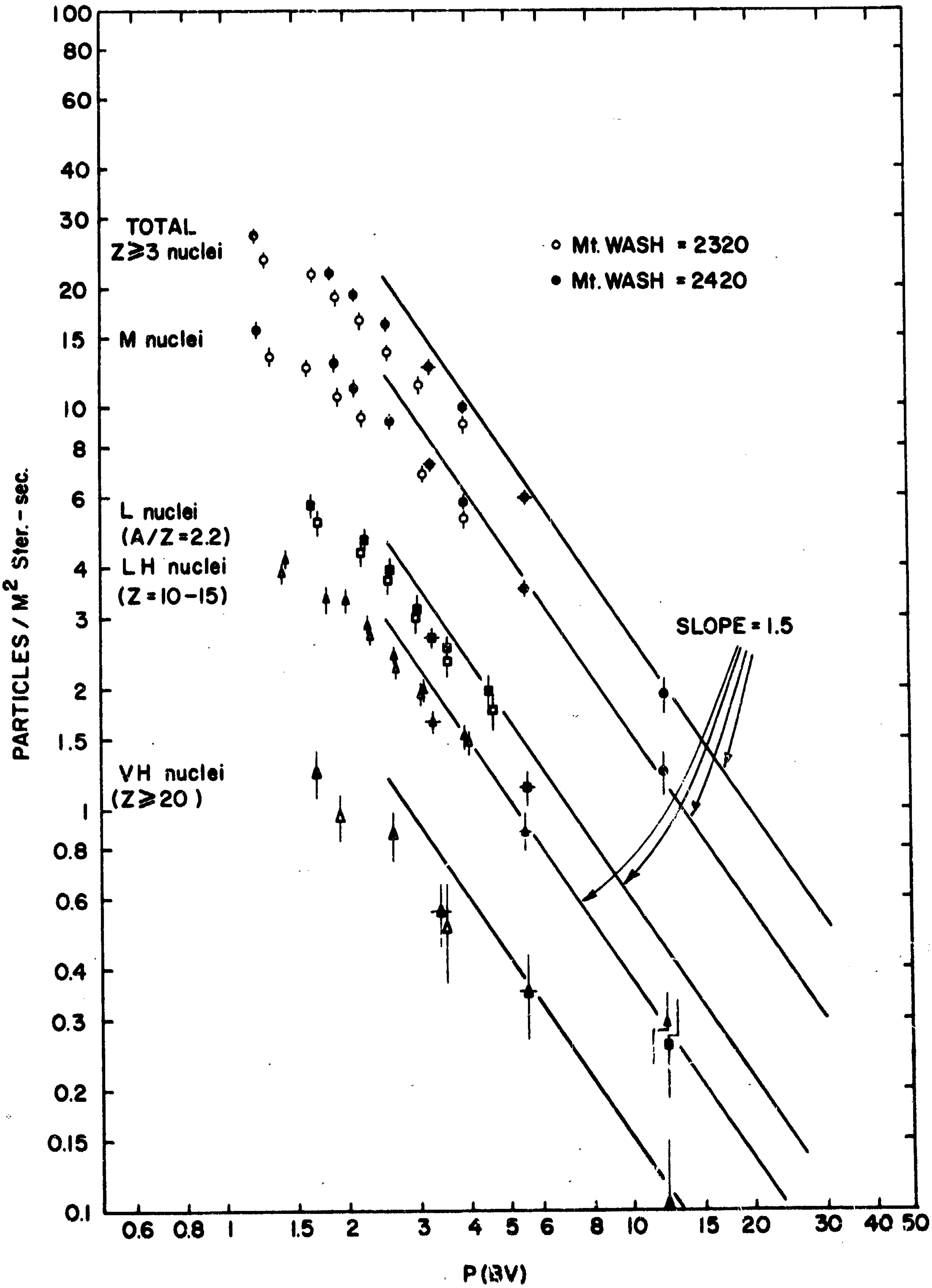

100
80
60
40
30
20
15
10
8
6
4
3
2
1.5
1
0.8
0.6
0.4
0.3
0.2
0.15
0.1
0.6
0.8
1
1.5
2
3
4
5
6
8
10
15
20
30
40
50
PARTICLES / M² Ster. - sec.
P (BV)
TOTAL
Z≥3 nuclei
M nuclei
L nuclei
(A/Z = 2.2)
L H nuclei
(Z = 10-15)
VH nuclei
(Z≥20)
○ Mt. WASH = 2320
● Mt. WASH = 2420
SLOPE = 1.5

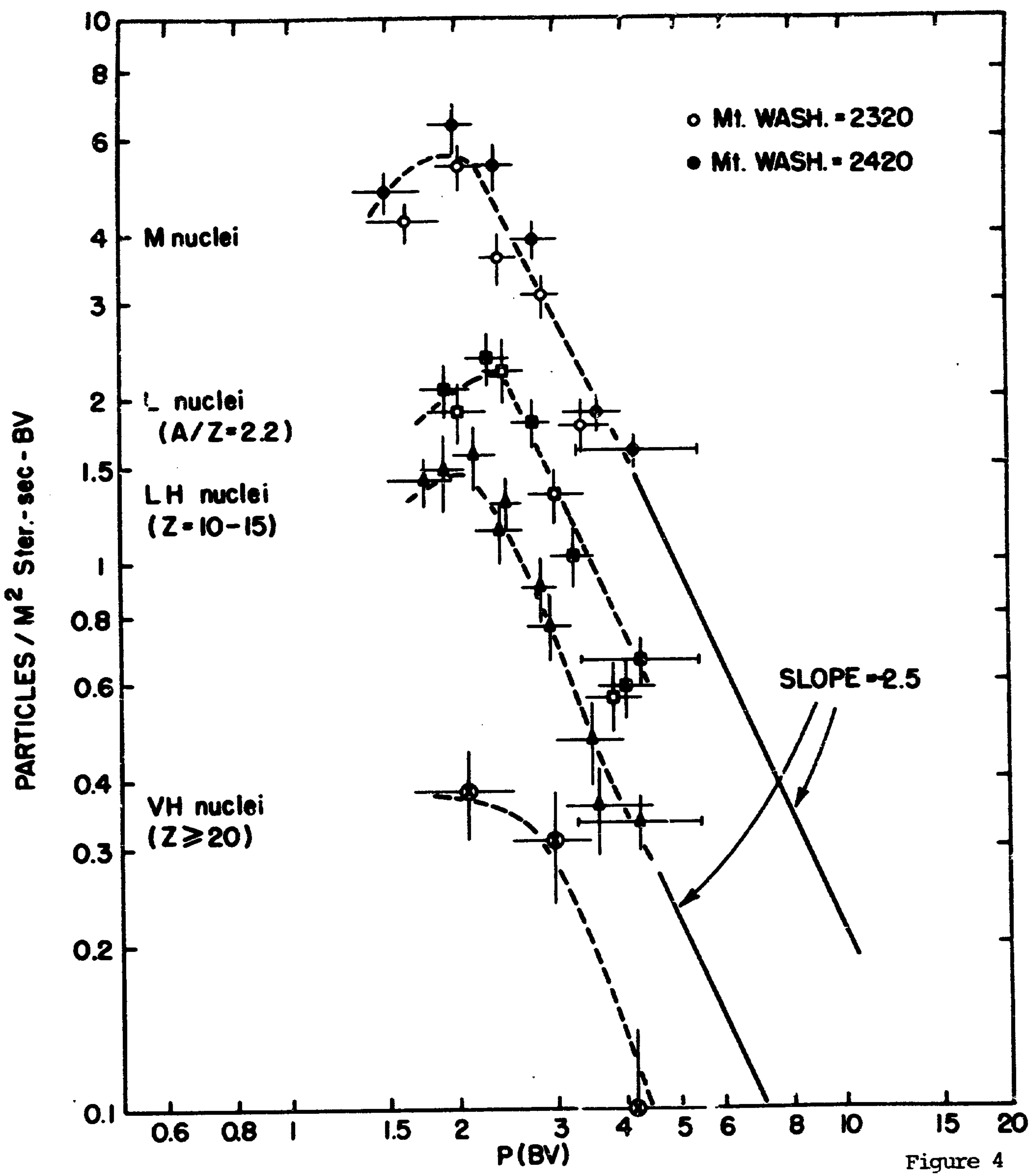

PARTICLES / M² Ster.-sec - BV
10
8
6
4
3
2
1.5
1
0.8
0.6
0.4
0.3
0.2
0.1
○ Mt. WASH. = 2320
● Mt. WASH. = 2420
M nuclei
L nuclei
(A/Z = 2.2)
LH nuclei
(Z = 10-15)
VH nuclei
(Z ≥ 20)
SLOPE = 2.5
0.6
0.8
1
1.5
2
3
4
5
6
8
10
15
20
P (BV)

Figure 4

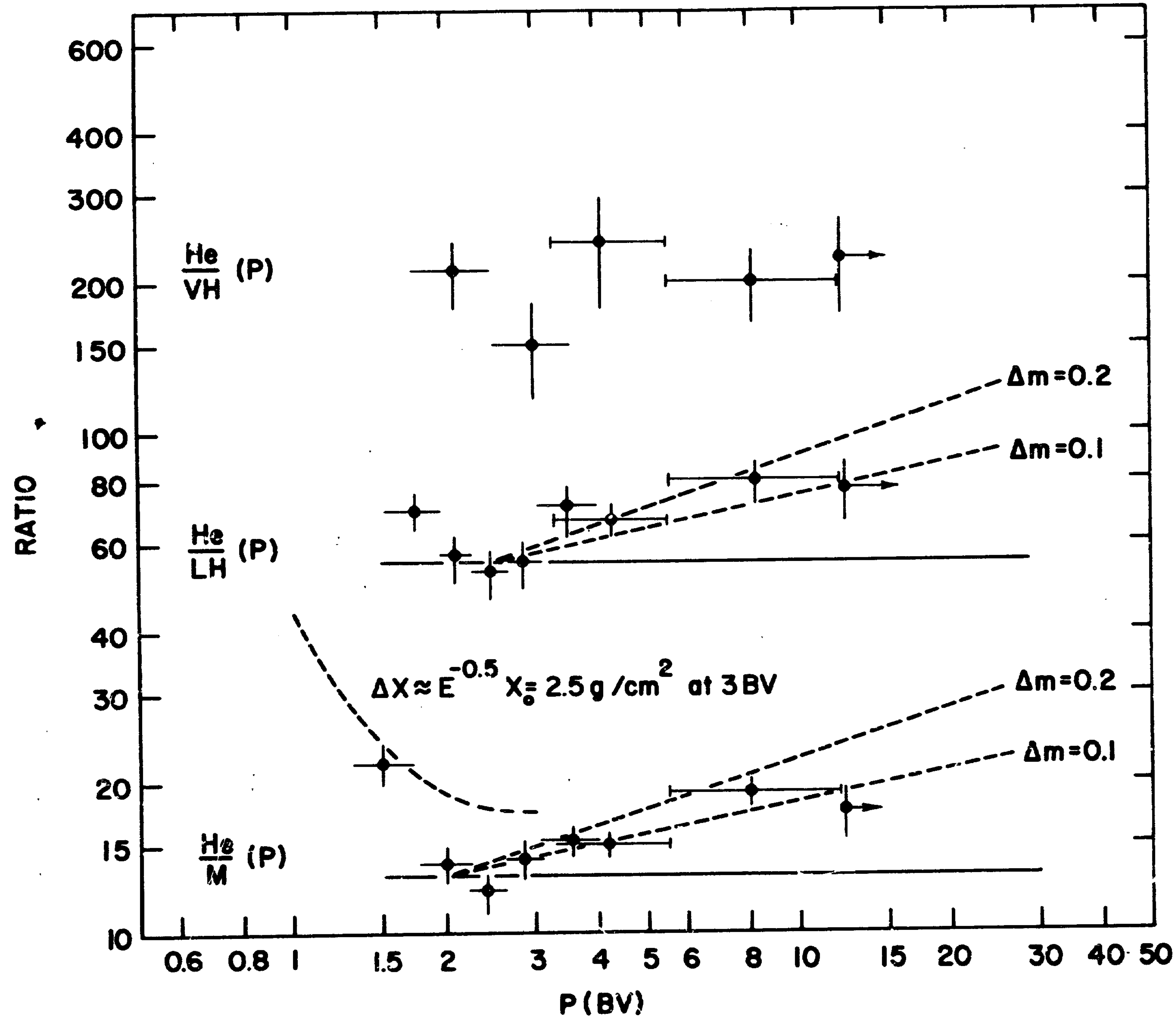

RATIO
600
400
300
200
150
100
80
60
40
30
20
15
10
He/VH (P)
He/LH (P)
He/M (P)
Δm=0.2
Δm=0.1
Δm=0.2
Δm=0.1
ΔX ≈ E^-0.5 X₀= 2.5 g/cm² at 3 BV
0.6
0.8
1
1.5
2
3
4
5
6
8
10
15
20
30
40
50
P (BV)

N66-13361

Solar Modulation of Protons and Helium Nuclei During the Period 1963 - 1965*

W. R. Webber

ABSTRACT

13361

The low rigidity portions of the primary spectra of protons and helium nuclei have been measured on six occasions during 1963-1965 using a Cerenkov-scintillation counter carried to altitudes of 2-6 g/cm^2 by balloons. The range of rigidities over which detailed spectral measurements have been made is 0.4 - 2 Bv for protons and 0.8 - 4 Bv for helium nuclei. The measurements cover a period of decreasing solar modulation as evidenced by an increase in Mt. Washington neutron monitor rate from a value ~2300 in the summer of 1963 to ~2450 in 1965. The increase in neutron monitor rate was accompanied by much larger increases in the low energy protons and helium nuclei -- amounting to a factor of almost two at the lowest rigidities. The energy dependence of the modulation of both protons and helium nuclei is consistent with a $1/\beta$ dependence for $0.45 \leq \beta \leq 0.85$. However, at the same velocity, the modulation for protons is ≥ 2 x that for helium nuclei. The modulation thus produces identical changes in the rigidity spectra of the two components. This model is inconsistent with a simple diffusion model for the 11-year variation such as suggested by Parker (1963). However, a model in which diffusion and energy loss occur simultaneously and are of approximately equal importance is explored and found to be capable of producing the observed modulation.

Author

* Work supported under NASA Research Grant No. NsG 281-62.

According to our data we propose the following recipe for the 11-year modulation of galactic cosmic rays near the sun. "Start with a basic solar wind. Add a generous portion of turbulence and scattering. Add an equal amount of Fermi deceleration. Mix together thoroughly and allow to diffuse near the sun for one month at $2 \times 10^{5°}$ K".

Our results on the modulation of protons and helium suggest that factors other than simple diffusion and convection in the model originally proposed by Parker (1963) play an important role in the 11-year modulation of galactic cosmic rays near the sun. In order to come to this conclusion, it is necessary to determine not only the energy dependence of the modulation for a single charge component but the relative modulation of charge components with different A/Z ratios -- such as protons and helium nuclei; light and medium nuclei; etc. The results presented in the previous two papers allow us to do this for the above charge groups during a period from 1963-1965. During this time the Mt. Washington neutron intensity at the times of the balloon flights increased from 2297 to 2445, or ~6.5%, reaching a level during the 1965 flights within 2-3% of the sunspot minimum level in 1954. The data on the changes in intensity of the protons and helium nuclei as a function of energy relative to the changes in neutron monitor intensity measured during this interval is summarized in Figure 1.

Between $\beta = 0.45 - 0.85$ the modulation of both helium nuclei and protons is seen to be reasonably similar and to have a $1/\beta$ dependence. This velocity dependence is in essential agreement with that observed for these components <u>individually</u> by experiments carried out on the IMP-1 satellite which was in operation over part of the period covered by our study, (Gloeckler 1965), (McDonald and Ludwig 1965). However, and this is important, at the same velocity the change in the proton intensity is at least a factor of 2 greater than the helium nuclei. This implies that if we measure the ratio of differential energy/nucleon intensities of protons and helium at times of different modulation, the ratio should be different. (See Figure 2 of accompanying paper.) At a time of greater modulation, the ratio is seen to be clearly smaller at lower energies. Conversely, if the ratios of differential rigidity intensities are compared as a function of modulation, little change is observed. (See Figure 1 of accompanying paper.) This suggests that although the actual amount of modulation depends on $1/\beta$, it is, nevertheless, effectively rigidity dependent.

We should point out that these results are in disagreement with the conclusions of Gloeckler (1965) who upon comparing his own results on the modulation of low energy helium with those of McDonald and Ludwig (1965) on protons (grouped into somewhat different time intervals) concluded that the modulation of these two components were the same at a given velocity at low energies. This might indeed be true at the values of $\beta = 0.2 - 0.45$ covered in these experiments and still not apply in the range covered by our measurements. To investigate the character of the modulation further, we have compared our results with the modulation that could be inferred by making regression curves of differential intensities of protons and helium nuclei with neutron monitor data for the complete solar cycle -- using the data presented in the review article by Webber (1965). This data is shown in Figure 2. Since here the fractional modulation is plotted as a function of rigidity the fact that the proton and helium modulation are similar is equivalent to our earlier statements. The composite data gives a significantly greater fractional modulation and a somewhat flatter rigidity dependence of this modulation than our balloon data. This is an average over the entire solar cycle, however, and the greater fractional modulation simply reflects the fact that the modulation has caused the average response energy of the neutron monitor to increase thus increasing $\Delta j/\Delta N$. Indeed, the points where $\Delta j/\Delta N = 1$ reflect the change in this response energy. The values of 7 and 15 Bv obtained from the figure are consistent with the modulation we describe here extending to neutron monitor energies as well.

Consider our results in terms of the diffusion model of Parker (1963) in which one considers an equilibrium condition established between the sweeping out of galactic cosmic ray particles by the solar wind and their inward diffusion through scattering by irregularities in the magnetic field. For an isotropic particle distribution, one obtains a modulation of the form:

$$j\ (v,r) = j_o\ (v,R)\ \exp - \frac{3}{v} \int_r^R \frac{U(r)}{\lambda(r)}\ dr$$

where v = particle velocity, R is the boundary of the interplanetary medium and r is the location of a point inside, U(r) is the velocity of the solar wind and $\lambda(r)$ is the M.F.P. between "scatterings". Assuming U and λ are both constant with r gives:

$$j\ (v,r) = j_o\ (v,R)\ \exp - \frac{3U\ (R-r)}{\lambda v}$$

The actual energy or rigidity dependence of such a modulation is almost completely described in terms of the variation of λ with rigidity. Parker has discussed the variation of λ for a simple picture containing two parameters -- the scale size of the irregularity (scattering center), ℓ, and the particles radius of curvature ρ. Very simply, if $\rho \ll \ell$, $\lambda(v)$ = const; if $\rho \sim \ell$, $\lambda(v) \sim \rho/\ell$; and if $\rho \gg \ell$, $\lambda(v) \sim \rho^2/\ell^2$.

We have already seen that the modulation is $\sim 1/v$ at low energies. This suggests that $\lambda(P)$ = const. and that $\rho \ll \ell$, a generally accepted condition in the interplanetary medium at low energies. However, at the same v the modulation of protons and helium is different. This is not indicated by this model. A rigidity dependence which might explain this velocity splitting could be introduced by assuming $\lambda(v) \sim \rho/\ell$ or ρ^2/ℓ^2. However, the modulation itself would then depend on $1/v^2$ or $1/v^3$ at low rigidities in contradiction with our measurements. Unless one is prepared to introduce a new concept of scattering, then it seems that our results cannot be explained on the basis of this picture alone.

What other possibilities exist for a general modulation mechanism? Recall the arguments of Ehmert (1960) who suggested that the 11-year modulation was explainable in terms of a heliocentric electric field (i.e. potential difference between the orbit of earth and a few hundred AU). Ehmert demonstrated that the variations at high energies could be related directly with the measurements of the changes in the differential spectrum of protons and helium nuclei measured in the period 1955-1959 by McDonald and Webber (1959). The actual change in the differential spectrum at low energies depends on the assumed initial spectrum in such a model. Ehmert originally assumed that the proton and helium nuclei spectra were identical (power laws in kinetic energy) at low energies. As a result of the modulation of such spectra in an electric field, the changes in helium nuclei are somewhat larger than protons at a fixed rigidity. This splitting was not observed in the measured spectra of McDonald and Webber.

Recent measurements confirm the splitting of the two spectra at low energies and suggest that this occurs before the particles are modulated in the solar system. Using this new data, Freier and Waddington (1965) have revived the electric field model as an explanation for the 11-year modulation. A study of the modulated spectra presented by Waddington and Freier shows that at the same rigidity the modulation of protons and helium nuclei are almost identical. Thus for what are now believed to be reasonable initial low energy spectra passage through an electric field produces a modulation indistinguishable from a "rigidity" dependent one.

The fairly well known characteristics (particularly the turbulence-diffusion aspect) of the outflowing solar solar plasma and magnetic fields do not lend themselve in a simple manner to a description of the modulation process in terms of an electric field -- either static or dynamic. However, one can retain the idea of diffusion in the Parker sense if one assumes that in addition to the intensity change caused by diffusion-convection, diffusive deceleration (inverse Fermi effect) and betatron deceleration are equally important in this expanding outward moving interplanetary field. This idea was first applied to the modulation of galactic cosmic rays in Forbush events by Laster, Lenchek and Singer (1962). Their calculation of the modulation produced in an expanding gas cloud gave a modulation much like that to be expected for a simple electric field. Webber and McDonald (1964) suggested that this type of energy loss may be a most important part of the 11-year variation. At present, a rigorous calculation of the spectral dependence and magnitude of the modulation to be expected from this effect has not been made for the 11-year variation. However, a number of simple calculations show, Parker (1963,1965), Dorman (1963) and Quenby (1965), that the modulation to be expected from inverse Fermi energy loss and betatron deceleration in the interplanetary medium is at least as large as that expected from the diffusion-convection process alone.

These calculations have been carried out for protons only and give no information on the charge dependence of these energy loss terms and in particular whether they can produce the observed rigidity and velocity dependence of the modulation.

Let us now consider the inverse Fermi effect (which is the dominant energy loss process) from the point of view of particles of different charge to mass ratio. In this energy loss process, the particle deceleration is caused by the induced electric field:

$$\underline{E} = -\frac{1}{c}\,\underline{U} \times \underline{H}$$

due to the velocity U of the scattering centers relative to the earth (solar wind velocity).

The energy loss per nucleon in the interaction of a particle with an individual scattering center (or with an electric field) is:

$$\Delta\varepsilon_{\,nuc} = \frac{Z}{A} \; e\,\underline{E} \cdot \underline{\ell}$$

where ℓ is a scale length. The calculation of the energy loss of a particle moving with velocity v with a scattering center (assumed to be a rigid hard sphere $\rho << \ell$) of velocity $U << v$ gives for a headon collision:

$$\left(\frac{\Delta\varepsilon}{\varepsilon}\right)_{nuc} = \pm \frac{2\,v\,U}{C^2}$$

Note that this fractional energy loss is independent of charge to mass ratio $\frac{Z}{A}$. We recognize the other simple types of scattering process possible, that is, when $\rho >> \ell$ or $\rho \simeq \ell$. In these cases, however, "scattering" occurs only after the summation of many smaller scatterings. In effect, the particle is continuously being scattered or what is equivalent -- the change in energy in a given small scattering depends only on the (relatively small) dimensions of the scattering center itself and not on the particles radius of curvature. As a result, the energy change per collision becomes:

$$\left(\frac{\Delta\varepsilon}{\varepsilon}\right)_{nuc} \simeq \pm \frac{Z}{A}\left(\frac{B_o\ell}{pc}\right)\frac{vU}{C^2}$$

In the interplanetary medium, the average energy loss per collision is determined by the relative velocity of recession of the different scattering centers, (or effective scattering radius). This in turn depends on the geometry of the expanding interplanetary region as well as possible variations of U with radius. For example, assuming an isotropic velocity distribution of particles and a uniformly expanding spherical region of radius R and surface expansion velocity U, the relative velocity of the individual centers, $\Delta U = (\frac{\lambda}{R})$ (where λ is the scattering M. F. P. discussed earlier). This situation may not be realistic for the interplanetary medium, however, since it is known that U is essentially constant along a solar radius vector. In this case there is expansion only in the direction at right angles to the radius vector. In this case $\Delta U = \frac{2}{3}(\frac{\lambda}{r})\,U$ where r is the distance from the sun. Since the mean number of collisions/unit time is v/λ then:

$$\frac{d\varepsilon_{nuc}}{dt} = -\alpha_s\,\varepsilon;(\rho >> \ell);\ \alpha_s = \frac{4}{3}\frac{v^2}{c^2}\frac{U}{r}$$

and

$$\frac{d\varepsilon_{nuc}}{dt} = -\alpha_t\,\varepsilon;(\rho \gtrsim \ell);\ \alpha_t = \frac{Z}{A}\left(\frac{B_0\ell}{pc}\right)\frac{\alpha_s}{2}$$

(at the earth, for example, with $v \approx c$, $U = 4 \times 10^7$ cm/sec $\alpha_s \approx 3 \times 10^{-6}$ / sec).

Now during a time dt the particles will diffuse a distance dr by a random walk. After n collision in an infinite isotropic diffusing medium the average particle will move a distance $d^2 = 2N\ \lambda^2$ from its starting point. One can define an average velocity for diffusion over a distance d as $v_d = \frac{2\lambda v}{d}$ so that a particle will take a time $t = \frac{d^2}{\lambda v}$ to move a distance d in the medium. If we take $\lambda = 2 \times 10$ cm and d = 10 AU, then $t = 5 \times 10^6$ sec for a particle to diffuse into the center of the solar system. Thus, $\left(\frac{\Delta\varepsilon}{\varepsilon}\right) \approx 1$ and it seems unavoidable that this process will produce a significant change in particle energy. As a result according to Liouville's theorem, there is a change in the differential energy spectrum given by: $\Delta j\varepsilon/j \approx \Delta\varepsilon/\varepsilon$ or in the differential momentum spectrum by $\Delta jp/j \approx 2\Delta P/P$. An additional change will occur because of the spectrum of the radiation. Since the spectrum is a complicated function at low energies the change can be treated separately by an iteration process and we shall neglect this effect here.

Using the fact that $dt = -\frac{dr}{v_d}$ we can write:

$$\frac{dj}{j} = -\alpha \frac{dr}{v_d}$$

Taking $j = j_o$ at $r = R$ and integrating gives:

$$j(\varepsilon, r) = j_o(\varepsilon_o, R) \exp -\frac{\alpha\; r\,(R-r)}{2\lambda v}$$

This modulation is seen to have much the same form as that resulting from diffusion-convection given on p-4. It cannot be compared directly in magnitude since no account of the spectrum or of betatron deceleration effects has been taken in this simple treatment. However, we may compare the charge to mass dependence of the modulation for different types of scattering by inserting the appropriate values of α and λ. This gives:

$$j(\varepsilon, r) = j_o(\varepsilon_o, R) \exp -\frac{Z}{3A}\left(\frac{v^2}{C^2}\right)\left(\frac{B.\ell}{pc}\right)\chi \qquad (\rho \geq \ell)$$

and

$$j(\varepsilon, r) = j_o(\varepsilon_o, R) \exp -\frac{2}{3}\left(\frac{v^2}{C^2}\right)\chi ; \; (\rho \ll \ell)$$

We see that for $\rho \ll \ell$ the charge to mass dependence is contained in χ as with diffusion-convection and the inverse Fermi energy loss cannot explain the observations. (Note that this term becomes relatively less important than diffusion-convection at low energies for this type of scattering).

For ($\rho \geq \ell$) the fractional modulation at low energies is $\frac{Z}{A} \cdot \frac{1}{v}$ -- becoming $\frac{Z}{A} \cdot \frac{1}{p^2}$, at high energies. Such a modulation is in agreement with the observations at low energies, but is somewhat too strong a function of P at high energies. Thus although the data at low energies could be explained by the inverse Fermi process alone it is likely that both this process and diffusion-convection play a role in both energy ranges -- with the relative mangitude of each varying with energy. This possibility is further heightened by the fact that a continuous distribution of scattering lengths (and M.F.P.) probably exists in interplanetary space. Even with such a distribution the diffusion convection picture cannot explain the results, however.

Finally we should note that there is need to investigate the effects of the spectrum term itself on the fractional and relative modulations as well as the effects of betatron deceleration. This later effect is, in fact, very similar to the diffuse scattering ($\rho \geq \ell$) inverse Fermi effect -- for in both cases a net loss of energy is continuously occurring.

FIGURE CAPTIONS

Figure 1 Ratios of fractional changes measured in low energy protons and helium nuclei to those observed in neutron monitors. The energy dependence of the modulation of both protons and helium nuclei is ~$1/\beta$ but at the same velocity the fractional change of protons is ~2 x as great.

Figure 2 Data presented in Figure 1, plotted (squares) as a function of rigidity and showing equal proton and helium modulation at the same rigidity. Circles show proton and helium modulation derived from all available data extending over the entire solar cycle and discussed in the text.

REFERENCES

Dorman, L. I., (1963) Proc. Int. Cosmic Ray Conf. (Jaipur) 2, 73.

Ehmert, A., 1960, Proc. Moscow Conf. on Cosmic Rays, 4, 142.

Freier, P. S. and C. J. Waddington, 1965, Space Science Reviews 4, 313.

Gloeckler, G.,1965, Ph.D. Thesis, University of Chicago.

Laster, H.,A. H. Lenchek and S. F. Singer, 1962,J.Geophys. Res.,67, 2639.

McDonald, F. B. and W. R. Webber, 1959, Phys. Rev. 115, 194.

McDonald, F. B. and G. H. Ludwig, 1964, Phys. Rev. Letters 13, 783.

Parker, E. N.,1963, "Interplanetary Dynamical Processes". Interscience, New York and earlier references.

Parker, E. N. 1965, Planet. Space Sci., 13, 9.

Quenby, J. J., (to be published, 1965), Handbuch der Physik, 47.

Webber, W. R. and F. B. McDonald, 1964, J. Geophys. Res. 69, 3097.

Webber, W. R. (to be published, 1965), Handbuch der Physik, 47.

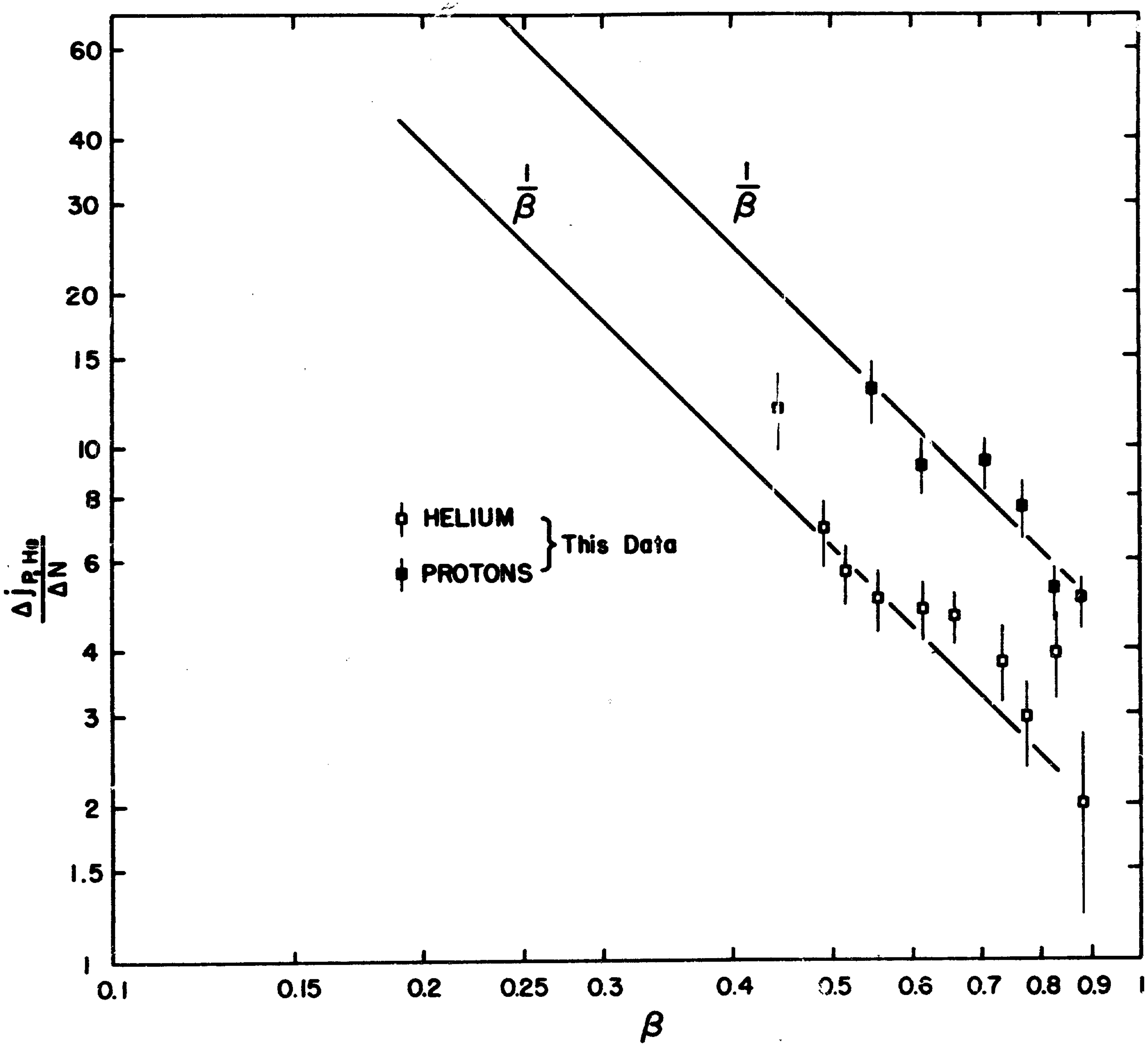
60
40
30
20
15
10
8
6
4
3
2
1.5
1
0.1
0.15
0.2
0.25
0.3
0.4
0.5
0.6
0.7
0.8
0.9
1
β
$\frac{\Delta j_{P, He}}{\Delta N}$
$\frac{1}{\beta}$
$\frac{1}{\beta}$
HELIUM
PROTONS
This Data

Figure 1

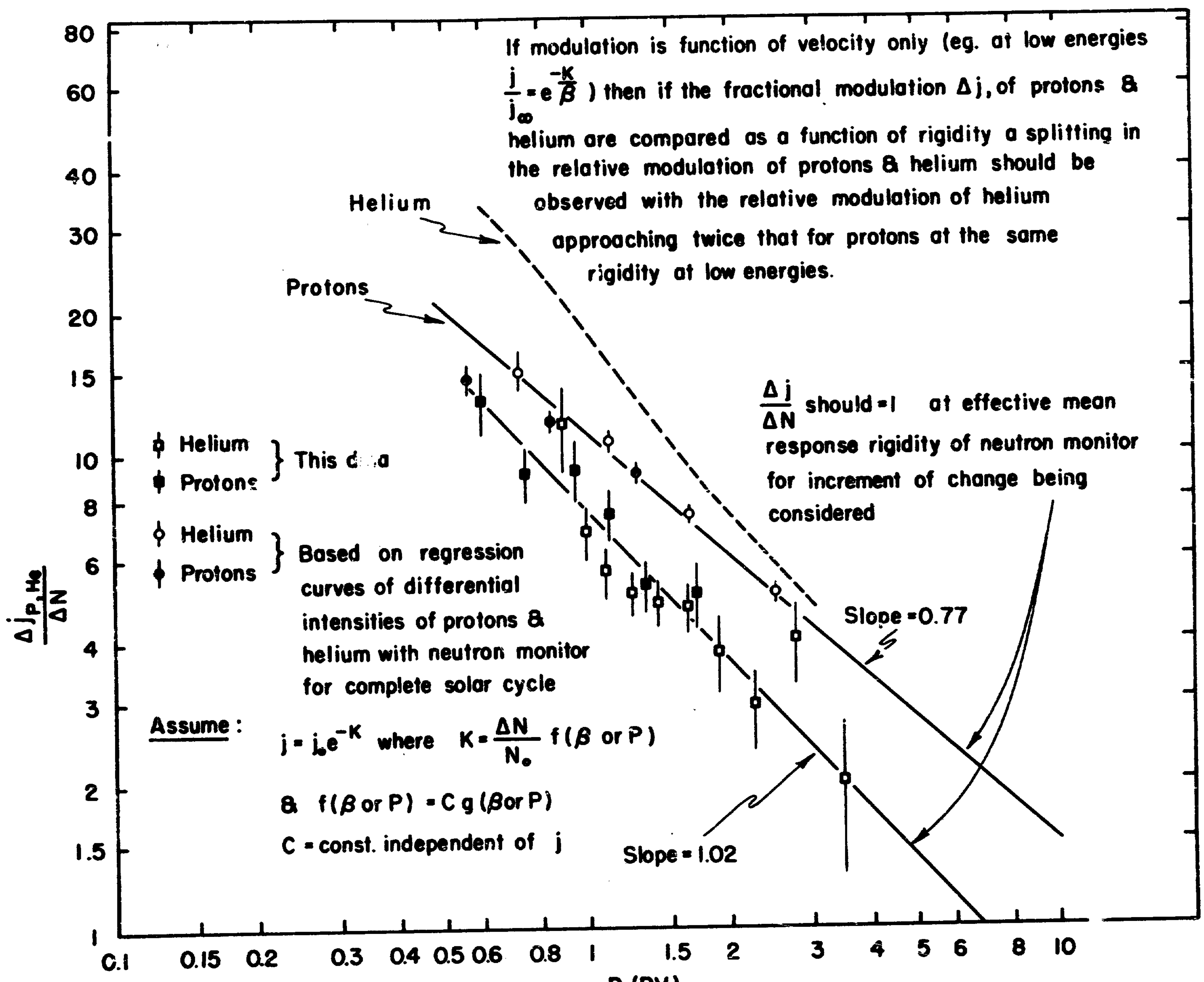

If modulation is function of velocity only (eg. at low energies $\frac{j}{j_\infty} = e^{-\frac{K}{\beta}}$) then if the fractional modulation Δj, of protons & helium are compared as a function of rigidity a splitting in the relative modulation of protons & helium should be observed with the relative modulation of helium approaching twice that for protons at the same rigidity at low energies.
Helium
Protons
Helium
Protons
This data
Helium
Protons
Based on regression curves of differential intensities of protons & helium with neutron monitor for complete solar cycle
$\frac{\Delta j}{\Delta N}$ should = 1 at effective mean response rigidity of neutron monitor for increment of change being considered
Slope = 0.77
Slope = 1.02
Assume:
$j = j_\infty e^{-K}$ where $K = \frac{\Delta N}{N_\infty} f(\beta \text{ or } P)$
& $f(\beta \text{ or } P) = C\, g(\beta \text{ or } P)$
C = const. independent of j
$\frac{\Delta j_{P,He}}{\Delta N}$
P (BV)

Figure 2

N66-13362

RAPPORTEUR PAPER ON "SPECTRA"

by

C. J. Waddington

This paper attempts to summarize some of the more striking and interesting results reported to this conference during the sessions on "Spectra". Inevitable, due to the limited space available and the large number of papers presented in these sessions, some form of selection has been essential and it has been necessary to omit any reference to some important and interesting results which have not conveniently fitted into the framework of this report. This selection reflects the author's personal bias and should not be taken to imply any judgment on the scientific worth of these omitted papers.

The sessions on Spectra, together with a few papers in other sessions, covered essentially five different aspects of cosmic ray studies. Each of these will be considered in turn.

(1) X-ray and γ-ray astronomy:

Following a review paper by Oda(invited paper) which summarized current development in this field, several papers were presented to this conference on high energy x-ray and γ-ray observations made from balloons or sounding rockets. Previously only one point source of high energy (15-60 kev) x-rays had been reported in the literature. Details of this observation of the Crab Nebula with a detector flown on a balloon were given to this conference by Clark (SPEC 2) while McCracken (SPEC 2a) reported the observation of another point source in the vicinity of Cygnus A, using a detector very similar to that employed by Clark. The angular resolution of this detector was inadequate to distinguish between Cygnus A and Cygnus X-1, the source of soft x-rays detected previously, which are some 6° apart. However, it seems reasonable to postulate that McCracken did indeed observe the latter source, since Cygnus A does not appear to be a strong source of soft x-rays. A third observation of point sources of energetic x-rays came from Hayakawa et al (ACCEL 6) who reported rocket observations on 5-20 keV photons and saw point sources coinciding with Scorpio X-1 and Cygnus X-1. These workers also reported observations on the general isotropic background which revealed x-rays having the same spectral form as those observed for point sources but having appreciably greater intensity than that observed for any individual source. In general, these observations on x-ray sources and on the isotropic background indicate that the subject of x-ray astronomy is active and rapidly developing, and a field that should have been covered in much greater detail in a conference on cosmic radiation.

Gamma-ray astronomy, on the other hand, still has some resemblence to the discipline of exobiology, in that as yet neither subject has any definitive data to impede theoretical speculation. No point source of energetic, $E > 10$ MeV, γ-rays has been detected thus far nor is there definitive evidence for a general background. Thus, the experimental data consists solely of flux limits for the background and for various likely point sources. At this conference, Cobb et al (SPEC) reported the lowest flux limit yet obtained for any object, quoting a limit for the Crab Nebula of less than 5.10^{-5} γ/cm^2 sec for the flux of γ-rays having $E \geq 100$ MeV as well as a number of higher limits for other possible astronomical sources. These limiting values were obtained from a spark chamber array flown on a high altitude balloon near the equator and illustrate the advantages in reduction of background that can be obtained by equatorial flights. Finally, at much higher energies, Fruin et al (SPEC 3) described observations made with groundbased Cerenkov detectors which set upper limits of 10^{-11} to 10^{-12} γ/cm^2 sec on the fluxes of γ-rays with $E > 10^{13}$ eV from a number of quasars and other plausible sources. These limits are very similar to those obtained with similar techniques by Chudakov et al (1963) for a number of other celestial objects.

(2) Electrons in the Primary Cosmic Radiation:

The observation and detailed study of primary electrons in the cosmic radiation is of great interest both to astrophysicists and radio astronomers. Current knowledge of the properties of these particles was summarized in an invited paper by Meyer. A number of new results were reported at this conference which related to the intensity, energy spectrum and charge ratio.

The various results reported for the intensity are shown in Figure 1 which illustrates the wide spread that exists in these values. Shown are the integral intensities reported by Agrinier et al (SPEC 8), Rubtsov (SPEC 6), Daniel and Stevenson (SPEC 9) and Waddington and Freier (SPEC 10), together with the integral spectrum between 0.5 and 3.0 GeV calculated from the differential spectrum of $dJ/dE = 11 \times E^{-1.6 \pm 0.4}$ electrons/m^2sec. ster. GeV reported by L'Heureux and Meyer (SPEC 5). It is apparent from this figure that the results of Rubtsov are in disagreement with those reported by other workers. Since the counter array used in this experiment has not been calibrated with a beam of electrons of known energy and since it represents a rather complex and devious method of electron detection, it would appear that the acceptance of these results must await further experimental confirmation.

Observations on the energy spectrum of the electrons are collected in Table I which lists the values of the integral and differential exponents of the quoted spectra on the assumption that this can be represented by a power law of the form $dJ/dE = KE^{-\gamma}$ over the range of energies covered in each experiment. Included in this table are the results of Bleeker et al (SPEC 7) who reported a value for the spectrum but were unable to determine an absolute intensity. An examination of this table shows that at the lower energies this spectrum is apparently not as steep as that of the primary cosmic radiation, but that at higher energies, there is some indication of a steepening. If verified, this behavior should

A. E. Chudakov, V. L. Dadykin, V. I. Zatsepin and N. M. Nesterova, Jaipur Conf. 4, 199 (1963).

provide an interesting indication of the nature and propagation of these electrons, although the possibility that these changes in the form of the spectrum are simply the consequence of residual solar modulation effects should not be disregarded. None of the results reported thus far have been accurate enough to permit any study of the effect of solar modulation but it would appear from the two values quoted by Waddington and Freier for 1963 and 1964 and the agreement between the value reported here by Agrinier et al and that reported previously, that solar modulation effects are not grossly more serious than those observed for protons of similar rigidity.

Agrinier et al and Daniel and Stephens both reported using the east-west effect to examine the positron-negatron ratio of ~4 and 15 GeV electrons respectively. Agrinier et al found that their data was consistent with the electrons all being negatively charged and reported that even in the limiting case of an infinitely steep energy spectrum $e^-/(e^+ + e^-) > 0.62$. This result is in agreement with the negatron excess reported by Meyer in his review paper for electrons of rather lower energy. At very high energies, ~15 GeV, Daniel and Stephens examined this problem but have as yet results of extremely limited statistical weight and can not really draw meaningful conclusions.

It was pointed out by several authors that the general run of the intensities shown in Figure 1 are considerably too great to be accounted for solely by the secondary production of electrons during the passage of the nucleonic cosmic radiation through reasonable amounts of interstellar matter. The essentially primary nature of these electrons is also suggested by the negatron excess observed by Meyer and by Agrinier et al and it appears reasonably well established by now that the electrons observed near the earth mainly originate in accelerative processes.

(3) Protons and Helium Nuclei:

Studies of the low and intermediate energy protons and helium nuclei in the primary cosmic radiation present one of the most direct and critical ways of investigating the processes of solar modulation. The shapes of the low energy spectra of nuclei having different charge to mass ratios and the temporal variations of the differential intensities represent data which must be explainable by an acceptable model of solar modulation. However, only in the past few years has it been possible to make measurements of good statistical weight and small apparent systematic error on the protons and the helium nuclei. As a consequence, it is only now at this conference that results have been reported which reliably measure the temporal changes of these components and thus impose severe limitations on the possible modulation processes.

In the intermediate energy range, from the atmospheric cut-off for balloon borne detectors of ~80 MeV per nucleon, to the relativistic region of ≥ 1 GeV per nucleon, the results of greatest statistical weight were those presented by Ormes and Webber (SPEC 12,13). These are illustrated in Figures 2 and 3 which show the differential proton and helium rigidity spectra observed in 1963 and in 1964. The effects of solar modulation can be clearly seen in these figures and it may be noted that over this time period the protons at a given rigidity clearly experienced a larger increase than did the helium nucle. A comparison of the energy per nucleon spectra, i.e. velocity spectra, showed this differential behavior even more clearly. A similar effect was noted by Waddington and Freier (SPEC 10) whose results, which also cover 1963 and 1964 but are of lower statistical weight, are in good agreement with those of Ormes and Webber, suggesting that there are no serious systematic errors present in either of these measurements. This general agreement is largely supported by several other results reported here on proton or helium nuclei measured at times comparable either with 1963 or 1964, Neelakanton (SPEC 17), Fichtel et al (SPEC 19) and Balasubrahmanyan et al (SPEC 31), and even possibly with the somewhat discordant results presented by Courtier and Linney(SPEC 21). However, this agreement is not perfect and it must be emphasized that there is no external evidence to prove that Ormes and Webbers' results do not suffer from systematic errors of as much as 5%. As a consequence, the lack of statistical errors on Figures 2 and 3 should not be taken too seriously when absolute values are being considered, although such systematic errors, if present, should not be so serious in the study of comparative changes. It thus seems that it is now possible to make rather precise studies of the temporal behavior of these particles provided sufficient care is taken in the analysis and in correcting for background effects. These results have already placed stringent requirements on the models of solar modulation, and should lead to greatly improved models.

One word of caution may be interposed here. Many of the earlier results, those for example, on the helium nuclei, appear to exhibit gross differences even when periods of apparently similar solar modulation were compared. However, most of these results were obtained at times of high solar modulation, when interplanetary conditions were extremely disturbed. It is possible that the large measure of agreement being obtained at present is more a function of the relative solar inactivity than of more reliable experimental data, and that violent disagreements may again appear with the onset of the new solar cycle and increased solar activity.

At high energies, > 5 GeV per nucleon, Neelakantan and Shukla (SPEC 16) and Agarwal et al (ISOT2) reported observations on the energy spectrum of helium nuclei and the intensities of protons and helium at 16.8 GV rigidity which appear to be an improvement on those previously reported, but do not represent any drastic change.

Some of the most interesting results on these nuclei were those reported on the low energy, E < 80 MeV per nucleon, particles observed with satellites. Fan et al (SPEC 22) reported observations on low energy helium nuclei made between late 1963 and the end of 1964. Figure 4 shows the steady increase in differential intensity and the flattening of the energy spectrum with decreasing solar activity that typified those nuclei having $40 \leq E \leq 80$ MeV per nucleon. It also shows evidence for a component of still lower energy helium nuclei, $7 \leq E \leq 20$ MeV per nucleon, which falls sharply with increasing energy. These particles are apparently associated with even steeper proton energy spectra and show large temporal variations although there is apparently always a finite intensity present. A similar turn-up in the energy spectrum of the helium nuclei observed in 1965 was reported by Balasubrahmanyan et al (SPEC 31), Figure 5, but these workers did not extend their measurements to quite such low energies as did Fan et al, and, possibly as a result, did not observe an associated turn-up in the proton spectrum except at times associated with definite solar activity. The origin of these low energy particles appears to be quite obscure at present. They could have been accelerated on the sun or in the interplanetary medium. Alternatively, they could be particles of such low rigidity that they can preferentially leak through the solar modulation barrier.

A final result of interest in this section was the report by Balasubrahmanyan et al (SPEC 31) that between 1963 and 1965 and for energies between 50 and 100 MeV per nucleon, the helium nuclei apparently showed a larger increase in intensity than did the protons. This is the reverse of what was observed by Ormes and Webber (SPEC 13) and Waddington and Freier (SPEC 10) between 1963 and 1964 for $E \geq 100$ MeV per nucleon. The most logical explanation of this discrepancy would appear to be that in 1965 the low energy additional component of helium nuclei described above was of such a magnitude as to produce this effect. This would imply an appreciable steady intensity of these nuclei at or near solar minimum which is sharply diminished at other times.

(4) Isotopic Composition:

Prior to this meeting there had been a number of reports on the relative abundance of the He^3 and He^4 nuclei which had, with just one exception, depended on obtaining experimental mass resolution between these nuclei in nuclear emulsion detectors. At this conference, several new determinations of the ratio, Γ, of He^3

to ($He^3 + He^4$) were reported, two of which depended on electronic dE/dx versus total E measurements. The resolution obtained in these observations was clearly superior to that obtained in even the most painstaking and careful emulsion measurement, O'Dell et al (SPEC 33) and it seems clear that emulsions inherently lack the uniformity necessary to permit unambiguous separation even between isotopes as dissimilar as He^3 and He^4. The various ratios reported as a function of rigidity or energy per nucleon are given in Table II. Of these results that due to Balasubrahmanyan et al (SPEC 31) is a preliminary value taken from data showing rather clear resolution on OGO-I, that due to Hofmann and Winckler (SPEC) shows similarly good resolution and is from a balloon flight made at a time, May 1965, when solar modulation was apparently at a minimum. The emulsion data reported by O'Dell et al (SPEC 33) shows fair resolution which, however, is not as clear as that of the previous experiments, while Biswas et al (SPEC 18) reported results having barely adequate resolution. Finally, Agarwal et al (ISOT2) used a variable pressure gas Cerenkov counter to study this ratio at an extremely high rigidity. These results are at present of limited statistical weight, but it is to be hoped that they will be improved in the near future since a measurement of this ratio at high energies will be of considerable importance, particularly in view of the suggestions that the fragmentation path length measured by the L-nuclei may be energy dependent. Examination of Table II shows reasonable agreement between the various reported results, particularly when it is appreciated that the apparently anomalous value for $\Gamma(R)$ reported by O'Dell et al is for a range of rigidities higher than that of the other experiments, where the shape of the energy spectrum is varying rapidly.

(5) Heavy Nuclei, $Z \geq 3$:

Four years ago at the Kyoto Conference, it finally became possible to state that general agreement had now been obtained on the relative abundance of the fragmentation nuclei, lithium, beryllium and boron, L-nuclei, to the heavier, S-nuclei. This agreement applied essentially to the integral value of the L/S ratio measured above 1.5 GeV per nucleon, i.e. to nuclei having a mean energy of 3-4 GeV per nucleon. At this conference, papers have been presented which discuss the variation of this ratio with energy and which show an unusual and unexpected variation in this ratio of very low energies.

In the intermediate energy range, the data of greatest statistical weight was that presented by Webber et al (SPEC 30). Similar comments regarding the significance of these statistical errors relative to possible systematic errors should be applied to these results as were applied in Section 3 to the results of Ormes and Webber on protons and helium nuclei. Figure 6 shows the L/M ratio, where M-nuclei have $6 \leq Z \leq 9$, plotted both as a function of rigidity and energy per nucleon as observed by these authors. It can be clearly seen that this ratio increases as the rigidity or energy decreases, with an indication that it reaches a maximum at about 400 MeV per nucleon. On these data the evidence for a maximum is not conclusive, but other experiments reported here which are discussed below clearly showed that at low energies the ratio falls appreciably. The general trend and magnitude of the values shown in this figure agreed well with the results reported by Anand et al (SPEC 27) and by Freier and Waddington (SPEC 24), both of whom observed values for the L/M ratio which were appreciably higher at 0.3 - 0.5 GeV per nucleon than at higher energies.

Another interesting consequence of the great statistical weight of the results obtained by Webber et al is that they were able to compare the energy spectra of the various charge groups with those of the helium nuclei. This comparison is shown in Figure 7 and indicates that possibly the M and LH-, $10 \leq Z \leq 15$, nuclei have energy spectra whose exponent in the power spectrum, here assumed to be of the form $dJ/dP = KP^{-\gamma}$, is 0.1 to 0.2 greater than that of the helium nuclei. Confirmation of this result would be most important, suggesting as it does that appreciable composition changes may exist between the 10^9 - 10^{10} eV per nucleon typical of these measurements, and the 10^{14} eV and above typical of air shower experiments.

The rather unexpected decrease observed in the L/M ratio at low energies was just one of a number of observations reported here which showed that previous simple minded ideas of the production and propagation of the low energy cosmic ray nuclei must be drastically modified. In its simplest form the model customarily assumed for production and propagation suggests that one initially starts with some unspecified cosmic ray source(s) which inject nuclei into the interstellar matter with a particular energy and charge spectra. These nuclei then propagate through the interstellar medium undergoing fragmentation and ionization losses which change the charge and energy spectrum respectively. The presence of L-nuclei shows almost certainly that fragmentation plays an important role in the overall propagation and in order to explain the data on these nuclei and on the He^3 nuclei at low energies it seems reasonable to assume that the relativistic particles, $E \gtrsim 1$ GeV per nucleon have traversed approximately 3 g/cm^2 of interstellar matter, while those of some 200 - 300 MeV per nucleon have traversed as much as 6 g/cm^2. Now the traversal of such quantities of matter might be expected to produce, as a result of ionization energy losses, very obvious shaping of the low energy end of the energy spectra, with nuclear species of increasing Z being more and more depressed in intensity and more and more sharply cut-off at low energies relative to, for example, the helium spectrum. Apparently this does not happen and there appears to be little or no evidence for appreciable shaping of the energy spectra by ionization loss. It is thus necessary to make a clear distinction between the amount of matter traversed which causes fragmentation and that traversed while the de-acceleration due to ionization loss dominates the accelerative processes acting on the nuclei. In the light of the evidence presented to this conference, it would seem that accelerative processes other than ionization losses are present and dominate during the traversal of most of the matter responsible for fragmentation.

The first report that indicated that something unexpected was occurring at lower energies was the observation by Waddington and Freier (SPEC 25) that the VH-nuclei, $20 \leq Z \leq 28$, which should be those most seriously affected by ionization losses, appeared to have a low energy spectrum similar in shape to that of the helium nuclei. Furthermore, the intensity was that expected from the VH-helium ratio measured at high energies, whereas ionization loss should have depressed the intensity of the VH-nuclei by more than a factor of two. These results are shown in Figure 8 and indicate that these nuclei have passed through appreciably less than 2 g/cm^2 while being influenced solely by ionization loss. More spectacular reults, apparently indicating the same thing, were reported by Comstock et al(SPEC 23) and Balasubrahmanyan et al(SPEC 31),who both reported the observation of appreciable numbers of very low energy heavy nuclei,having an essentially flat energy spectrum in an energy range where the spectrum of the helium nuclei was falling sharply. Figure 9 shows the spectra reported by Comstock et al (SPEC 23) for various nuclei. A comparison of these spectra with that shown in Figure 4 for the helium nuclei shows that far from exhibiting a more steeply falling spectrum these heavy nuclei have much flatter spectra. This is, of course, quite inconsistent with the pure ionization loss hypothesis. Another very interesting aspect of these satellite data is illustrated in Table III which gives the abundances relative to carbon at 100 MeV per nucleon and greater than 600 MeV per nucleon as observed by Balasubrahmanyan et al(SPEC 31). There seems to be a virtually complete absence of lithium and beryllium nuclei at these low energies,but appreciable quantities of boron. As a consequence, the L/M ratio is appreciably less than that observed by,for example, Webber et al, at 300 MeV per nucleon. This general tendency for the relative abundance of the L-nuclei to fall at low energies was also observed by Comstock et al and by Fichtel et al (SPEC 28) and must be accepted as being well established. Whether it is due to energy dependent changes in the fragmentation parameters, which seems most likel particularly in view of the abundance changes within the L-nuclei group,or to some othe cause,must await further experimental study.It is, for example,conceivable that many of these low energy nuclei are of solar origin and that the observed spectra is a combination of solar and galactic components. Philosophically, this is an unattractive assumptions, as it demands a fortuitous coincidence between the intensities of the two components, but it would explain in a natural way the apparent lack of lithium and beryllium at low energies, although then the presence of appreciable amounts of boron becomes puzzling.

These data at low energies are extremely important and it is interesting to compare the various results for checks on the consistency. While the overall agreement between the two satellite experiments is quite good, there are some discrepancies in points of detail. Comstock et al reported appreciably more L-nuclei than did Balasubrahmanyan et al and also claimed that oxygen was more abundant than carbon, the reverse of what is observed at higher energies and what Balasubrahmanyan et al reported. It is not clear at present whether these differences are statistically significant.

The absolute intensity values observed in these satellite experiments appear to be in reasonable agreement with each other and with the values reported by Fichtel et al. It is also interesting to note that the high energy intensity of silicon reported by Comstock et al is in very good agreement with a value quoted by Waddington and Freier (SPEC 25) from a balloon borne detector.

A final observation of a rather different nature concerns the intensity of nuclei appreciably heavier than iron, Z=26. Webber et al and Waddington and Freier each reported systematic observations on rather more than 300 VH-nuclei, $20 \leq Z \leq 28$. The first group saw one probable Z≈40 nucleus and one possible Z≈40 nucleus, while the second group saw just one Z≈32 nucleus. However, at this conference, Walker et al (TECH 9) reported the first results from a new technique which should greatly improve knowledge on the abundance of these nuclei. These workers find that certain crystals in meteoritic material show evidence for damage which was most probably caused by stopping VH-nuclei and that by suitable treatment short tracks appear whose length depends rather critically on the charge of the stopping nucleus. These crystals then behave like very insensitive nuclear emulsions which have had an exposure time equal to the lifetime of the meteorite and, as a consequence, there are large numbers of tracks in small volumes of the crystal. As yet, Walker et al have been unable to calibrate this technique and as a result they did not wish to quote a value for the relative abundance of the $Z \geq 30$ nuclei, however, examination of their data suggests that the ratio of VH-nuclei to still heavier nuclei is about $1:10^{-4}$. This value would suggest that these very very heavy nuclei have an abundance somewhat similar to that of the cosmic abundances, rather than showing the typical cosmic ray overabundance of high charge nuclei. This behavior is what would be predicted by Colgate (ACCE-4) on the basis of his theory of a supernova origin for cosmic rays.

TABLE I

Form of the Electron Energy Spectrum. On assumption that:

$$\frac{dJ}{dE} = KE^{-\gamma}$$

Author	Differential γ	Integral γ^{-1}	Energy Range GeV
L'Heureux and Meyer	1.6 ± 0.5	(0.6)	0.5 - 3.0
Waddington and Freier	1.6[a]	(0.6)	0.5 - 5.0
Bleeker et al	1.9 ± 0.4	(0.9)	2.0 - 15.0
Rubtsov	(2.8)	1.8	3.5 - 8.0
Agrinier et al	(3.0)	2.0 ± 0.5	4.6 - 8.0
Daniel and Stephens	(2.2)	1.2[a]	16 - 50

[a]These are emulsion experiments in which the statistics are really too limited to permit a reasonable determination of γ or γ^{-1}.

TABLE II

Values of the ratio of He^3 to $(He^3 + He^4)$, Γ (R or E), as a function of energy per nucleon or rigidity.

Technique	(R)	ΔR GV	Γ(E)	ΔE MeV/Nucleon	Date	Authors
$\frac{dE}{dx}$ v. E	-	-	0.10-0.15	~50-100	1965	Balasubrahmanyan et al (SPEC 31)
$\frac{dE}{dx}$ v. E	0.39 ± 0.09	~0.8	0.19 ± 0.05	80-150	1965	Hofmann and Winckler(SPEC)
Emulsion	0.32 ± 0.07	0.85-1.12	0.11 ± 0.03	115-210	1963	Biswas et al (SPEC 18)
Emulsion	0.11 ± 0.04	1.2-1.5	0.10 ± 0.03	215-368	1963	O'Dell et al (SPEC 33)
Gas Cerenkov	0.45 ± 0.23	~16.0	-	-	1965	Agarwal et al (TSCT2)

TABLE III

Abundances of various elements relative to Carbon as observed by Balasubrahmanyan et al (SPEC 31)

Element	Abundance	
	E=100 MeV per nucleon	E > 600 MeV per nucleon Under 2.8 g/cm^2 of atmospher
Li	0.01	0.3
Be	0.01	0.2
B	0.3	0.4
C	1.0	1.0
N	0.2	0.3
O	0.8	0.8
F	-	0.04
Ne	-	0.14

FIGURE CAPTIONS:

Fig. 1 Flux values of electrons reported by various groups at this conference, see text.

Fig. 2 The differential rigidity spectra of protons observed in 1963 and 1964, statistical errors are less than the size of the points, Ormes and Webber (SPEC 13).

Fig. 3 The differential rigidity spectra of helium nuclei observed in 1963 and 1964, Ormes and Webber (SPEC 13).

Fig. 4 The differential energy spectra of helium nuclei observed by satellite at a number of periods between 1963 and 1964. Notice that in order to compare these results with those of other workers, the energy scale should be multiplied by four, so that the energies are expressed as energies per nucleon. Fan et al (SPEC 22).

Fig. 5 The differential energy and rigidity spectra of protons and helium nuclei as observed from satellites and balloons in 1965, Balasubrahmanyan et al (SPEC 31).

Fig. 6 The ratio of L to M-nuclei as a function of energy per nucleon and of rigidity, Webber et al (SPEC 30).

Fig. 7 The ratio of the differential intensities of helium nuclei to those of various other charge groups plotted as a function of rigidity, Webber et al (SPEC 30).

Fig. 8 The differential energy spectrum of VH-nuclei as observed in 1964. The curve labeled VH(1964) shows the expected form of this spectrum if the VH-nuclei had passed through just 2 g/cm^2 of interstellar hydrogen and had an energy spectrum similar to that of the helium nuclei shaped by

Fig. 8 (continued)

ionization energy loss, Waddington and Freier (SPEC 25).

Fig. 9 The differential energy spectra of several different species of nucleus as observed on OGO-I. Comstock et al (SPEC 23).

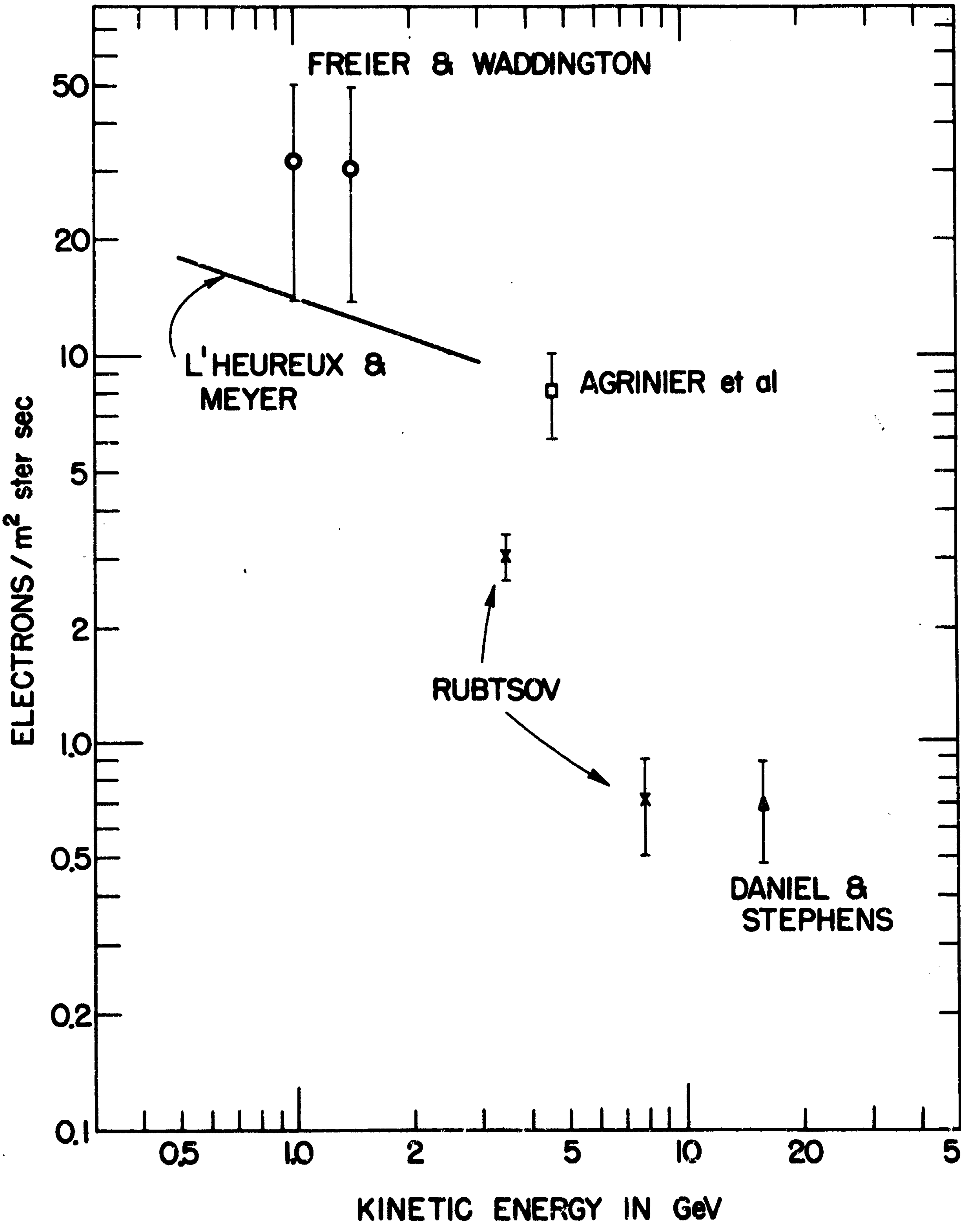
FREIER & WADDINGTON
L'HEUREUX & MEYER
AGRINIER et al
RUBTSOV
DANIEL & STEPHENS
ELECTRONS / m² ster sec
KINETIC ENERGY IN GeV
50
20
10
5
2
1.0
0.5
0.2
0.1
0.5
1.0
2
5
10
20
50

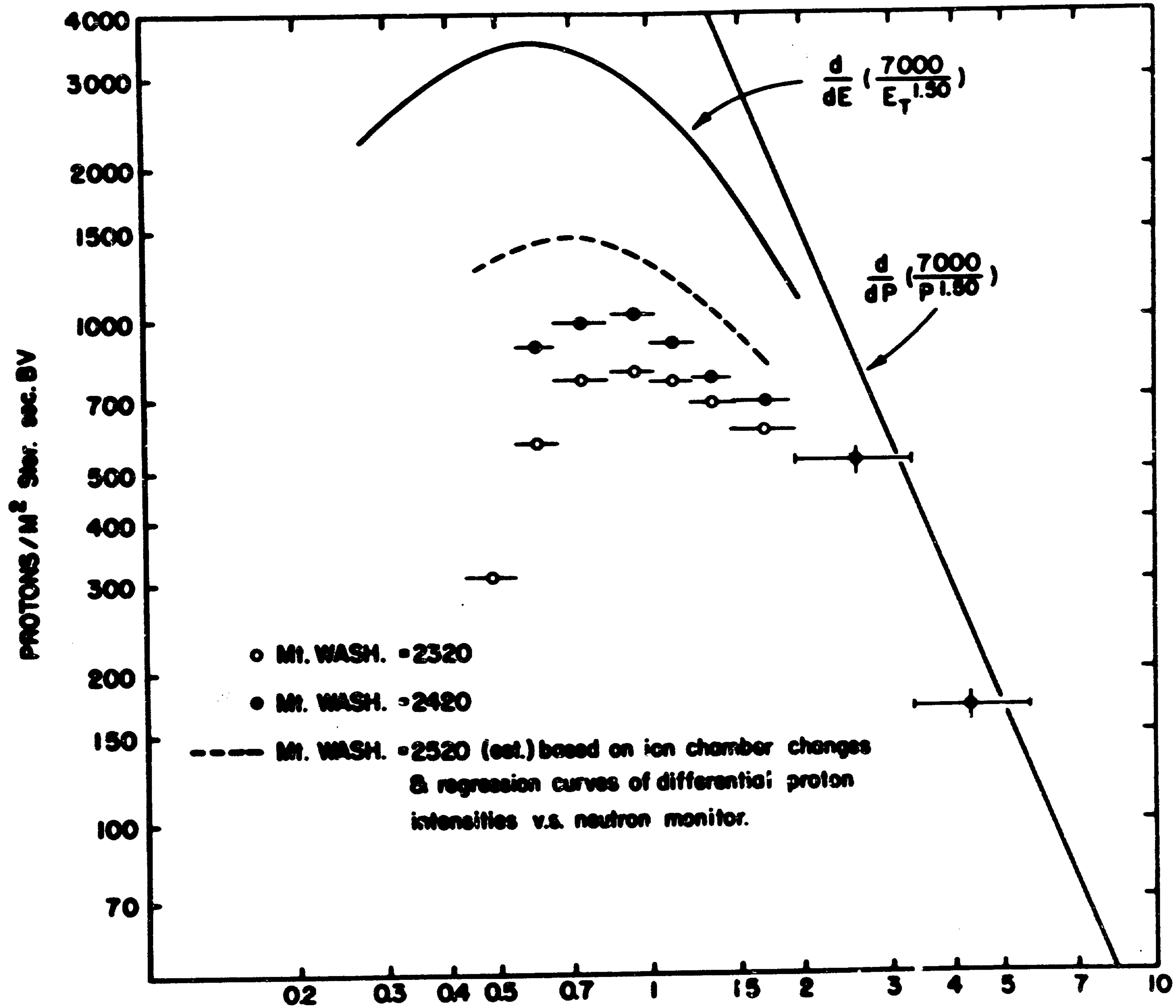

4000
3000
2000
1500
1000
700
500
400
300
200
150
100
70
PROTONS/M² Ster. sec. BV
0.2
0.3
0.4
0.5
0.7
1
1.5
2
3
4
5
7
10
$\frac{d}{dE}\left(\frac{7000}{E_T^{1.50}}\right)$
$\frac{d}{dP}\left(\frac{7000}{P^{1.50}}\right)$
○ Mt. WASH. #2320
● Mt. WASH. #2420
– – – Mt. WASH. #2520 (est.) based on ion chamber changes & regression curves of differential proton intensities v.s. neutron monitor.

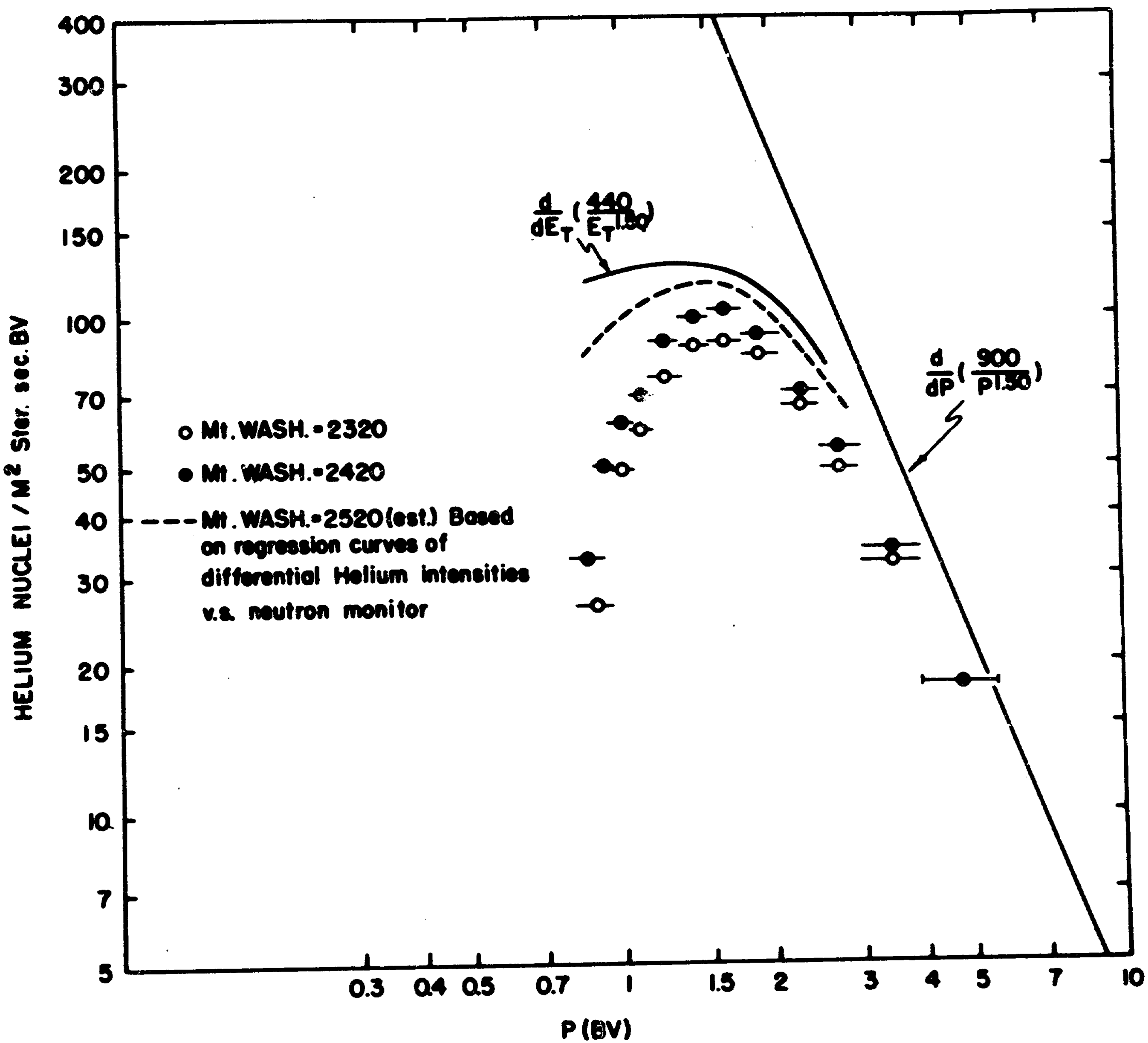

HELIUM NUCLEI / M^2 Ster. sec. BV
400
300
200
150
100
70
50
40
30
20
15
10
7
5
0.3
0.4
0.5
0.7
1
1.5
2
3
4
5
7
10
P (BV)
$\frac{d}{dE_T}\left(\frac{440}{E_T^{1.50}}\right)$
$\frac{d}{dP}\left(\frac{900}{P^{1.50}}\right)$
o Mt. WASH. = 2320
● Mt. WASH. = 2420
Mt. WASH. = 2520 (est.) Based on regression curves of differential Helium intensities v.s. neutron monitor

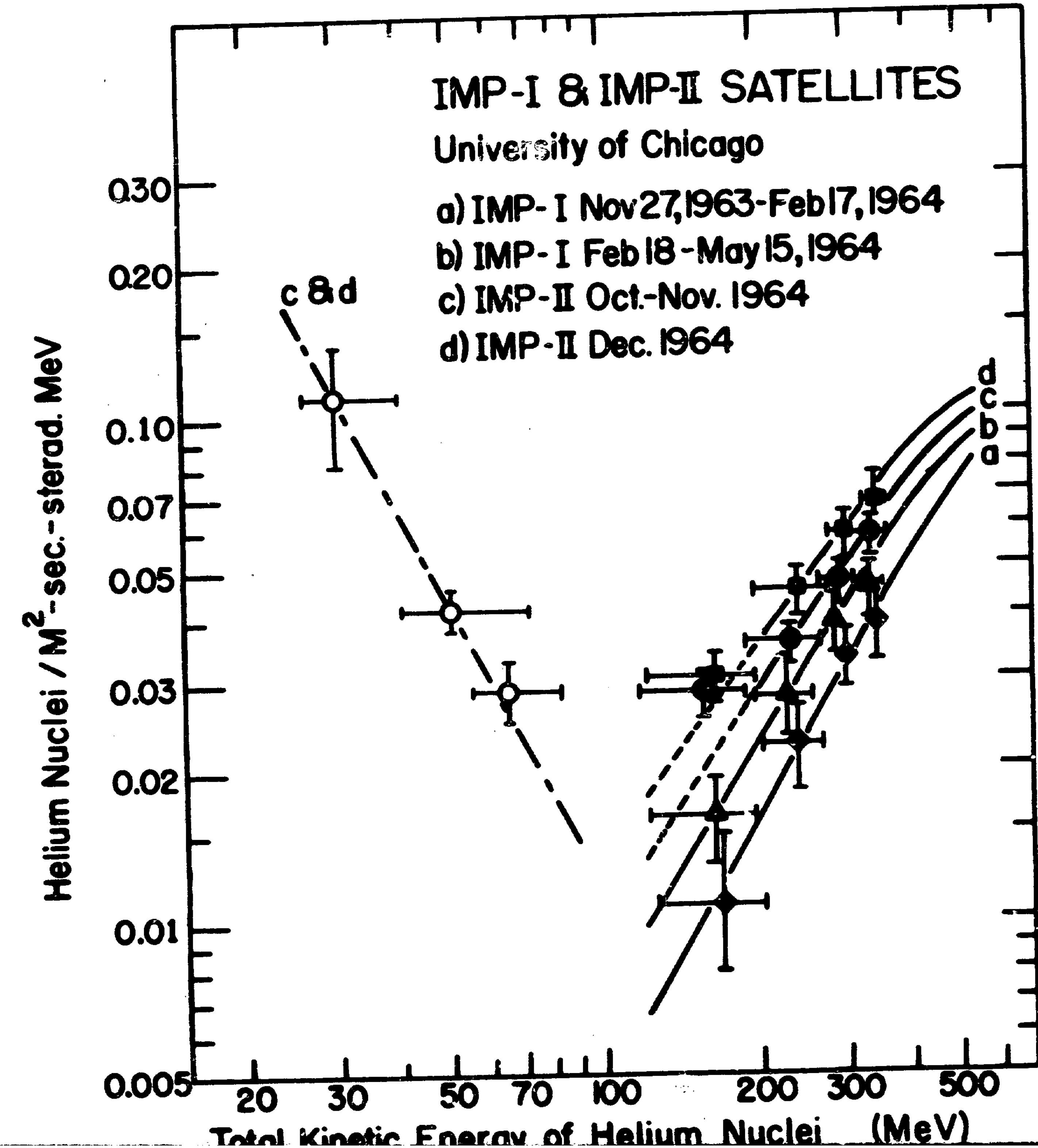
IMP-I & IMP-II SATELLITES
University of Chicago
a) IMP-I Nov 27, 1963-Feb 17, 1964
b) IMP-I Feb 18-May 15, 1964
c) IMP-II Oct.-Nov. 1964
d) IMP-II Dec. 1964
c & d
a
b
c
d
Helium Nuclei / M^2-sec.-sterad. MeV
0.30
0.20
0.10
0.07
0.05
0.03
0.02
0.01
0.005
20
30
50
70
100
200
300
500
Total Kinetic Energy of Helium Nuclei (MeV)

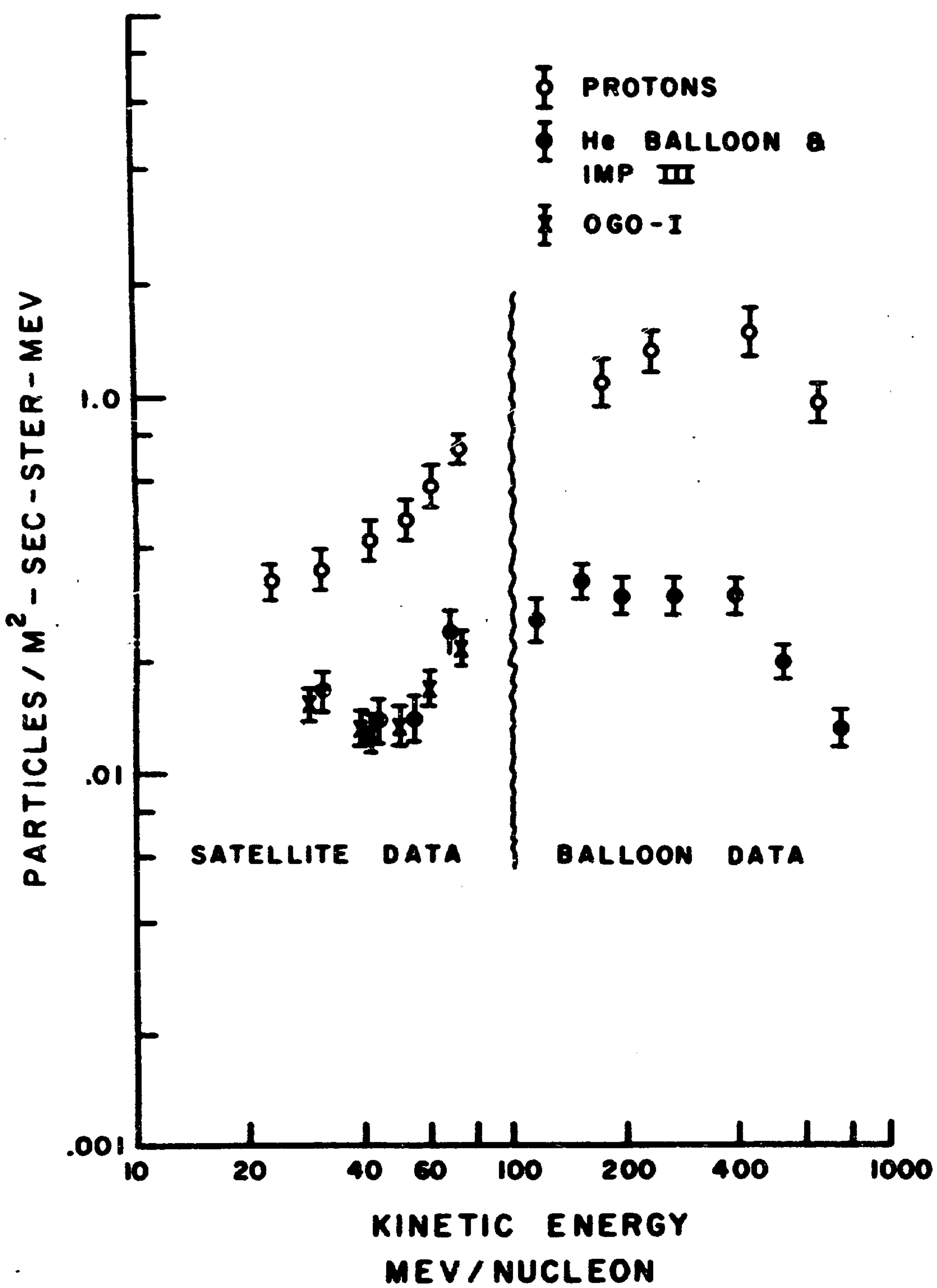
PROTONS
He BALLOON &
IMP III
OGO-I
SATELLITE DATA
BALLOON DATA
PARTICLES / M² - SEC - STER - MEV
1.0
.01
.001
10
20
40
60
100
200
400
1000
KINETIC ENERGY
MEV/NUCLEON

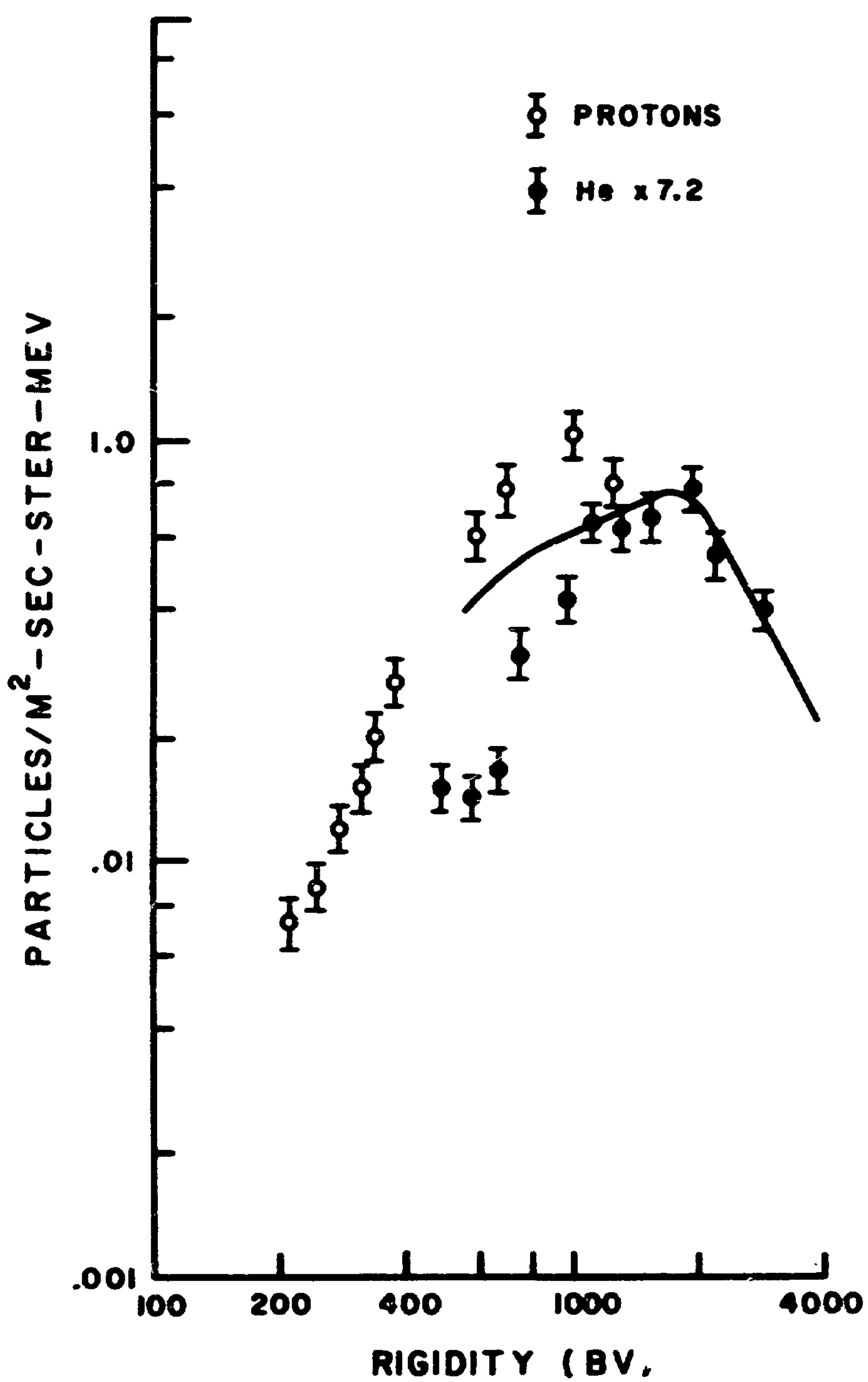
PROTONS
He x 7.2
PARTICLES/M²-SEC-STER-MEV
1.0
.01
.001
100
200
400
1000
4000
RIGIDITY (BV.

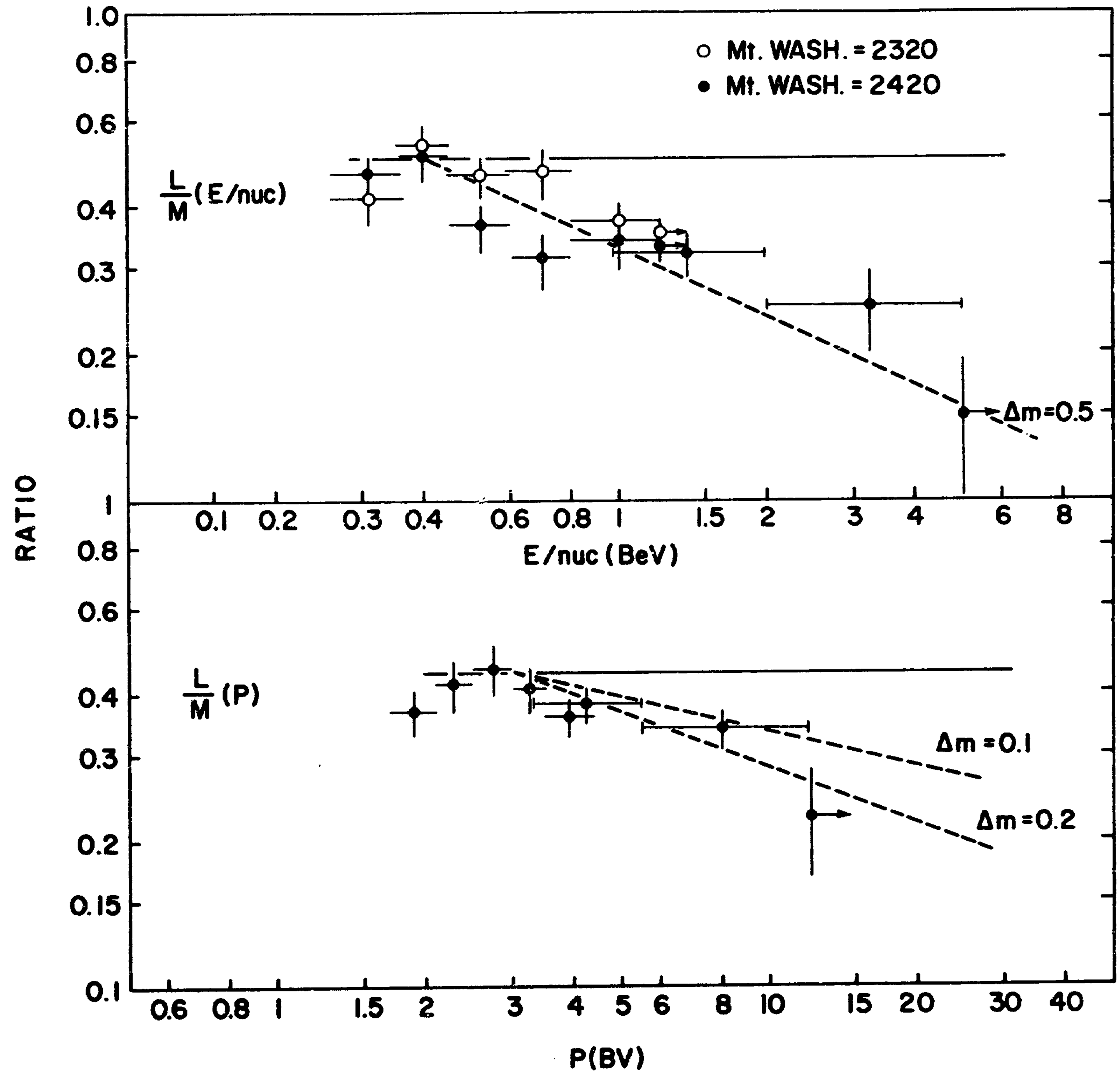

Mt. WASH. = 2320
Mt. WASH. = 2420
L/M (E/nuc)
Δm=0.5
E/nuc (BeV)
RATIO
L/M (P)
Δm=0.1
Δm=0.2
P(BV)

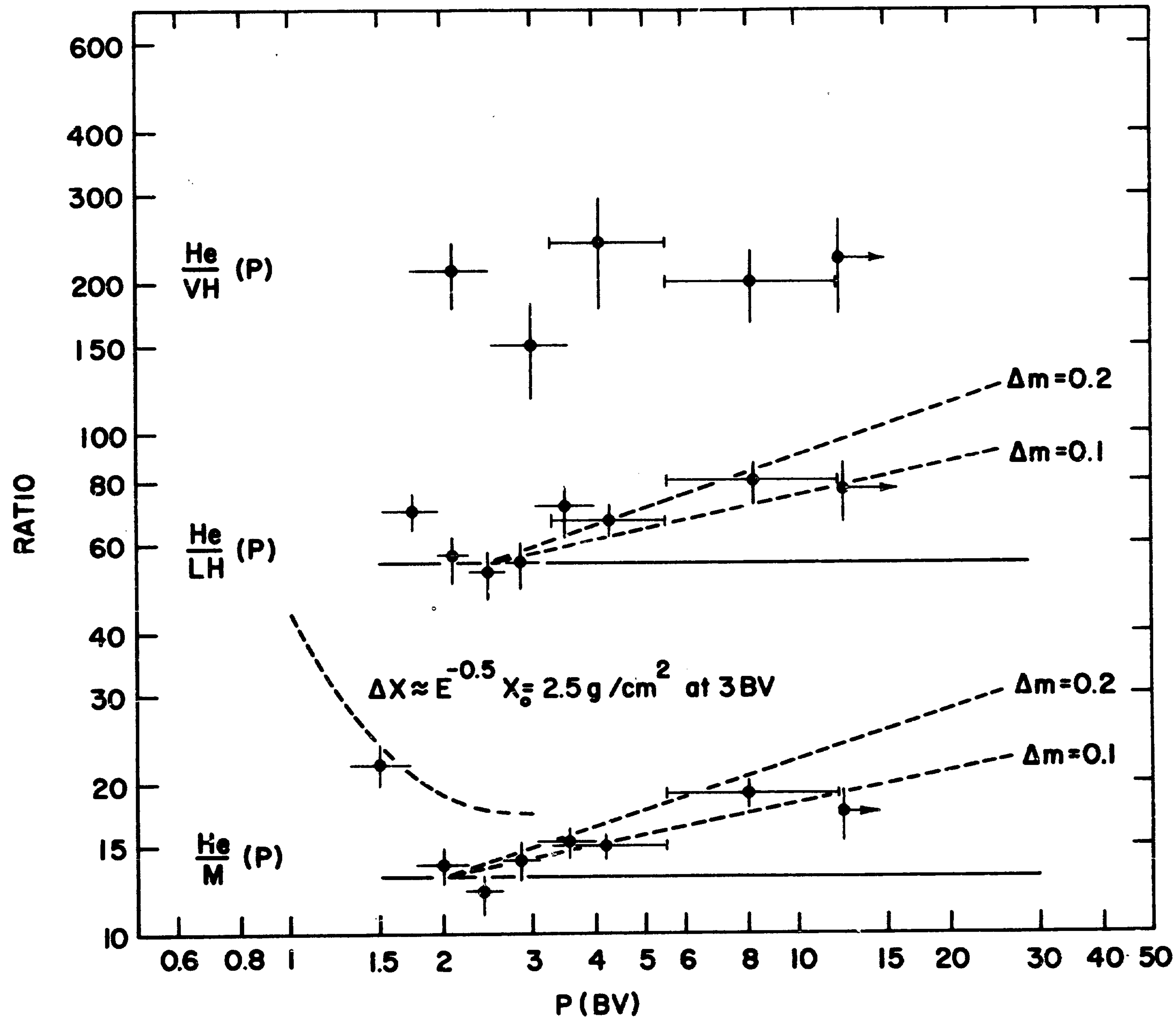

RATIO
600
400
300
200
150
100
80
60
40
30
20
15
10
He/VH (P)
He/LH (P)
He/M (P)
Δm=0.2
Δm=0.1
Δm=0.2
Δm=0.1
ΔX≈E^-0.5 X₀= 2.5 g/cm² at 3BV
0.6
0.8
1
1.5
2
3
4
5
6
8
10
15
20
30
40
50
P (BV)

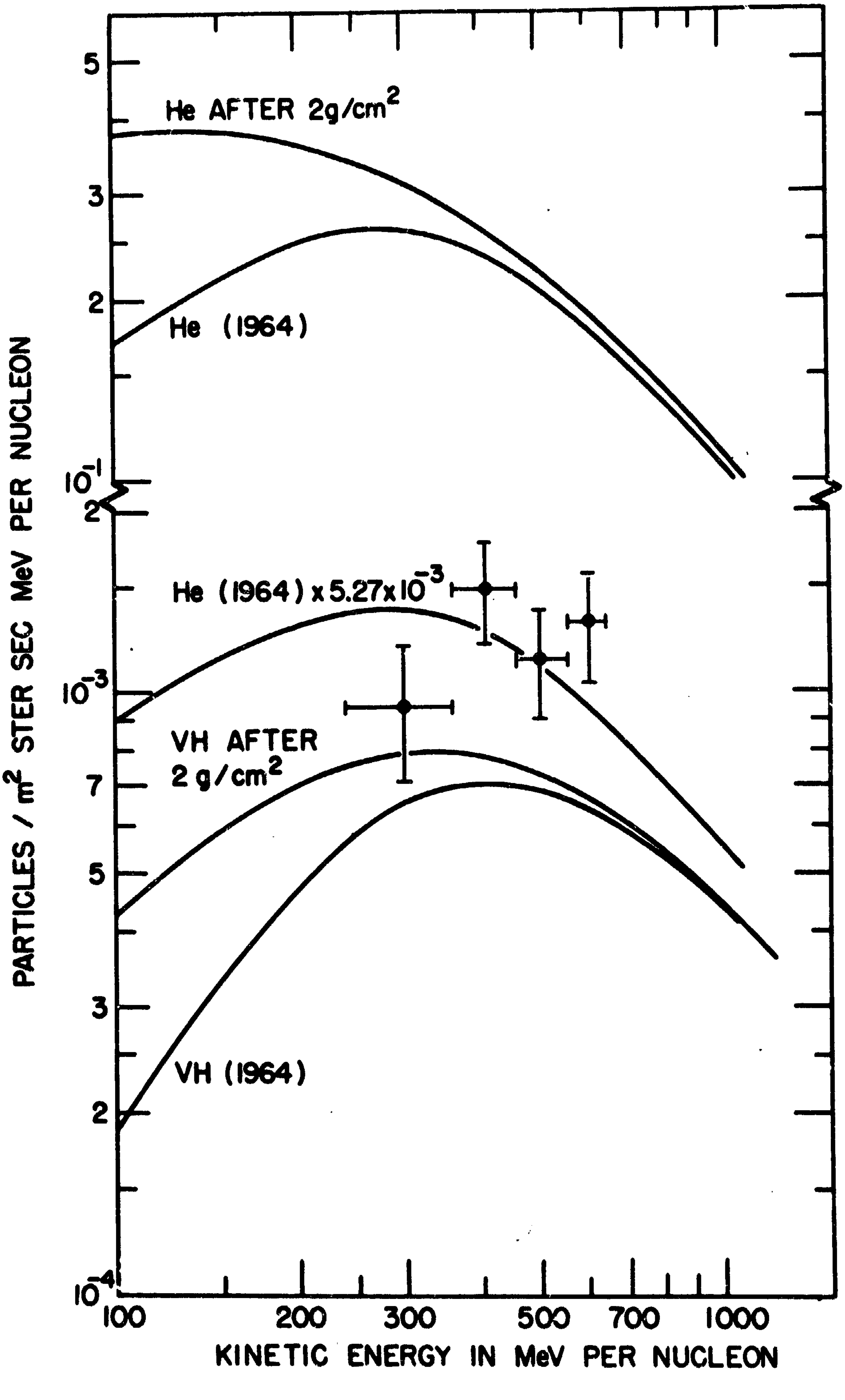

He AFTER 2g/cm²
He (1964)
He (1964) x 5.27x10⁻³
VH AFTER 2 g/cm²
VH (1964)
PARTICLES / m² STER SEC MeV PER NUCLEON
KINETIC ENERGY IN MeV PER NUCLEON
5
3
2
10⁻¹
2
10⁻³
7
5
3
2
10⁻⁴
100
200
300
500
700
1000

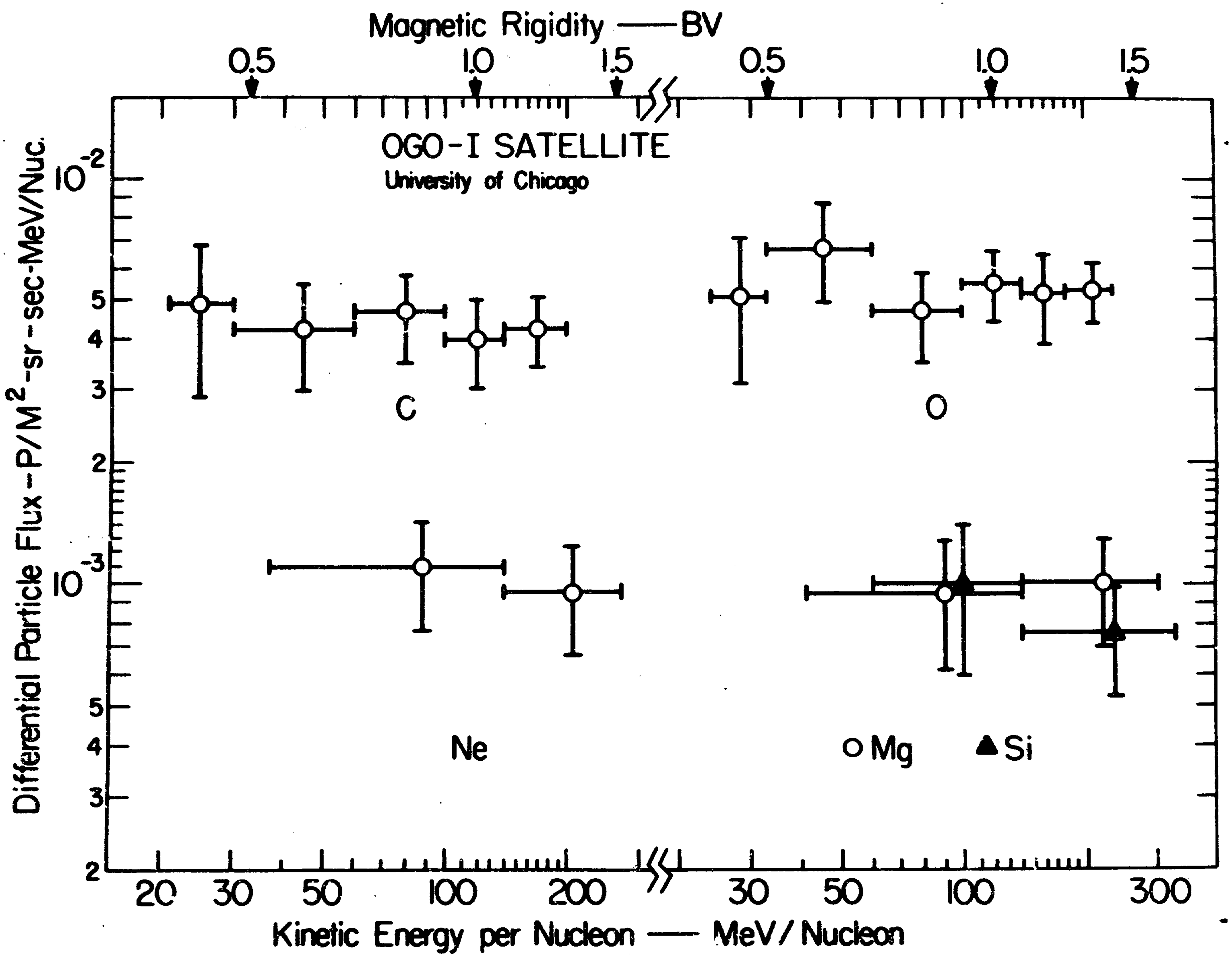

Magnetic Rigidity —— BV
0.5
1.0
1.5
0.5
1.0
1.5
OGO-I SATELLITE
University of Chicago
C
O
Ne
○ Mg
▲ Si
10^{-2}
5
4
3
2
10^{-3}
5
4
3
2
Differential Particle Flux – P/M²-sr-sec-MeV/Nuc.
20
30
50
100
200
30
50
100
300
Kinetic Energy per Nucleon —— MeV/Nucleon